Solubility of Fluorinated Polymers in Supercritical Carbon Dioxide

Von der Fakultät für Mathematik, Informatik und Naturwissenschaften der Rheinisch-Westfälischen Technischen Hochschule Aachen vorgelegte Dissertation zur Erlangung des akademischen Grades eines Doktors der Naturwissenschaften genehmigte Dissertation

vorgelegt

von

M.Sc.
Sherif Medhat Fahmy

aus Kairo/Ägypten

Berichter: Universitätsprofessor. Dr. Martin Möller
Universitätsprofessor. Dr. Franz-Joseph Wortmann

Tag der mündlichen Prüfung: 22.12.2005

Dedication

This thesis is dedicated to the soul of my parents, Mr. Medhat Fahmy and Mrs. Olfat Rashad, for their loving supports throughout my whole life. They are always and forever be in my heart and my mind.

Sherif Fahmy

"There is no limit in doing chemistry in carbon dioxide, just because it's neat and green candidate, and green is the color of money"

S.K. Ritter in C&EN July 16, 2001

The work presented in this dissertation has been done partially in the time from 01.08.2001 to 31.08.2002 at the Department of Macromolecular Chemistry III/ Materials, University of Ulm, and in the time from 01.09.2002 to 30.11.2004 at the Chair for Textile Chemistry and Macromolecular Chemistry, Institute for Technical Chemistry and Macromolecular chemistry, Aachen University of Technology under supervision of Prof. Dr. rer. nat. Martin Möller.

Content

List of Abbreviations

Chemicals

CO_2	Carbon dioxide
PERC	Perchloroethylene
PVDF	Polyvinylidene fluoride
HFP	Hexafluoropropene
PEA	Polyethylacrylate
PBA	Polybutylacrylate
PEHA	Polyethylhexylacrylate
PVAc	Polyvinyl acetate
PODA	Polyoctadecylacrylate
PMA	Polymethylacrylate
EMA	Ethylmethacrylate
PEO	Polyethylene oxide
PS	Polystyrene
PTFE (Teflon)	Polytetrafluoroethylene
Tefoln-AF_{160}	DuPont's Teflon commercial product
PVF	Polyvinyl fluoride
F8H2A	1H, 1H, 2H, 2H Perfluorodecylacrylate
DME	Dimethyl ether
PMMA	Polymethymethacrylate
PLLA	Poly(L-Lactide)
sPS	Syndiotactic polystyrene
PET	Polyethylene terephthalate
DMF	N,N- Dimethylformamide
DMAc	N, N- Dimethylacetamide
THF	Tetrahydrofuran
PFOA	1,1- Dihydrochlorofluorooctylacrylate
Freaon-113	1,2-Trichloro-1,2,2-trifluoroethene
HFX	Hexafluoro-m-xylene
PDMS	Polydimethylsiloxane
Kynar 741	Polyvinylidene fluoride M_w=323 kg/mol (Elf Atochem)

Solef1010	Polyvinylidene fluoride M_w=226 kg/mol (Solvay)
DMSO	Dimethyl sulfoxide
NMP	N- methylpyrroldidone
Krytox	Perfluoropolyether (DuPont's Product)

Units & Sympole

PVT	Pressure/temperature/volume correlation diagram
T_c	Critical Temperature
P_c	Critical Pressure
$\alpha(T)$	Temperature viral coefficient
s	Second
ΔH_{mix}	Change in Enthalpy on mixing
ΔS_{mix}	Change in Entropy on mixing
ΔU_{mix}	Change in internal energy on mixing
χ_i	Mole fraction i
χ_j	Mole fraction j
$\Gamma_{ij}(r,T)$	Intermolecular pair potential energy
$g(r,\rho,T)$	Radial distribution function
$\rho(P,T)$	Solution density
$\rho(r)$	Average density
ω	Interchange energy
Z	Coordination number
α	Polarizability
D	Dipole moment
Q	Quadruple moment
L+L (L+L)	Liquid/Liquid demixing line
L+S (L+S)	Liquid/Solid demixing line
LLV	Liquid/Liquid/Vapour transition line
UCST	Upper critical solution temperature
LCST	Lower critical solution temperature
LV	Liquid/Vapour transition line
P-x	Pressure-composition correlation diagram
P-T	Pressure-Temperature correlation diagram

T_c	Crystallization Temperature
M_w	Weight average molecular weight
M_n	Number average molecular weight
T_g	Glass transition temperature
T_m	Melting temperature
wt%	weight percentage
ppm	Part per million
δ	Chemical shift
dP/dT	Change pressure per time (depressurization time)
LCEP	Low critical end point
UCEP	High critical end point
ΔH_m	Change in Enthalpy on melting
μm	Micrometer
C^*_{VDF}	Temperature dependent fraction
f^{block}_{MMA}	MMA weight fraction in block copolymer
f^{random}_{MMA}	MMA weight fraction in statistical copolymer
Å	Angstrom
P^*	Intersection pressure
T^*	Intersection temperature
UCEP	Upper critical end point
LCEP	Lower critical end point

General

sc	Supercritical
VOC	Volatile Organic Compound
PRE	Peng Robinson equation of state
DSC	Differential Scanning Calorimetry
SEC	Size Exclusion Chromatography
^{13}C	^{13}C Nuclear Magnetic Resonance
NIST	National Institute of Standards
UV/vis	Ultraviolet-visible light source
SEM	Scanning Electron micrograph

SAFT	Statistical Associating Fluid Theory
EU	European Union
LPREI/CPREI	Laboratory of polymer reaction engineering
AUT	Chemical Process Engineering Institute, Aristotle University of Technology, Hellas
ATRP	Atom Transfer Radical Polymerization
GUC	German University in Cairo

CHAPTER 1

Introduction

1.1 Supercritical fluid technology as tool for environmental problem solving:

Rapid technological advances have many complex ecological issues on environment. As an example, pollution and waste management represent two of the most profound challenges of the 21st century. The proliferation of the use of organic solvents, halogenated solvents, and precious water in manufacturing and processing industries such as electronics, pharmaceuticals, dyes and coatings has created new innovative for the development of environmentally responsible and energy efficient processes.[1]

Although, volatile organic compounds (VOCs) are widely used in the chemical industry for various processes, they are often toxic and cause substantial costs regarding safety measures.

As a result of the growing concern of the population and government regulations imposed on the use of these compounds (e.g., the Montreal Protocol in 1987 and the Clean Air Act Amendments in 1990), considerable time and money has been spent on finding alternate solvents and processes that are environmentally beginn. [2]

Green or environmentally friendly chemistry is however much more than simply replacing hazardous materials (solvents or reagents) with less hazardous ones and can be defined on the basis of three factors: [1] being environmentally friendly; being chemically efficient (highly selective) and being economically viable.

In the past decade, in an effort to meet these challenges, research groups have focused on making liquid and supercritical carbon dioxide ($scCO_2$) as a viable solvent alternate

Carbon dioxide (CO_2) has the potential to replace water and many others solvents in many applications, e.g., dry cleaning and extraction process. CO_2 has its own advantageous because it is inexpensive, non-flammable, environmentally begin and can be completely and easily removed from products. [2, 3] Also CO_2 is naturally occurring and readily available; it can be found in nature reservoirs and is a byproduct from the industrial production of ammonia, ethanol, hydrogen and natural gases. [3, 4] In particular in food industry, CO_2 is routinely handled on a commercial scale using pressurized and refrigerated tanks for storage. When released to the atmosphere, liquid CO_2 leaves no residue to contaminate either the environment or personnel. [3]

Processes that use CO_2 from atmospheric sources do not add directly to the green house effect (global warming caused by the entrapment of heat into the atmosphere by gases that are emitted into the environment), but rather aid in the reduction of emitted CO_2. In addition to the environment benefits, CO_2–based processes can also be more energy efficient than those based on water or other conventional solvents. Moreover, the low heat of vaporization of carbon dioxide significantly reduces the energy costs that are associated with water intensive processing industries and also eliminates the inevitable contamination problems associated with the pollution of water effluent streams.

In addition to highly versatile nature of CO_2 has been exploited in numerous industries and applications, CO_2 has been used for a decades for food freezing and for pH-control in the textile, pulp and paper industries. [5] Commercialization of CO_2 was initially done in the 1970's as a "natural" extractant in decaffeination processes of coffee and tea, and also in spice industries have used $scCO_2$ to replace dichloromethane and ethylene dichloride.[6] In 1997, Ford Motor Company switched some of their bumper-coating processes from hazard solvent-base paints and primers to utilize CO_2 technology.[7] More recently, Micell technologies has commercialized an innovative process wherein

molecular engineered surfactant molecules, combined with CO_2 provide as an environmentally friendly alternative to the traditionally hazardous solvents used today, such as percholoethylene (PERC).[8]

A steady stream of emerging technologies has brought CO_2 all the way from a potential alternative solvent in the early 1970's, to its ever growing present day use in many industries and applications. The most recent example is Dupont's announcement to build a $275 million dollar manufacturing plant that will employ carbon dioxide technology to produce teflon and other fluoropolymers.[9]

1.2 Content of the thesis:

The work presented in this thesis is directed towards investigation of the solubility (i.e. miscibility) and crystallization of polyvinylidene fluoride (PVDF) (i.e. segregation regime of fluorinated polymers to be immiscible with supercritical carbon dioxide solution). Effect of different PVDF's molecular weights, concentration and other parameters on the location of liquid/liquid demixing in pressure/temperature diagram have been investigated. In a similar approach, a novel work has been done regarding the crystallization (liquid/solid boundary) of PVDF from carbon dioxide media. Influence of molecular weights on the position of the crystallization line of PVDF has been studied as well.

Additionally, most low molecular weight organic molecules mix readily with supercritical carbon dioxide. The solubility of polymer in CO_2 is poor with the exception of fluoropolymers, polysiloxane and polyether carbonate. More recent investigation focuses on the enhancement of the miscibility of polymers by adding suitable co-solvent. Where, addition of co-solvent can alter the chemical nature of the fluids system. The thesis is made an attempt to answer the question whether the addition of a small amount of a carefully selected low and high molecular weights compound will affect phase segregation upon isobaric change of temperature (crystallization) or isothermal change of pressure (precipitation) for PVDF/ $scCO_2$ solutions. Although, due to the low polarity of $scCO_2$ (i.e. its ability to solubilize polar PVDF is limited), solubility of novel synthesized macromolecular stabilizers has been investigated. Formation of stable dispersion based on suitable amphiphilic surfactants can provide a

technical solution as processing aids in dispersion polymerization of PVDF in supercritical carbon dioxide. In the following, an outline of the contents and objectives of the different chapters are given.

Chapter 2: provides the literature survey describing thermodynamic principles of CO_2–polymer mixtures interaction relevant to the thesis. Effects of polymer concentration, molecular weight and polymer crystallization are described for binary mixtures of polymer-scCO_2. The impact of co-solvency on the solubility and crystallization PVDF/SCF is shown.

Chapter 3*:* reveals experimental studies on crystallization/precipitation of poly (vinylidene fluoride) from supercritical carbon dioxide solution by cloud point measurement technique, and the effects of different PVDF's molecular weight on the position of cloud point pressure in the PVT diagram is described as well. In a rather novel approach the influence of monomeric vinylidene fluoride on the precipitation/crystallization cloud point boundaries of PVDF has been studied, as monomer could alter the solubility parameter of the growing polymeric chains. This effect is of great interest during dispersion polymerization process of polyvinylidene fluoride in carbon dioxide.

Chapter 4*:* deals with the phase behaviour determination of a variety of macromolecular stabilizers originally intended to be used as detergents for dispersion polymerization in supercritical carbon dioxide. A series of amphiphilic molecules constituted from CO_2-philic and a CO_2-phobic segment has been synthesized, where variety of CO_2-philic groups spanning from perfluoro (meth)acrylates, silioxanes to fluoro-silicone compounds have been used. Effects of different molecular architectures and other parameters like concentration, and molecular weight of stabilizer on the solubility have been checked.

Chapter 5*:* focuses on the effect of added non-polymerizable low and high molecular weight compounds on the location of precipitation/crystallization boundaries of polyvinlidene fluoride (PVDF) in scCO_2, and the effects of these additives on the polymer morphology and degree of crystallinity have been described in details. The

impact of hexafluoropropene oxide (HFP) gases on the position of liquid/liquid & Liquid/solid segregation lines of the PVDF/scCO_2 mixtures has been illustrated.

Chapter 6*:* presents the effect of different molecular weight of polyvinylidene fluoride on positions at which either precipitation or crystallization lines in carbon dioxide take place. Furthermore, the effect of different PVDF molecular weight on the morphological changes of the polymer crystals has been discussed briefly.

1.3 References:

[1] A. Clifford, Fundamentals of supercritical fluids, Oxford University Press, Oxford, 1998.

[2] Wells S. L. and DeSimone M J.; Angew. Chem. Int. Ed. 2001, **40**, 518-527.

[3] McHugh M., Krukonis V.; supercritical fluid extraction-principles and practice, Butterworths, Boston, 1986.

[4] Steiner R.; Chem.Eng. 1993, **100**, 114.

[5] Barer S., Stern K.; catalytic activation of carbon dioxide, American chemical society, 1988.

[6] CO_2 dry cleaning: minimizing environmental impact, company Bulletin, MICELL Technologies, 2000.

[7] Moore S., Samdani S., Ondrey G., Parkinson G.; Chem. Eng. 1994, **101**, 32.

[8] Canelas D., DeSimone J. M.; Chem. Br. 1999, **38**.

[9] Anonymous A.; Chem. Eng. 1997, **104**, 66.

CHAPTER 2

Literature overview

2.1. Fundamentals of supercritical fluid:

A "Supercritical Fluid" (SCF) is defined as a substance above its critical temperature (T_c) and critical pressure (P_c). [1-4] The critical point represents the highest temperature and pressure at which the substance can exist as a vapour and liquid in equilibrium. The phenomenon can be easily explained with reference to the phase diagram for pure carbon dioxide (Fig. 2.1). This shows the conditions where carbon dioxide exists as a gas, liquid, solid or as a SCF. The curves represent the temperatures and pressures where two phases coexist in equilibrium; (at the triple point, the three phases coexist). The critical point for carbon dioxide occurs at a pressure of 73.8 bars and a temperature of 31.1 °C.

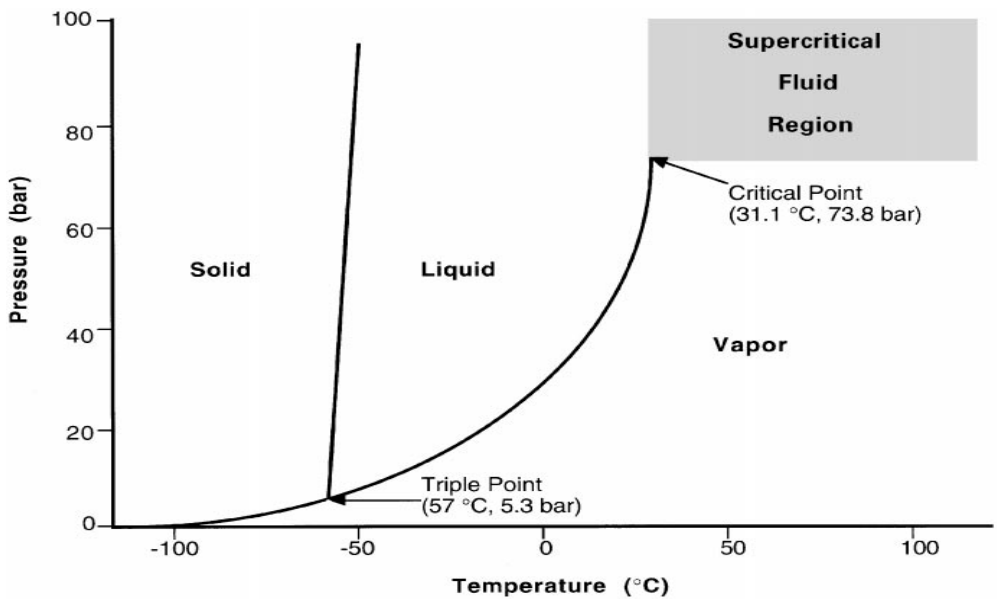

Figure 2.1: *phase diagram for pure carbon dioxide.* [1]

The density of $scCO_2$ can be adjusted to liquid-like values and the solubility of liquid or solid material in these media can be orders of magnitude higher than predicated from the ideal gas law. The bulk density of CO_2 at the critical point (d_c=0.466 g ml^{-1}) is the mean value of the densities of the liquid and the gaseous phase just before entering the supercritical region. It must be noted, however, that the local density of an SCF is subject to large fluctuations and may differ considerably from the bulk density, especially round the solute molecules. [1, 5]

For more practical applications, however, it seems more important that the high compressibility of the supercritical phase allows the bulk density of $scCO_2$ to be varied continuously in temperature and/or pressure. For example, the density of $scCO_2$ at 37°C is only 0.33 g ml^{-1} at 80 bar, but it rises to 0.80 gml^{-1} at 150 bar. (cf. Fig. 2.2)

The phase behaviour of the reaction mixture is of paramount importance for a chemical reaction in $scCO_2$. In order to exploit the physical properties of the supercritical state most effectively during a reaction, one will generally try to define conditions where a single homogeneous phase is present. On the other hand, it may be desirable to achieve controlled separation during work-up or to establish two-phase systems. It is therefore mandatory to carry out chemical reactions in $scCO_2$ using window equipped reactors that allow for the visual control of the reaction mixture. Furthermore, the expected phase behavior should be already considered during the design of a process to provide at least a rough estimate of promising reaction conditions.

The "solvent power" of a fluid phase is of course related to its polarity, but depends also strongly on the bulk density of the SCF directly. Normally the density values of carbon dioxide can be calculated from Peng-Robinson equation of state (PRE); this gives accurate results both for vapour and liquid phases. The pressure according to the PR equation is given by:

$$p = \frac{RT}{V-b} - \frac{a\alpha(T)}{V(V-b)+b((V-b)} \qquad (1)$$

Where,

$$a = 0.45724\frac{R^2T_c^2}{p_c}, \quad b = 0.0778\frac{RT_c}{p_c} \quad \text{and} \quad \alpha(T) = \left[1 + m\left(1 - \sqrt{\frac{T}{T_c}}\right)\right]^2$$

M= 0.37464+1.54226ω-0.26992ω^2 and ω=0.25, where a and b are constants, *α (T)* is the temperature virial coefficient taking into account the short range attractive forces between molecules and m is the acentric factor (i.e. compressibility factor) .

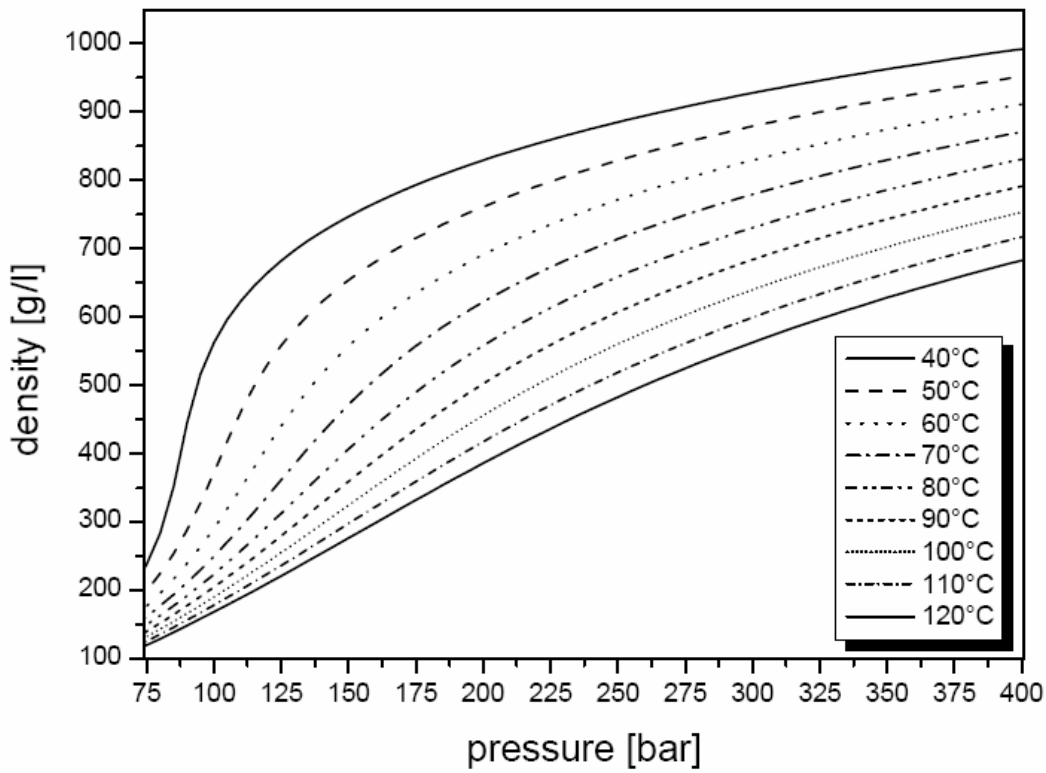

Figure 2.2: *Variation of the density with pressure for pure carbon dioxide above its critical temperature and pressure.* [6]

Table 2.1 shows a comparison of typical values for physical properties of a pure substance in different phases, including that of a SCF around the critical point. [6] It can be seen that the density of a SCF is approximately two orders of magnitude higher than that of the gas but still less than half that of a conventional liquid phase. The viscosity and diffusion coefficient (which is strongly related to viscosity) are also temperature and pressure dependent, and in general are at least one order of magnitude lower and higher, respectively compared to the liquid phase. If a chemical reaction is particularly fast, then it is feasible that diffusion of CO_2 could be the rate limiting factor; where an increase in the diffusivity could lead to reaction rate enhancement. This principle is particularly applicable to uni-molecular fission reactions (where increased diffusion allows an increase in reaction product rather than recombination) and highly efficient bimolecular processes such as free radical or enzymatic reactions. [2]

Table 2.1: *Comparison of physical properties of carbon dioxide in gases, liquids, and sc states* [2]

Property	Gas	SCF	Liquid
Density/ gml^{-1}	10^{-3}	0.4	1
Viscosity/ Pa S	10^{5}	10^{-4}	10^{-3}
Diffusivity / cm^2 S^{-1}	0.1	10-3	10^{-5}-10^{-6}

The disappearance of the distinction between liquid and gas phases can be demonstrated visually in an autoclave with a window, in which the meniscus between liquid and gas can be seen to disappear as the critical point is reached (Fig. 2.3).

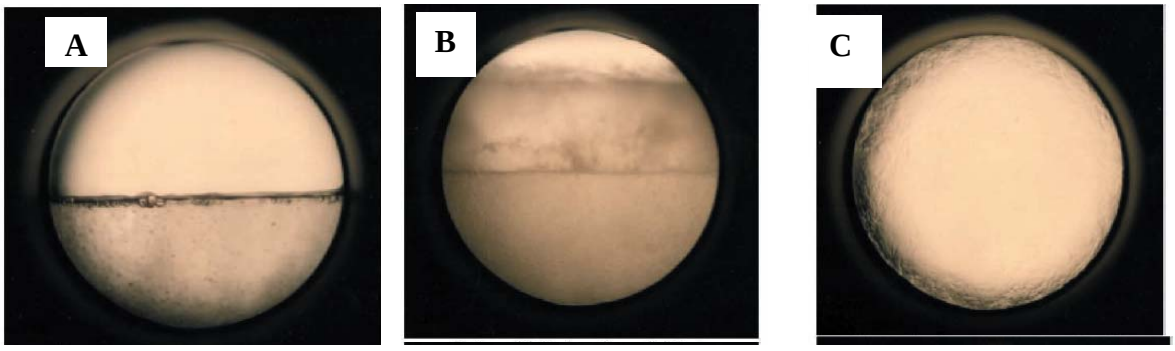

Figure 2.3.: *Photographs demonstrating the disappearance of the meniscus as the critical point is reached for a pure substance. Where, (a) shows a two phase liquid–gas system, with a clearly defined meniscus. (b) less defined meniscus, and(c) no meniscus is present and the system is now a single homogeneous SCF.* [2]

Historically, the high-pressure free-radical polyethylene polymerization process developed in the late 1930s represents the earliest applications of SCF solvents for polymers processing. Although these processes were commercialized in the late 1930s and early 1940s, a thorough understanding of the phase and kinetic behavior of these systems were still developing at this time. Ehrlich and co-workers were the first to develop fundamental phase behavior information that resolved much of the contradictory kinetic data that were actually obtained while operating in a two-phase region rather than the presumed one-phase region.[7]

Generally, the phase behavior of a polymer in a given solvent depends on polymer molecular weight, molecular weight poyldispersity, degree and type of chain branching as well as solvent quality.[8] To explore the dissolving power of SCF solvent for a polymeric compound in $scCO_2$, this necessitate the understanding of the thermodynamics of the polymer-SCF solution behavior.

2.2. Thermodynamics of polymer-SCF mixtures.

The principles of thermodynamics provide the vehicle for understanding the physicochemical properties of the components in solution. [9] A thermodynamics approach coupled with an experimental protocol in which solute and solvent properties are varied systematically elucidates the underlying chemical features of the components that fix the conditions needed to dissolve a polymer in an SCF solvent. This type of molecularly directed experimental approach provides the insight needed by polymer chemists to design polymers and copolymers that are miscible in SCF solvents at low pressures. In addition, it provides a rational methodology for choosing co-solvents to reduce operating pressures and temperatures needed to obtain a single phase.

To form a stable polymer-SCF solvent solution at a given temperature and pressure, the Gibbs free energy must be negative and at a minimum value. [9] The Gibbs free energy of mixing is given by:

$$\Delta G_{mix} = \Delta H_{mix} - T\Delta S_{mix} \qquad (2)$$

Where, ΔH_{mix} and ΔS_{mix} are the change of enthalpy and entropy on mixing of solute and solvent, respectively. Enthalpic interactions depend predominately on solution density and on polymer segment-segment, solvent-solvent, and polymer segment-solvent interaction energies. ΔS_{mix} depends on both the combinatorial entropy of mixing and the non-combinatorial contribution associated with the volume change on mixing, a so-called equation of state effect. [10] It is reasonable to assume that the combinatorial entropy of mixing a polymer with SCF solvent should not vary significantly with temperature and pressure near the conditions where the polymer dissolves in solution as long as the solvent density does not change dramatically. The combinatorial entropy always promotes the mixing of a polymer with a solvent. Although it is not possible to rigorously decouple the impact of energetic and entropic contributions to the Gibbs free energy of mixing, but it is possible to design phase behavior experiments that magnify or attenuate the impact of energetic relative to entropic contributions. For those situations, the principles of molecular thermodynamics provide a means for quantifying the interactions that govern the phase behavior of polymer-SCF mixtures. For a dense SCF solution, ΔH_{mix} is expected to be approximately equal to the change in internal energy on mixing,

$\Delta U_{mix}(where, \Delta U_{mix} = \Delta H_{mix} - \Delta nRT)$. The scaling of the solution energetics with density, assuming pairwise additivity, is shown in the following expression for the internal energy of an isotropic, homogeneous mixture relative, to ideal gas mixtures. [11]

$$\Delta U_{mix} \approx \frac{2\pi\rho(P,T)}{kT}\sum_{ij} x_i x_j \int \Gamma_{ij}(r,T) g_{ij}(r,\rho,T) r^2 dr \tag{3}$$

Where, x_i and x_j are mole fractions of components *i* and *j*, respectively. $\Gamma_{ij}(r,T)$ is the intermolecular pair potential energy of the solvent and the polymer segments, $g(r,\rho,T)$ is the radial distribution function, r is the distance between molecules, $\rho(P,T)$ is the solution density, and *k* is the Boltzmann constant (radial distribution is defined as the average density $\rho(r)$ at a distance r of a given particle).

Imbedded in equation 3 is the radial distribution function that describes the spatial positioning of molecules or segments of molecules with respect to one another. It is in this spatial description of the solution that the connectivity of the segments in the backbone of the polymer chain precludes the possibility of rigorously decoupling energetics from chain conformation in solution, i.e., the solution of segments is not random. Nevertheless, important generalities can still be gleaned from this approach. For example, given that the internal energy of the mixture is roughly proportional to its density, the solubility of a polymer is expected to improve by increasing the system pressure or using a denser SCF solvent.

However, the polymer will dissolve only if the energetic of polymer segment-solvent interactions outweighs polymer segment-segment and solvent-solvent interactions. In other words, the integral in equation 3 cannot be ignored completely. Stated differently, for certain polymer-SCF solvent mixtures, hydrostatic pressure alone will not overcome a mismatch in energetics between the components in solution. The balance of such interactions in solution is described by the interchange energy, ω defined as:

$$\omega = z\left[\Gamma_{ij}(r,T) - \frac{1}{2}(\Gamma_{ii}(r,T) + \Gamma_{jj}(r,T))\right] \tag{4}$$

Where, z is the coordination number, or number of different pairs in solution. [11] An approximate form of the attractive part of the intermolecular potential energy, $\Gamma_{ij}(r,T)$ for small molecule mixtures is:

$$\Gamma_{ij}(r,T) \approx -\left[c_1 \frac{\alpha_i \alpha_j}{r^6} + c_2 \frac{\mu_i^2 \mu_j^2}{r^6 kT} + c_3 \frac{\mu_i^2 Q_j^2}{r^8 kT} + c_4 \frac{\mu_i^2 Q_j^2}{r^8 kT} + c_5 \frac{Q_i^2 Q_j^2}{r^{10} kT} + complex* formation \right] \quad (5)$$

Where α is the polarizability, μ is the dipole moment, Q is the quadrupole moment, and $C_{1\text{-}5}$ are constants.[9] Equation 5 serves only as a guide for qualitatively evaluating the effects of intermolecular interactions on polymer-solvent phase behavior. Induction interactions are not shown in equation 5 since their contribution to the potential energy tends to be much smaller than dispersion and polar interactions. Equation 5 is not expected to describe rigorously the interaction of a polymer segment with another segment or with the solvent since segmental motion is constrained by chain connectivity.

Note that for nonpolar dispersion interactions, the first term in equation 5 depends only on the polarizability of the components in solution and not on temperature. Therefore, the pressures needed to dissolve a nonpolar polymer in a nonpolar SCF solvent should decrease as the polarizability of the solvent increases. Specific interactions such as complex formation or hydrogen bonding can also contribute to the attractive pair potential energy. Once again the strength of these "directional" interactions are also very temperature sensitive. Equations 3-5 describes how the solvent quality of a supercritical fluid can be tuned with changes in pressure as well as temperature, and a degree of flexibility not available with liquid solvents

2.3. Phase diagram of polymer-CO_2 mixtures:

Solubility of a polymer is a key factor for the homogeneous polymerization in $scCO_2$. Author has reported that solvent physical qualities of $scCO_2$ can be compared to those of toluene, hexane or acetone.[10] Meanwhile, phase diagram of polymer-CO_2 mixtures can be better understood on the base of phase diagram for binary mixture of low moleculer weight solutes.

Phase diagram of binary polymer-SCF mixtures.

2.3.1 Effect of physical properties of polymer.

Figure 2.4 (a) shows the schematic *P-T-x* phase diagram[11] of a typical binary mixture with a large difference in critical temperature, such as a small organic molecule and CO_2. The front and back faces of the rectangular prism show the *P-T* phase behavior of

pure component A and pure CO_2, respectively. The various surfaces inside the prism are the different phase boundaries. The SA-L surface (red) extends from the melting curve of pure A on the front face into the interior, where solid A (SA) is in equilibrium with the liquid phase (L). The SA-V surface (yellow), which signifies the phase boundary between solid A and the vapour phase (V), stretches from the sublimation curve of A inward. The V-L envelope (cyan) stems from the vaporization curve of A and is bounded by two surfaces representing vapour and liquid phases in equilibrium. The envelope ends at the locus of critical points, beyond which the vapour and liquid phases are indistinguishable.

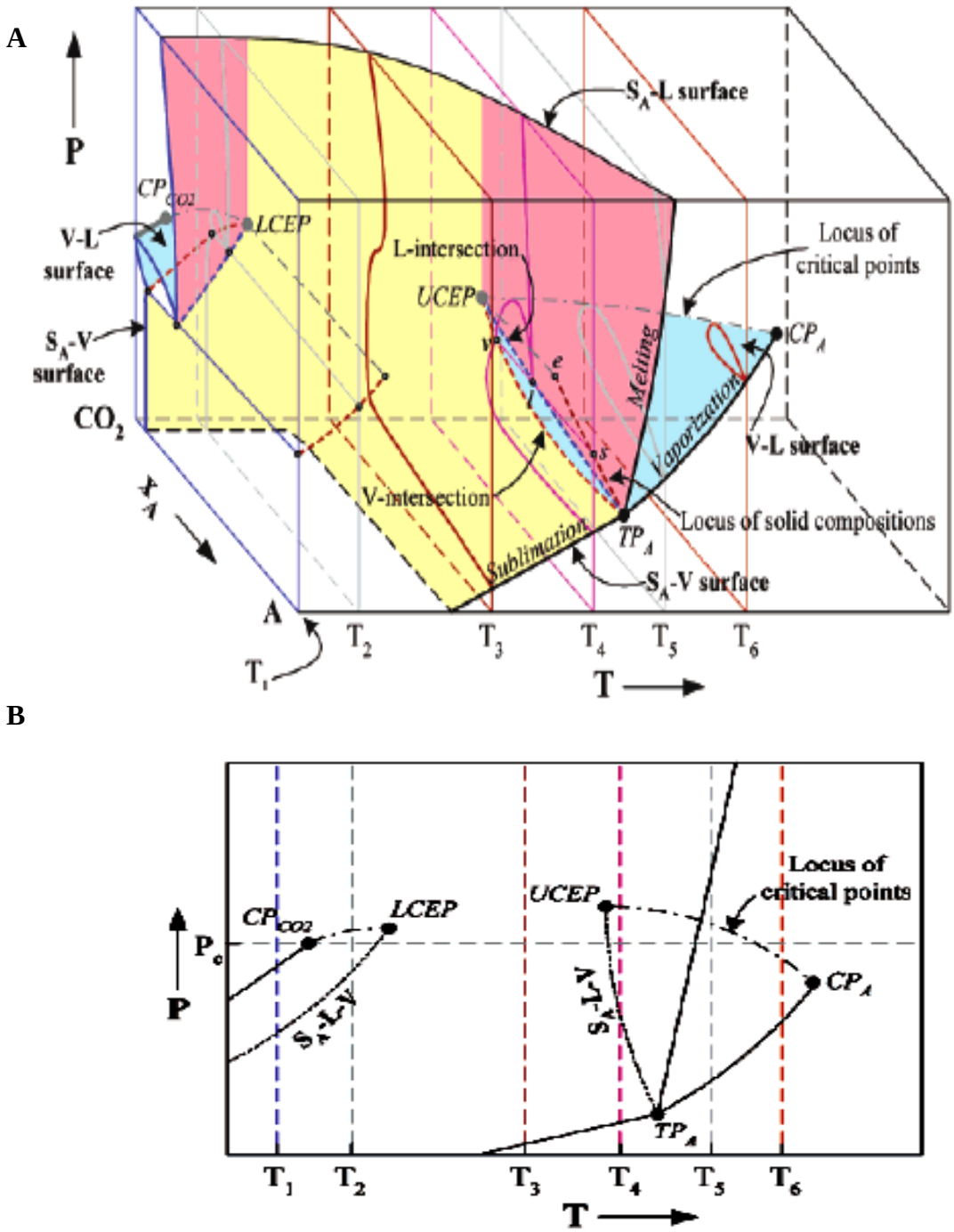

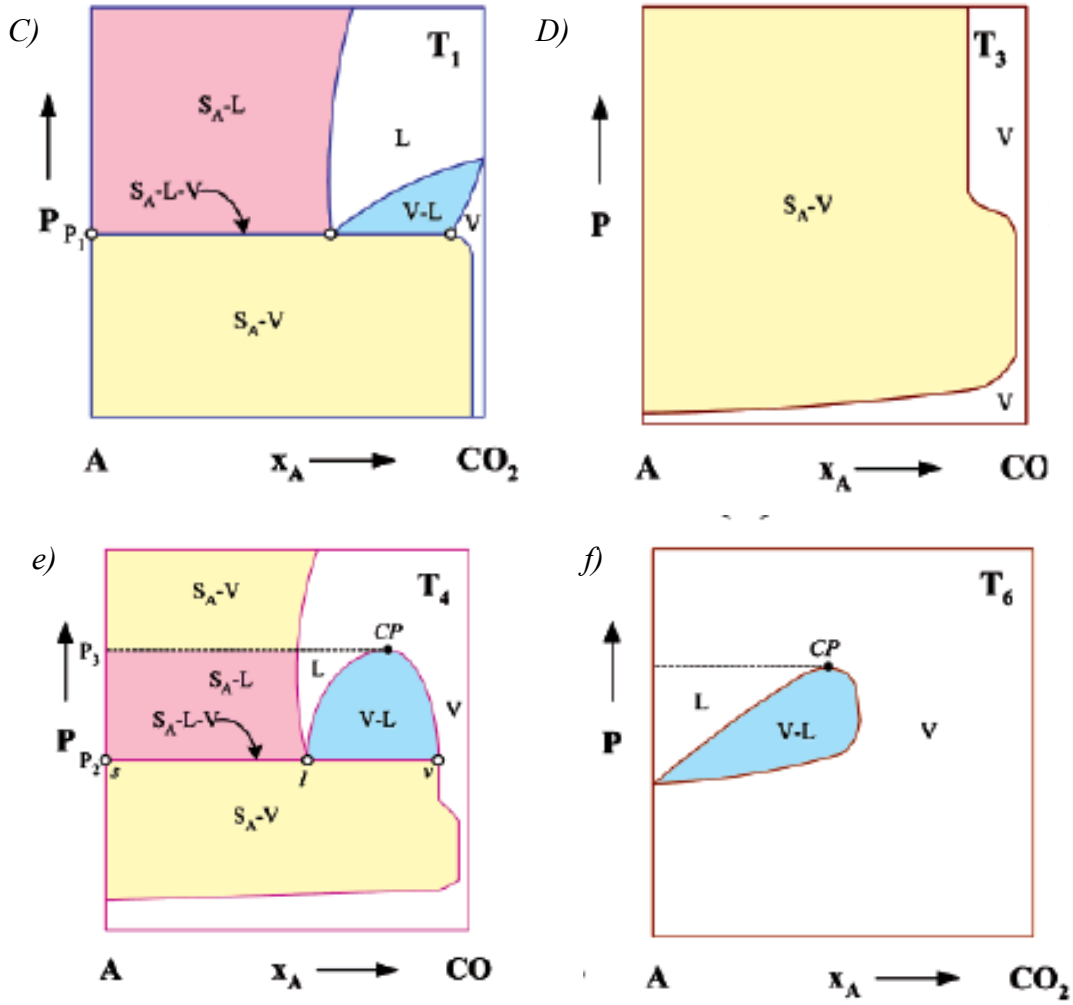

Figure 2.4 *Schematic phase diagram of the binary system A-CO_2. Diagram is not to scale. (a) P-T-x diagram; (b) P-T projection; (c) isothermal cut at T1; (d) isothermal cut at T3; (e) isothermal cut at T4; (f) isothermal cut at T6.(redrawn from ref. 11)*

The intersection between the upper V-L surface and the SA-L surface is the L-intersection curve (blue dotted curve). The lower V-L surface intersects the SA-V surface at the V-intersection curve (orange dotted curve). These V- and L-intersection curves extend from the triple point of A (TPA) and end by intersecting the locus of critical points at the upper critical end point (UCEP). Similarly, such curves on the low-temperature side intersect the locus of critical points at the lower critical end point (LCEP). The V- and L-intersection curves represent the vapour and liquid phases that are in equilibrium with each other as well as with solid A (SA-L-V equilibrium). The locus of solid phase compositions (curve e, TPA) is on the front face of the prism because the solid phase is pure A. Therefore, SA-L-V equilibrium exists for any temperature between the UCEP and TPA. For example, at temperature *T*4, the solid, liquid, and vapour equilibrium composition is given by points s, l, and v, respectively. At the UCEP temperature, the solid phase is given by point e, while the vapour and

liquid phases merge into a single fluid phase at point UCEP. The section of the SA-L surface between the LCEP and UCEP temperatures thus represents equilibrium between solid A and the fluid phase (also marked with yellow as the SA-V surface). Figure 2.4 (b) is the *P-T* projection of the three-dimensional prism in Figure 1a, showing the pure component melting, sublimation, and vaporization curves as well as the locus of critical points. The SA-L-V region (e-Upper critical end point-Triple point (TP) A, Figure 2.4 (a)) appears as the SA-L-V curve in the projection, because the liquid and vapour phases in equilibrium, while having different compositions, must have the same pressure and temperature. Also, for three-phase equilibrium in a binary system, the degree of freedom is unity. The *P-T* projection is especially useful for showing the regions of pressure and temperature in which various phase equilibria may exist. However, it does not show the compositions of the phases in equilibrium, which is an important piece of information for process design.

Figure 2.4 (c-f) shows the isothermal cuts section of the binary phase diagram at different temperatures. At *T*1, which is below the critical temperature of pure CO_2, the isothermal cut features the regions of SA-L, SA-V, and V-L equilibria (Figure 2.4 (c)). The SA-L-V equilibrium (at *P*1) forms the boundary among the various regions. Such a boundary does not exist in the isothermal cut at *T*3, which is between the LCEP (*LCEP; Lower critical end point*) and UCEP (*UCEP; upper critical end point*) a temperature (Figure 2.4 (d)). The solid is always in equilibrium with a vapour-fluid phase. Notice that the phase boundary illustrates that solubility of a solute is generally higher at high pressures, with a significant change in the vicinity of the critical pressure of CO_2. It is this portion of the phase diagram that is usually displayed as an isotherm curve in a solubility diagram. As the temperature is further increased to *T*4 (higher than the UCEP), the SA-L-V equilibrium (at *P*2) that forms the boundary among the various regions reappears (Figure 2.4(e)). Since the vapour and liquid phases are indistinguishable above *P*3, solid A is in equilibrium with the supercritical fluid phase (referred to as the SA-V equilibrium). At a higher temperature *T*6 (Figure 2.4 (f)), there is only a V-L region and a solid phase is not present.

Furthermore, Figure 2.5 [10, 12] shows that it is possible to induce the single fluid phase into two phases either by isobarically lowering temperature by crossing the UCST curve (arrow I) or increasing the temperature through crossing the LCST curve (arrow II). At high temperatures, the LCST curve does not reach a distinct end point since polymers

do not have critical points. Also, the LLV line for a polymer-solvent mixture essentially superpose onto the vapor pressure curve of the solvent. Indeed that the LCST curve is more sensitive to pressure since it is typically at temperatures in the vicinity of the solvent critical temperature, where the solvent is highly compressible. Hence, increased hydrostatic pressure decreases the molar volume of the solvent and reduces the free volume difference between the solvent and polymer. Numerous polymer-solvent phase behaviour studies are available in the literature demonstrating the effect of solvent quality on the location of the LCST for type III mixtures. [13-21]

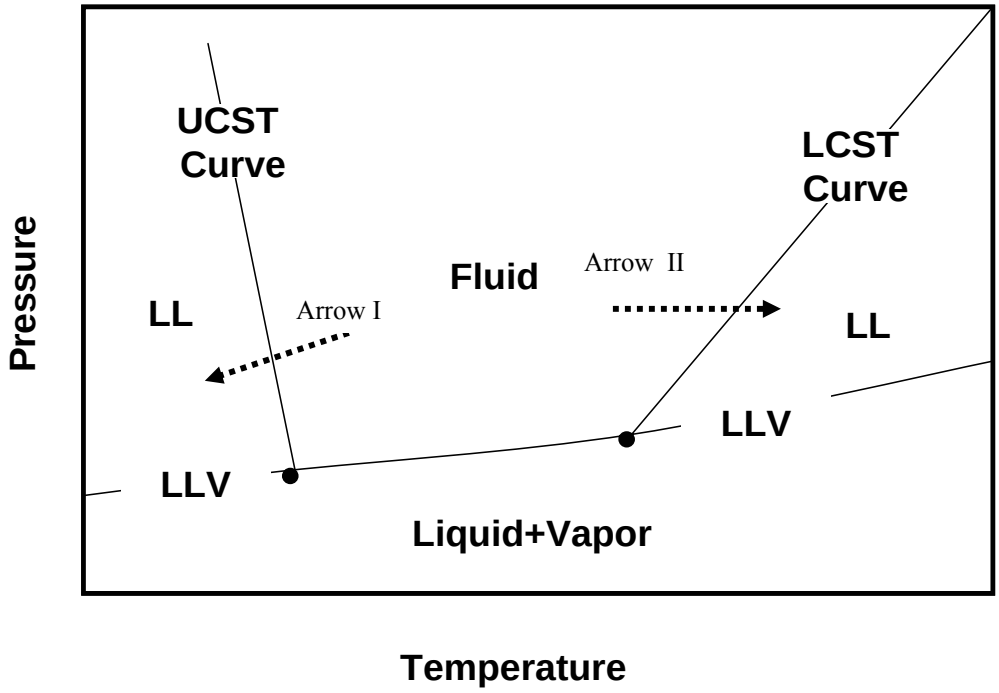

Figure 2.5: *Schematic pressure-temperature phase diagrams for binary mixtures of low molecular weight solvent with low molecular weight solute. L+L represent a liquid-liquid region; L+V represent a liquid- vapor regime, arrow I and II represent the possible phase transitions from homogenous solution.* [8]

Actually polymer-solvent diagram in Figure 2.5 represents a multicomponent phase behavior, since all polymers have a molecular weight polydispersity fixed by the synthesis technique used to make the polymer. For polymer-solvent mixtures the transition from a transparent single phase to an opaque two-phase system at either the UCST or LCST is termed a cloud-point which is the multicomponent analogue of a binodal point. [22- 28]

2.3.2 Effect of polymer concentration:

It was reported [16, 29-31] that similarities were found between the phase behavior of polymers in supercritical fluid mixtures and small molecules, as illustrated in Figure 2.6. A distinction between small molecule and polymer-SCF solvent behavior is given by the fact that the curves in the small molecule diagram are the locus of points for mixtures with differing compositions, and the curves in polymer-SCF solvent diagram are at essentially one fixed composition. Figure 2.6 shows that the maximum/minimum temperature for the temperature-composition curve of polymer-SCF solution is relatively insensitive to composition in the range of 3-15wt % polymers. The pressure maximum/minimum of a pressure-composition (P-X) curve is also insensitive to composition. This means that a single cloud-point curve in the composition range of 3-15 wt % polymer defines the maximum pressure of the P-T trace of the P-x curve that is, cloud-point curves with compositions between 3 and 15 wt % essentially superpose.

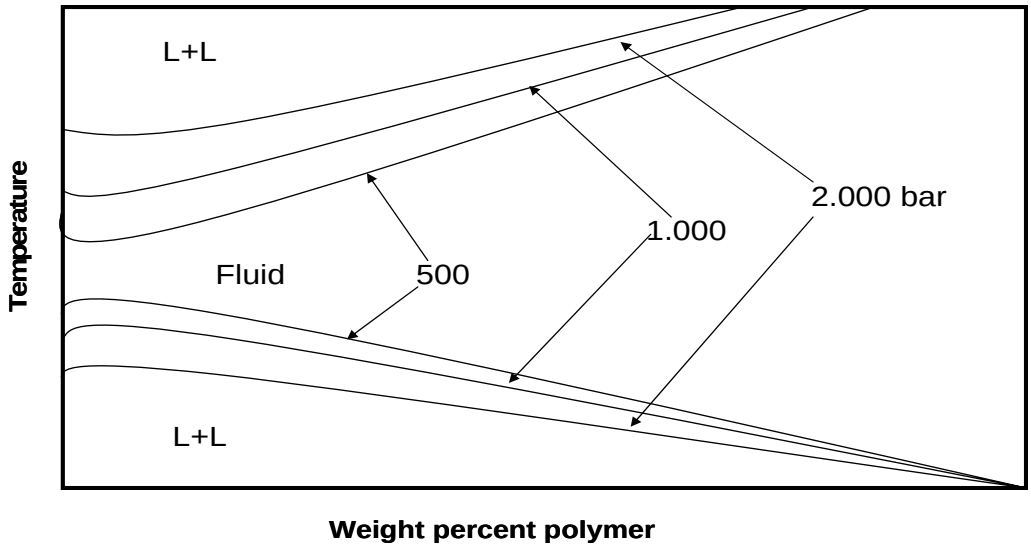

Figure 2.6: *Schematic representation of the impact of pressure on The UCST (maximum) and LCST (minimum) temperature for a polymer-solvent mixture. The curves are relatively flat at the maximum (minimum) in the range of 3-15 wt % polymers. L+L represent a two-phase region. (Redrawn from ref.8)*

2.2.3 Effect of the polymers molecular weight:

McHugh et al. [8] have showed that, the effect of polymer molecular weight on the phase behavior in a SCF solvent is analogous to that observed in a liquid solvent. Figure 2.7 shows a schematic representation of the diminishing effect of polymer molecular weight on the UCST curve of a liquid solvent for a molecular weight greater than ~100.000 g/mol. The same diminishing effect is observed within polymer-SCF mixtures for both

the UCST and LCST curves which suggests that phase behavior experiments should be conducted with molecular weights near 100000g ml^{-1} molecular weight. If molecular weight effect is a concern, it is possible to obtain a straight-line extrapolation of the effect of molecular weight by plotting the inverse UCST temperature versus the inverse square root of molecular weight from several cloud-point curves.

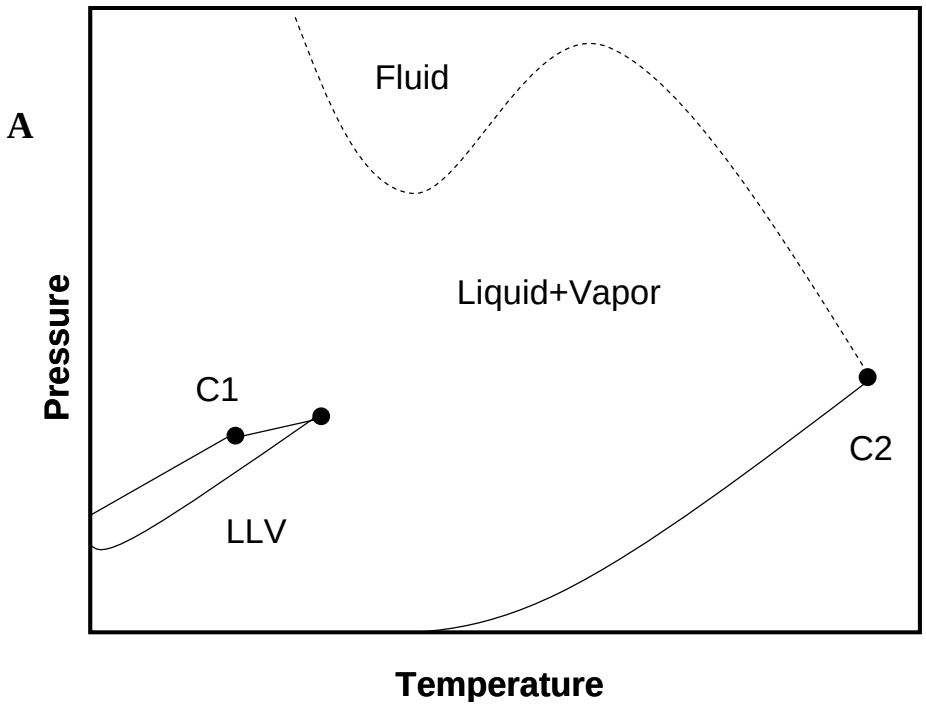

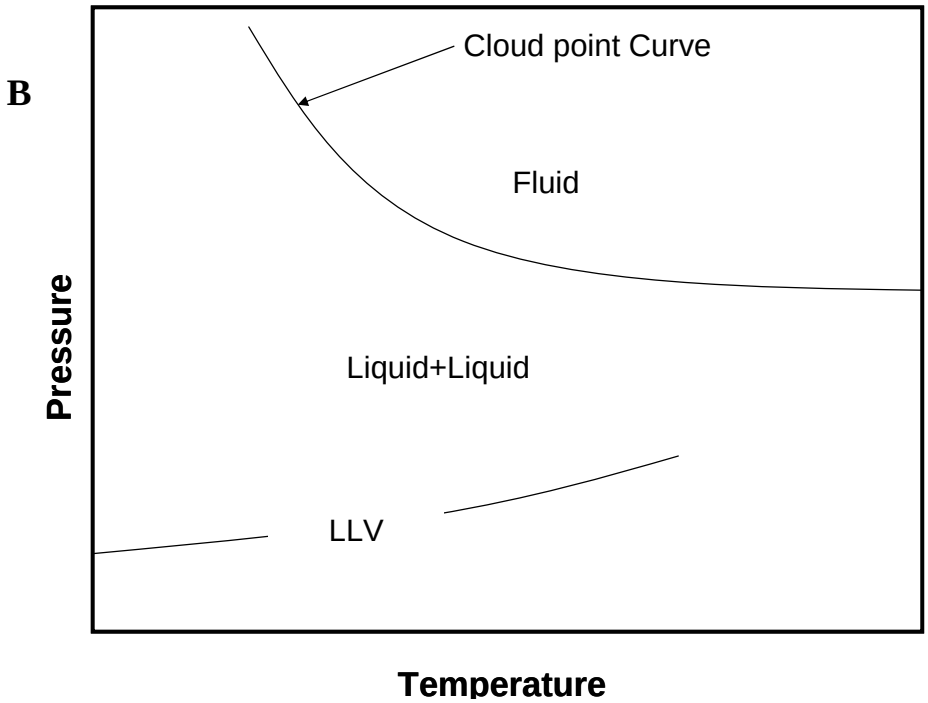

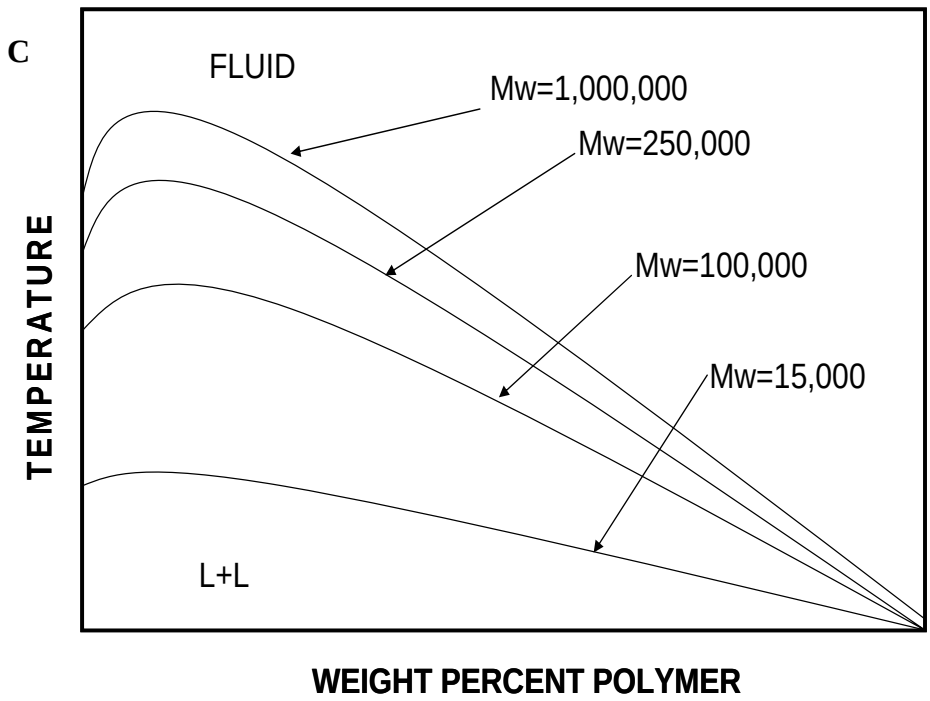

Figure 2.7: *Schematic pressure-temperature phase diagrams for binary mixtures of low molecular weight solvent; (A) with a low molecular weight solute, and (B) with a high molecular weight polymer.* [8]*The influence of polymer molecular weight on the phase behaviour of polymer-SCF solvent mixture at an arbitrary pressure, the same type of behavior is expected if pressure is substituted for the temperature axis(C).(redrawn from ref. 13)*

2.3.4 Effect of polymer solidification:

Most interesting issue concerning polymer solubility in a given supercritical fluid solvent was recorded to be extremely low at temperatures less than the solidification temperature (crystallization temperature; T_c) of semicrystalline polymers. This behavior was found to be dependent on solvent quality and hydrostatic pressure exerting between polymer and sc fluid. For all practical purposes the solubility is so low at temperatures below the solidification boundary; where most of polymer fractionation or extraction processes would not be operated in this regime. Figure 2.8 shows how the polymer's solidification can affect the phase behavior of polymer-SCF mixtures.

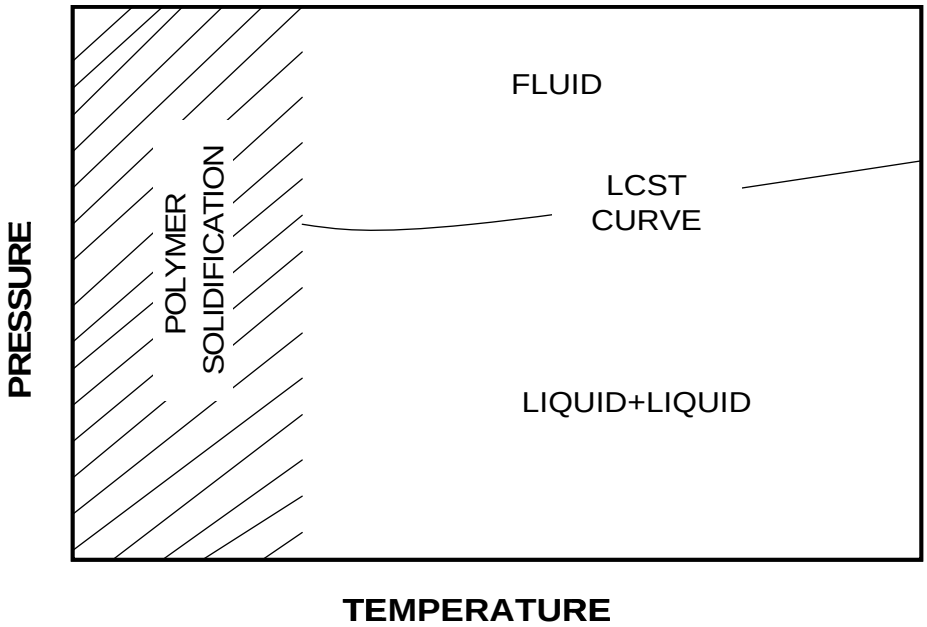

Figure 2.8: *Effect of polymer crystallization on the phase behavior of polymer in supercritical carbon dioxide. (Redrawn from ref. 8)*

2.4. Solubility of (co) polymers in a solutions of $scCO_2$:

The pressures and temperatures needed to dissolve a polymer in CO_2 depend from one side on the intermolecular forces between solvent-solvent, solvent-polymer segment and polymer segment-segment pairs in a solution as given by the interchange energy; and from another side on the free volume difference between the polymer and CO_2.[32-36] Krukonis has shown that CO_2 at or near room temperature and at pressures below 600 bar dissolves many poly(dimethyl)- & poly(phenylmethyl) silicones, perfluoroalkylpolyethers, chloro- and bromotrifluoroethylene polymers.[12,37-38] Beckman and co-workers have described the solubility of poly(perfluoropropylene oxide) and poly (dimethyl siloxane) in CO_2.[39] Barton[40, 41] and Kiran[42] have also reported on the high solubility of poly(dimethyl siloxane) in CO_2 at approximately 450 bar. In general, polymers are reported to have high solubility in CO_2 whereas, all of them possesses some degree of polarity due to presence of oxygen or other electronegative groups such as chlorine or bromine incorporated into the backbone of the polymer. The only exceptions are the silicone and siloxane type polymers. Where, higher solubility of the poly (dimethyl) and poly(phenyl methyl) silicones in CO_2 is likely due to the very flexible nature of these polymers that endows them with much larger free volumes as compared to other polymers.

An interesting aspect regarding solubilities of polymer in sc solutions is how much polarity is needed to make a polymer soluble in CO_2. This question has been answered by Rindfleisch et al. [43] Where they observed after determining the cloud points curves (c.f Figure 2.9) of polyacrylates in CO_2, example are poly(ethylacrylate) (PEA), poly(butyl acrylate) (PBA), poly(ethylhexyl acrylate) (PEHA) and poly (octadecyl acrylate) (PODA). A common observation was noticed, as the alkyl tail group length on the acrylate increases the effective polarity decreases and solubility in CO_2 becomes harder. Since reduced dipole interactions scale inversely related with the square root of the molar volume.[9]

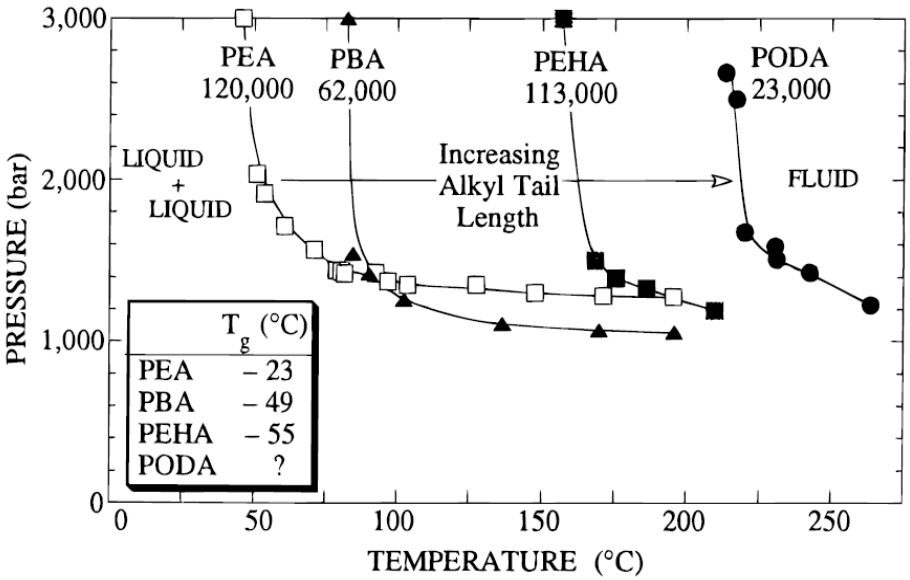

Figure 2.9: *Impact of the nonpolar alkyl tail of the acrylate group on the cloud-point curves of poly (ethyl acrylate) (PEA), poly (butyl acrylate) (PBA), poly (ethylhexyl acrylate) (PEHA), and poly (octadecyl acrylate) (PODA) in CO_2. Listed on each curve is the respective weight average molecular weight, (M_w). The polymer concentration is ~5 wt% in each case.* [43]

McHugh et al. [8] have reported that, CO_2 is a very weak supercritical solvent that is sensitive to polymer architecture, chemical type and intermolecular potential energy of the polymeric repeating units. By comparing the locations of cloud point curves of poly(methacrylate) (PMA) and poly(vinyl acetate) (PVAc) (cf.Figure 2.10) we can notice that at 30 °C the PMA cloud-point curve is 1500 bar higher than the PVAc curve even though the molecular weight of PVAc is four times greater than that of PMA. Both PMA and PVAc are polar, but the T_g for PVAc is approximately 21°C higher than the T_g of PMA. The slightly higher T_g of PVAc is a reflection of stronger polar interactions between vinyl acetate groups as compared to methyl acrylate groups when these groups are attached to a polymer chain. Moreover, CO_2 can more easily access the carbonyl

group in PVAc than in PMA, which makes PVAc more soluble in CO_2 with decreasing temperature. Easier access to the carbonyl group in PVAc also makes it easier for CO_2 to form a weak complex with PVAc especially at moderate temperatures. [34]

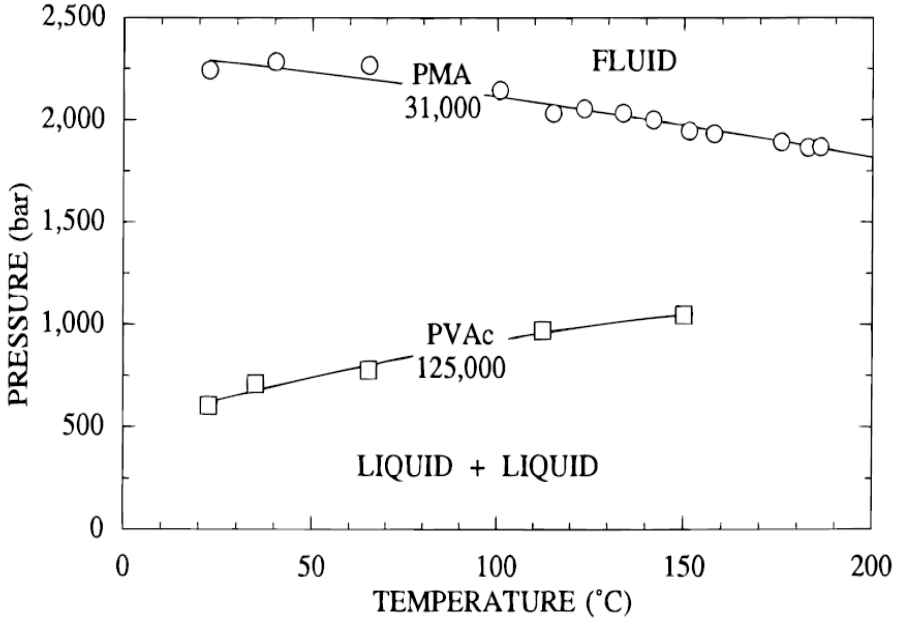

Figure 2.10: *Comparison of the CO_2-poly (methyl acrylate) (PMA) and CO_2-poly (vinyl acetate) (PVAc) cloud-point curves. The weight average molecular weight, Mw, is given in the figure, and the polymer concentrations are ~5 wt % in each case.* [43]

Table 2.2 summarizes the solution behavior of a variety of polymer referencing to their solubilities in sc CO_2:

Table 2.2: *A list of experimental solubility data for some polymers in scCO_2 investigated so far:*

Polymer	**Temp. °C**	**Pressure bar**	**M_w x10^{-3}**	**Ref(S)**
Poly (dimethylsiloxane)	25-185	250-600	39-370	42
Poly (isobutylene)	50-200	150-750	2-486	40, 44, 45
Poly(vinylidene fluoride) (PVDF)	120-220	1700-2200	~200	46
PVDF w/Acetone	90-220	1700	~200	46
PVDF w/DME	100-220	300-1700	~200	46
PVDF w/ Ethanol	100-220	1700	~200	46
Poly(1,1-dihydroperfluorooctyl acrylate)	30-80	100-300	1200	47, 48, 53
Poly(vinyl Acetate) (PVAc)	20-160	500-1000	125	43
Poly (methyl acrylate)	20-200	1700-2200	31	43

(continued)

Poly (ethyl acrylate)	50-200	1200-3000	119	43
Poly (propyl acrylate)	100-180	1200-1500	140	43
Poly (butyl acrylate)	80-200	1000-3000	62	43
Poly(ethylhexyl acrylate)	150-220	1100-3000	113	43
Poly (octadecyle acrylate)	210-260	1000-2600	23	43
Poly(butyl methacrylate)	120-230	1100-3000	320	43
Poly(ethylene-co-18 mol% methylacrylate)	80-280	1500-2800	~100	43
Poly(ethylene-co-31mol% methylacrylate)	80-280	1500-2800	~100	43
Poly(ethylene-co-41 mol% methylacrylate)	80-280	1500-2800	~100	43
Poly(tetrafluoroethylen-co-19 mol% hexafluoropropen)	180-250	1000-3000	210	43
Poly(tetrafluoroethylen-co-48 mol% hexafluoropropen)	170-230	1000-2800	210	50
Poly(vinylidene fluoride-co-22 mol% hexafluoropropen)	100-230	700-900	191	43, 51
Poly(vinylidene fluoride-co-74 mol% chlorotetrafluoroethylene)	120-210	1000-2750	85	49
Polytetrafluoroethylene (Teflon AF160)	50-180	500-1000	400	43
Polytetrafluoroethylene (Teflon AF240)	60-180	500-1000	n/a	52
Poly (vinyl fluoride) (PVF)	<300	Insol.	120	54,55
Poly(acrylic acid)	<280	Insol.	54	54
Polyethylene oxide	140	800-1500	13	56
Poly (acryl amide) (PAA)	Insol.	Insol.	160	56
Poly(styrene) (PS)	Insol.	Insol.	80	54, 56
Poly(tetrafluoroethylene$_{47.8}$-co-vinyl – acetate$_{52.2}$)	80-120	550-1000	53	57

Entries that show a polymer with a notation "polymer/cosolvent" indicate that a cosolvent is added to the solution.

Generally, predicting polymer solubility in CO_2 is of paramount importance for polymerization in $scCO_2$. To exploit the physical properties of CO_2 most effectively during polymerization, defining a condition at which polymer forms a single homogenous phase plays a crucial rule. It might be desirable to achieve a controllable

polymer separation during work out. However, recent investigation regarding polymer miscibility in $scCO_2$ indicates that partial fluorination of polymer might increases miscibility but it does not guarantee dissolution at moderate conditions. [58,-61] Another aspect for the formation of stable polymer solutions or dispersions is the viscosity of solution. From one side the extremely low viscosity of sc solutions is favourable for an efficient polymerization process; on the other side it favours aggregation and precipitation of the growing polymeric chain. Influencing the viscosity by addition of special viscosity modifiers will be important for retarding segregation in metastable colloidal solution stage. Examples for such an approach are statistical copolymers of styrene (29 mol %) with a fluoroacrylate (F8H2A). Concentrations of 1–5wt% increase the viscosity of pure CO_2 by a factor of 5 to 400.[62, 63]

2.5 Fluoropolymer-CO_2 interaction behaviour :

Fluoropolymers are treated as a self-standing section due to their specialty-end applications in the medical and electronics industry and as separation membranes. Very little systematic phase behaviour studies have been done on fluoro-copolymer-$scCO_2$ mixtures. Since fluorinated polymers and copolymers, and in particularly poly(tetrafluoroethylene) (PTFE), have generally been considered to be resistant to dissolution in most common solvents.[64] Recent studies show that it is possible to dissolve PTFE and its copolymers in many halogenated solvents including tertiary perfluoroamines, perfluorinated olefins, perfluorokerosenes, perfluorinated oils, and polyhexafluoropropylene oxide oligomers.[64-66] Table 2.3 summaries chemical structures of fluoro-monomeric units constituting fluoro-copolymer so far.

Table 2.3: *Chemical structure of the repeating units in several fluorocopolymers* along *with their IUPAC nomenclature.*

Copolymer	Monomer 1	Monomer 2
Poly(vinylidene fluoride$_{78}$-co-hexafluoropropene$_{22}$) P[VDF_{78}-co-HFP_{22}]	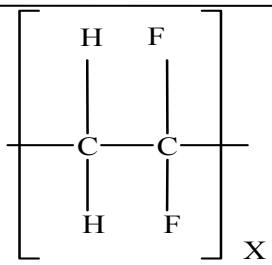	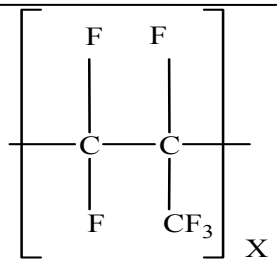

Poly(tetrafluoroethylene$_{81}$-co-hexafluoropropene$_{19}$)
P[TFE$_{81}$-co-HFP$_{19}$]

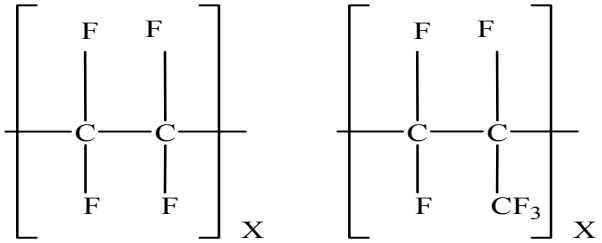

Poly (vinylidene fluoride$_{26}$-co-chlorotetrafluoroethylene$_{74}$)
P [VDF$_{26}$-co-CTFE$_{74}$]

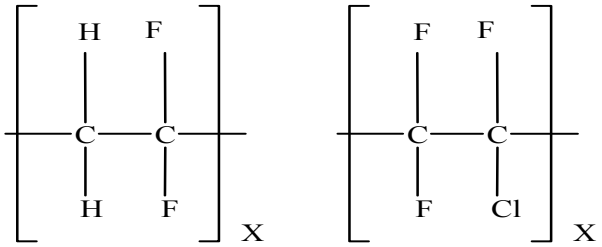

Poly[(tetrafluoroethylene$_{35}$-co-perfluoro-(2,2-dimethyl-1,3-dioxole)$_{65}$]
P[TFE$_{35}$-co-PDD$_{65}$]

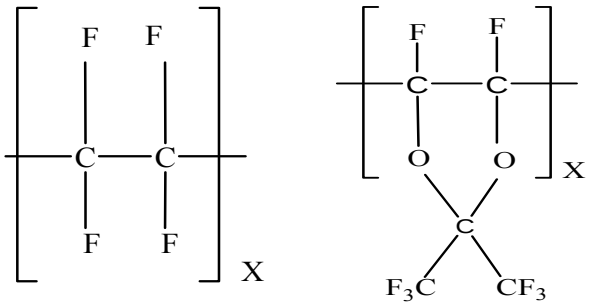

Recent studies revealed that is possible to dissolve these fluoropolymers in halogenated solvents but only at very high temperatures (T>300°C), [64, 67] e.g. PTFE remains insoluble until its melting point is reached. To dissolve most of the other fluoropolymers higher pressures and temperatures are required.

Poly (vinylidene fluoride) (PVDF) was first reported to be completely insoluble [54] in $scCO_2$, but it was found out that this was due to some high degree of crosslinked material in the sample. Moreover very high molecular weight PVDF (M_w=530 kg/mol) was chosen for the measurement. For a non crosslinked sample with a M_w=200 kg/mol, 130°C and 1600bar were needed to ensure complete solubilization in $scCO_2$. Increasing temperature from 135 to 215°C resulted only in minor decreases of the cloud point pressure from 1700 to 1600 bar. [32] Below 130°C PVDF crystallized and became insoluble in $scCO_2$. On the contrary poly (vinyl fluoride) does not dissolve in CO_2 even at temperatures as high as 300°C and pressures up to 2750 bar. The extreme conditions needed to dissolve these polymers are explained by the very strong interactions of the polar segments which are also pointed out in the high melting temperatures ~170°C for

PVDF and ~185°C for PVF. For solubilization of crystalline compounds the heat of fusion must be overcomed, dissolution of rather nonpolar polymers in a weakly interacting solvent is generally not possible below the melting temperature. Introduction of a co-monomer into the polymeric backbone of PVDF can however lower the critical solution curve dramatically as illustrated in Figure 2.11. Already pressures of 400-1000 bars are sufficient to dissolve the copolymer of PVDF with 22 mol% of hexafluoropropylene units P(VDF-*co*-HFP_{22}).[68, 69-70, 77]

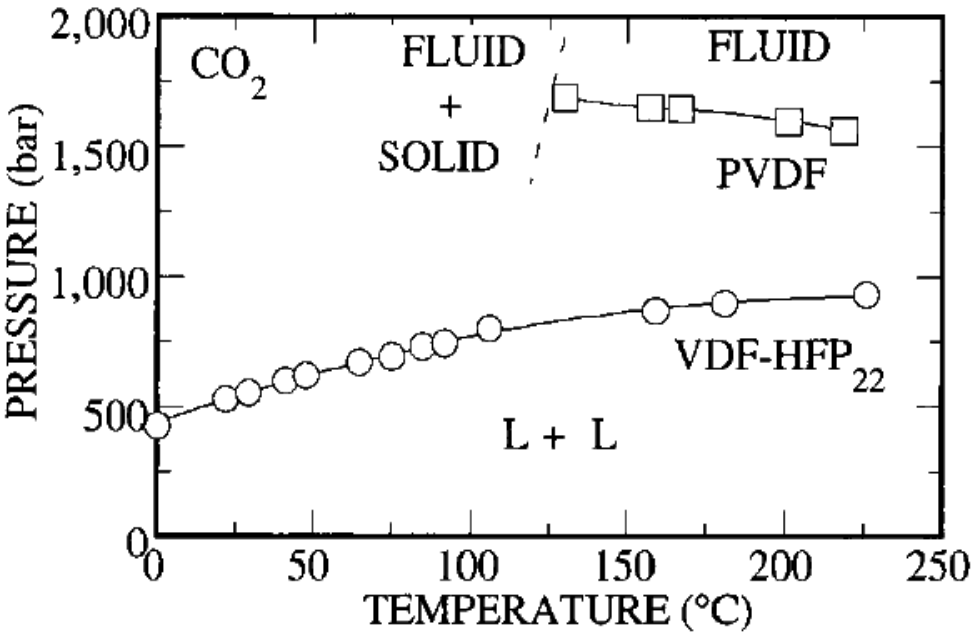

Figure 2.11: *Cloud point behavior of poly(vinylidene fluoride) (PVDF, M_w=200 kg/mol) and of poly (vinylidene fluoride-co-22mol% hexafluoropropylene) P [VDF-co-HFP_{22}] M_w=85 kg/mol) in a ~ 5wt% solution.*[75]

2.6 Effect of co-solvent on the cloud point of polymers in $scCO_2$:

A co-solvent can greatly enhance polymer solubility in a given solvent due to several factors. If the solvent is highly expanded, the addition of a dense liquid cosolvent reduces the free volume difference between the polymer and the solvent resulting in a reduction in the pressure needed to obtain a single phase.[72] If the cosolvent provides favourable physical interactions, such as polar interactions, the region of miscibility should expand more than expected from just a density effect.[73] In the case where a polar cosolvent is used with a polar polymer, cloud-points monotonically decrease in pressure and temperature as long as the cosolvent does not form a complex with the

polar repeat units in the polymer chain.[72,73,74] The cloud point will decrease much more dramatically if the polar cosolvent can form a complex with the polymer since the interaction energy of complex formation, such as hydrogen bonding, is typically an order of magnitude greater than expected from dispersion or polar interactions. Decoupling effect of a cosolvent from that of hydrostatic pressure is sometimes complicated since increasing the system pressure also reduces the free volume difference between the solvent and the polymer and increases the probability of interaction between polymer, solvent, and cosolvent segments in solution.[76] McHugh et al[76] have investigated the phase behavior of semicrystalline polyester resin comprising 53.4 mol % adipic acid and 46.6 mol % 1,4-cyclohexanedimethanol (M_w= 5960 g mol^{-1}, and M_n =2060 g mol^{-1}) in sc CO_2 with and without cosolvents . (cf. Figure 2.12).

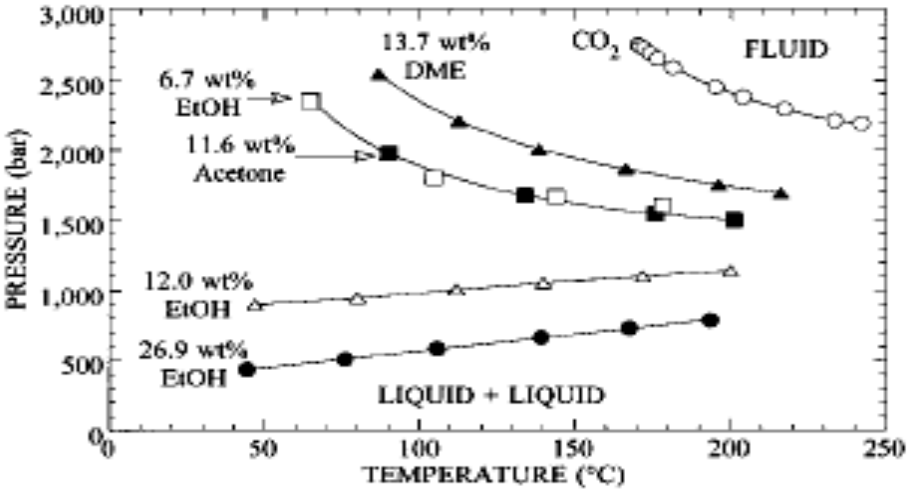

Figure 2.12: *Impact of co-solvent on the phase behavior of polyester of 53.4 mol % adipic acid and 46.6 mol % 1, 4-cyclohexanedimethanol (Mw= 5960 g.mol^{-1} and M_n =2060 g.mol^{-1}) in scCO_2 with and without cosolvents.* [76]

Experimentally, acetone was observed to be a better cosolvent than dimethyl ether (DME), where acetone cloud-point curve is at lower pressures and temperatures for the same concentration of cosolvent. The author has argued the higher cosolvency of acetone due to dipole moment exerted by acetone rather than DME. In contrast, the shift in the cloud-point curve with only 6.7 wt % ethanol was equal to that observed with 11.6 wt % acetone added to the solution. The location of the polyester/CO_2/6.7 wt % ethanol cloud-point curve was a result of hydrogen bonding between the hydroxyl group on the ethanol and ester groups in the polymer, because the dipole moment of ethanol is lower than that of acetone and both cosolvents should have similar densities. The cloud-

point curve shifted to even lower temperatures and pressures when 12.0 and 26.9 wt % ethanol was added to the solution.

Other authors reported[75] on the cloud point data for the system of poly(methylmethacrylate) PMMA-CO_2-methyl methacrylate (MMA) in the temperature range of 26 to 250°C,and at pressure as high as 2500 bar. With cosolvent concentrations of 10.4, 28.9, and 48.4 wt%; PMMA does not dissolve in pure CO_2 up to 255°C and 2550 bar; as shown in Figure 2.13. The cloud point curve for the PMMA-CO_2-10.4 wt% MMA system exhibits a negative slope that reaches 2500 bar at105°C. On other hand, with 28.9 wt% MMA the cloud point curve remains relatively flat at ~900 bars for temperature between 25 and 170°C. With 48.4 wt% MMA the cloud point curve exhibits a positive slope that extends to 20°C and ~ 100 bars.

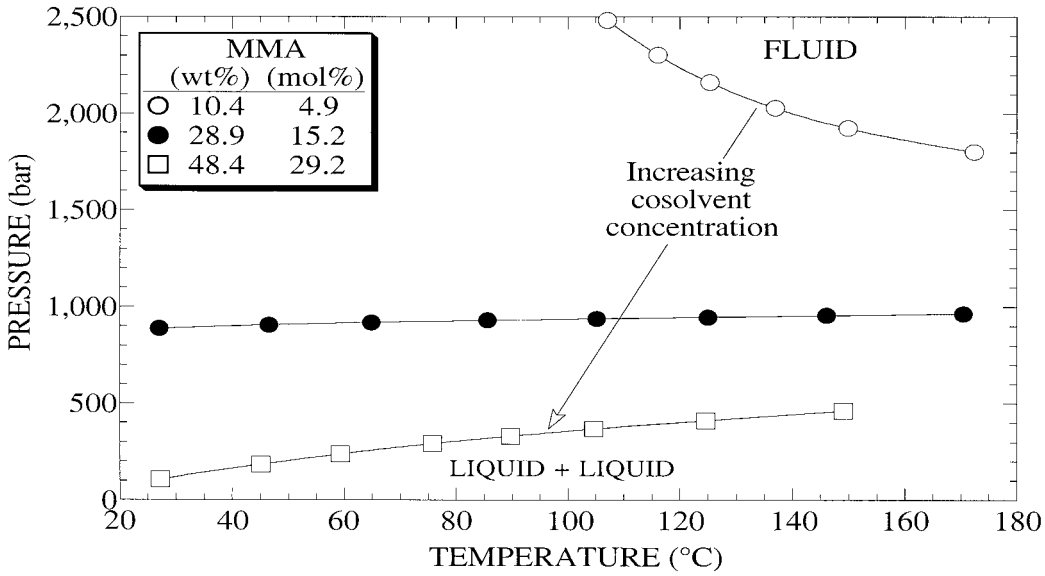

Figure 2.13 *Experimental cloud point curves for the PMMA-MMA-CO_2 system with different MMA concentrations. The concentration of PMMA is about 5.0 wt %.* [75]

2.7 Crystallization technique from $scCO_2$.

Crystallization from supercritical fluid is similar to conventional batch crystallization, where the crystals are obtained by slowly cooling down a saturated solution according to an optimum cooling protocol. This allows the desired supersaturation level to be maintained, as well as a constant crystal growth rate. If the solvent is a SCF; high pressure is required: therefore, not only temperature but also pressure can be used to trigger nucleation and growth of the crystals. The interest in crystallization from $scCO_2$ comes from a number of attractive features: the possibility of tuning crystal size

distribution [77], producing large crystals, [78] and of purifying solid materials from impurities. [79, 80]

For polymers, the crystallization from dense fluids offers a new pathway for polymer separation and purification, polymer modification, or formation of microstructures with unique morphologies. The rate by which the solid-fluid boundary is approached, degree undercooling that is imposed, as well as the pressure and the fluids influences the outcome and can be used as tuning parameter.

Crystallization from $scCO_2$ can be carried out in a simple apparatus, especially a stirred pressure resistant vessel. First the supercritical solution is prepared by loading inside the stirred autoclave with the proper amounts of SCF and the compound of interest. Then, the stirrer is switched off, and the temperature and/or pressure of the solution are varied according to the protocol adopted for the process until the crystals are formed.

Several studies [81] have been reported on the crystallization of poly (bisphenol A carbonate) ($M_{w=}$ 4.4 x 10^{4} g/mol) being synthesized in supercritical carbon dioxide. Where, others show that carbon dioxide as a dispersing media can induce a degree of crystallinity inside polymer beads. Moreover, temperature and pressure as well as time of treatment to $scCO_2$ can significantly affect the crystallization of polycarbonate. Forbes et al [82] have investigated the plasticizing and the thermal effects of CO_2 on the mechanism of crystallization and particle agglomeration of poly (L-Lactide) (PLLA). Other authors [82-86] have reported on the phase behavior of polyethylene and other polyolefins in n-alkanes + carbon dioxide fluid mixtures. Majority of these studies have been on liquid-liquid (L+L) phase transition. The L+L phase transition of polyolefins in these fluids displays lower critical solution (LCST) type behavior. In the presence of carbon dioxide the phase boundary shifts to higher pressures and the character of system gradually transform to an upper critical solution (UCST) type behavior. Even though limited in scope, several studies have also been carried out on the fluid-solid (F+S) phase transition in polymers solutions in pressurized or supercritical fluids. [85-86, 87] these studies show that the fluid-solid phase boundary is usually confined to a narrow temperature range (~5°C).

Handa et al. reported on the effect of CO_2 on the crystallization kinetics of syndiotactic polystyrene (sPS).[88,89] Where they measured T_m of sPS under several elevated pressures of CO_2 gas and showed that the crystallization rates of the sPS-CO_2 mixture were different from that of the neat sPS. Furthermore, they showed the presence of CO_2 induced morphological modifications of the sPS crystal. [90]Mizoguchi et al. reported that crystallization of polyethylene terephethalate (PET) occurred at a temperature below the T_g, of neat PET when it was crystallized under CO_2 and its isothermal crystallization rate increased with CO_2 content at a temperature over the T_g. [90, 91] The PET samples were crystallized under the pressurized CO_2 in an autoclave for a certain period of time and the crystallinity of the treated polymers were estimated from infra-red spectra and density measurements. The crystallization rate was obtained by changing the processing time in the autoclave. Kalospiros et al. has estimated crystallization rate of polymer-CO_2 system theoretically, assuming that the crystallization kinetic rate depend s only on the local degree of swelling inside the amorphous regions and the degrees of crystallinity itself, and they compared experimental data with the model predictions successfully.[91](cf. figure 2.14)

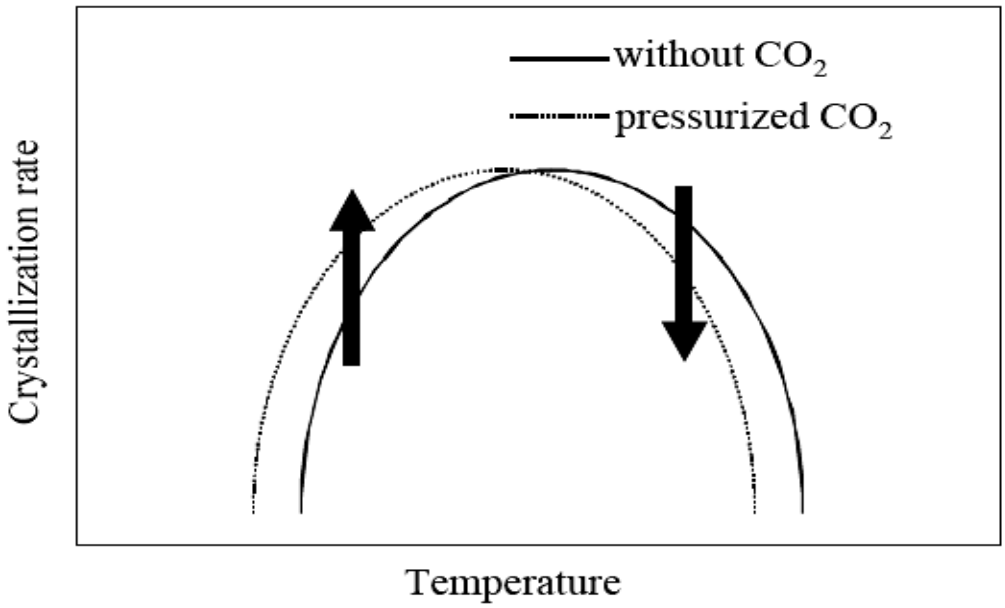

Figure 2.14: *Correlation diagram between rates of crystallization of polymer with temperature in presence and absence of carbon dioxide.* [91]

2.8 References:

[1] Jessop P. G., Ikariya T. and Noyori R.; Chem. Rev., 1999, **99**, 475.

[2] Stewart I. H. and Derouane E. G.; Curr. Top. Catal. 1999, **2**, 17.

[3] Baiker A.; Chem. Rev., 1999**, 99**, 453.

[4] Green Chemical Syntheses and Processes: Tester J. W., Danheiser R. L., Weinstein R. D., Renslo A., Taylor J. D. and Steinfeld I. J.; ACS Symp. Ser., 2000, **767**, 270.

[5] Jessop P. G. and Leitner W.; Chemical Synthesis using Supercritical fluids, Wiley-VCH, Weinheim, **1999.**

[6] Clifford A. A.; Fundamentals of Supercritical Fluids, Oxford Uni. press, oxford, **1998**.

[7] Ehrlich P., Mortimer G. A.; Adv. Polym. Sci. 1970, **7**, 386.

[8] Kirby C., McHugh M. A.; Chem. Rev., 1999, **99**, No. 2, 565-602.

[9] Prausnitz J. M., Lichtenthaler R.N., "Molecular thermodynamic of fluid phase equilibria, 2 nd ed.; Prentice Hall: Englewood Cliffs, NJ, **1986**.

[10] Patterson D.; Polym. Eng. Sci. 1982, **22**, 64.

[11] Kurnik, R. T.; Reid, R. C.; Fluid Phase Equilib. 1982, **8**, 93.

[12] Lee L. L.; Molecular Thermodynamics of Nonideal Fluids; Butterworth Publishers: Stoneham, MA, **1988**.

[13] McHugh M. A., Krukonis V.; J. Supercritical Fluid Extraction: Principles and Practice, 2nd ed.; Butterworth Publishers: Stoneham, MA, 1994.

[14] Rowlinson J. S., Swinton F. L.; Liquids and Liquid Mixtures, 3rd Ed. Butterworth Publishers: Boston, **1982**.

[15] Freeman P. I., Rowlinson J. S.; Polymer 1960, **1**, 20.

[16] Allen B., Baker C. H.; Polymer 1965, **6**, 181.

[17] Baker C. H., Clemson C. S., Allen G.; Polymer 1966, **1**, 525.

[18] Zeman L., Biros J., Delmas G., Patterson D.; J. Phys. Chem.1972, **76**, 1206.

[19] Zeman L., and Patterson D. J.; J. Phys. Chem. 1972, **76**, 1214.

[20] Saeki S., Konno S., Kuwahara N., Nakata M., Kaneko M.; Macromolecules, 1974, **7**, 521.

[21] Cowie J. M. G., McEwen I. J.; Macromolecules 1974, **7**, 291.

[22] Koningsveld R., and Staverman A. J. ; J. Polym. Sci.: Part C 1967, **16**, 1775.

[23] De Loos T. W., Lichtenthaler R. N., Diepen G. A.; Macromolecules, 1983, **16**, 117.

[24] De Loos T. W., Poot W., Diepen G. A.; Macromolecules 1983, **16**, 111.

[25] Koningsveld R., Staverman A. J.; J. Polym. Sci: Part A-2 1968, **6**, 305.

[26] Koningsveld R., Staverman A. J.; J. Polym. Sci: Part A-2 1968, **6**, 325.

[27] Koningsveld R., Staverman A. J.; J. Polym. Sci: Part A-2 1968, **6**, 349.

[28] Solc K.; Macromolecules 1970, **3**, 665.

[29] Irani C. A., Cozewith C.; J. Appl. Polym. Sci. 1986, **31**, 1879.

[30] Lee S.-H., LoStracco M. A., Hasch B. M., McHugh M. A.; J.Phys. Chem. 1994, **98,** 4055.

[31] De Loos Th. W., Poot W., Lichtenthaler R. N.; J. Supercrit.Fluids 1995, **8**, 282.

[32] Hyatt J.A.; J. Org. Chem. 1984, **49**, 5097.

[33] Walsh J.M., Ikonomou G.D., Donohue M.D.; Fluid Phase Equilib.1987, **33**, 295.

[34] Kazarian S. G., Vincent M. F., Bright F. V., Liotta C. L., Eckert C. A.; J. Am. Chem. Soc. 1996, **118**, 1729.

[35] O'Shea K. E., Kirmse K. M., Fox M. A., Johnston K. P.; J. Phys.Chem. 1991, **95**, 7863.

[36] Yilgor I., McGrath J. E., Krukonis V. J.; J. Polym. Bul. 1984, **12**, 499.

[37] Krukonis V. J., J. Polym. News 1985, **11**, 7.

[38] Hoefling T. A., Enick R. M., Beckman E. J.; J. Phys. Chem 1991, **95**, 7127.

[39] Hoefling T. A., Stofesky D., Reid M., Beckman E. J., Enick R. M.; J. Supercrit. fluids 1992, **5**, 237.

[40] Dris G., Barton S. W.; Polym. Mater. Sci. Eng. 1996, **74**, 226.

[41] Zhao X.; Watkins, R.; Barton, S. W.; J. Appl. Polym. Sci. 1995, **55**, 773.

[42] Xiang, Y.; Kiran, E. ; Polymer 1995, **36**, 4817.

[43] Rindfleisch F., DiNoia T. P., McHugh M. A ; J. Phys. Chem 1996, **100**, 15581.

[44] Gregg C. J., Stein F. P., Radosz M.; Macromolecules 1994, **27,** 4972.

[45] Gregg C. J., Stein F. P., Radosz M. ; Macromolecules 1994, **27**, 4981.

[46] Lora M., Lim J. S., McHugh M. A. ; J. Phys. Chem. 1999, **103**, 2818-2822.

[47] Luna-Barcenas G.; Mawson S., Takishima S., DeSimone J.M., Sanchez I.C., and Johnston K. P.; Fluid Phase Equilib. 1998, **146**, 325.

[48] Hsiao Y.-L., Maury E. E., DeSimone J. M., Mawson S., Johnston K. P.; Macromolecules, 1995, **28**, 8159.

[49] DiNoia T. P., McHugh M. A., Cocchiaro J. E., Morris J. B.; Waste Manage. 1997, **17**, 151.

[50] Mertdogan C. A., Byun H.-S., McHugh M. A., Tuminello W. H.; Macromolecules, 1996, **29**, 6548.

[51] Mertdogan C. A., DiNoia T. P., McHugh M. A.; Macromolecules 1997, **30**, 7511.

[52] DiNoia T. P., Conway S. E., Lim J. S., McHugh M. A.; Macromolecs, 2000, **33**, 6321- 6329.

[53] Mawson S., Johnston K. P., Combes J. R., DeSimone J. M.; Macromolecules, 1995, **28**, 3182.

[54] Rindfleisch F., DiNoia T.P., McHugh M.A.; J. Phys. Chem.1996, **100**, 15581.

[55] Lora M., Lim J.S., McHugh M.A.; J. Phys. Chem. B 1999, **103**, 2818

[56] O`Neill M.L., Cao Q., Fang M., Johnston K.P., Wilkinson S.P., Smith C.D., Kerschner J.L., Jureller S.H.; Ind. Eng. Chem. Res.1998, **37**, 3067.

[57] Baradie B., Shoichet M. S., Shen Z., McHugh Mark A., Hong L., Wang Y., Johnson J. K., Beckman E. J., and Enick R. M.; Macromolecules, 2004, **37(20)**, 7799-7807**.**

[58] Hachisuka H., Sato,T. T. I., Tsujita Y., Takizawa A., Kinoshita T.; Polymer J. 1990, **22**, 77.

[59] Kazarian S.G., Vincent M.F., Bright F.V., Liotta C.L., Eckert C.A.; J. Am. Chem. Soc.1996, **118**, 1729.

[60] O´Neill M.L.; Ind. Eng. Chem. Res. 1998, **37**, 3067.

[61] Meredith J.C., Johnston K.P., Seminario J.M., Kazarian S.G., Eckert C.A.; J. Phys.Chem. 1996, **100**, 10837.

[62] Huang Z., Shi C., Xu J., Kilic S., Enick R.M., Beckman E.J.; Macromolecules, 2000, **33,** 5437.

[63] Shi C., Huang Z., Kilic S., Xu J., Enick R.M., Beckman E.J., Carr A.J., Mendelez R.E., Hamilton A.D.; Science 1999, **286,** 1540.

[64] Smith P., Gardner K. H.; Macromolecules 1987, **18**, 1222.

[65] McCain G. H., Covitch, M. J.; J. Electrochem. Soc. 1984, **31**, 1350.

[66] Tuminello W. H., Dee G. T.; Macromolecules 1994, **27**, 669.

[67] Tuminello W.H., Dee G.T.; Macromolecules 1994, **27,** 912.

[68] Hoefling T.A., Stoefsky D., Reid M., Beckman E.J., Enick R.M.; J. Supercrit .fluids 1992, **5,** 237.

[69] Zhao X., Watkins R., Barton S.W.; J. Appl. Polym. Sci. 1995, **55**, 773.

[70] Krukonis V.J.; J. Polym. News 1985, **11**, 7.

[71] Yilgor I.., McGrath J.E., Krukonis V.J.; J. Polym. Bull.1984, **12**, 499.

[72] Cowie J. M. G., McEwen I. J.; J. Chem. Soc., Faraday Trans.1974, **70**, 171.

[73] Wolf B. A., Blaum G.; Polym. Sci.: Part B: Polym. Phys. 1975, **13,** 1115.

[74] Hasch B. M., Meilchen M. A., Lee, S.-H., McHugh M. A.; J. Polym. Sci.:

Part B, Polym. Phys. Ed. 1993, **31**, 429.

[75] LoStracco M. A., Lee S.-H., McHugh M. A.; Polymer 1994, **35,** 3272.

[76] Conway S. E., Lim J. S., McHugh M.A., Wang J. D., and Mandel F.S.; J. App. Polym. Sci. 2001, **81**, 2642–2648 .

[77] Tavana A., Randolph A.. D.; AIChE J. 1989, **35**, 1625-1630.

[78] C. Y. Tai, C. –S Cheng, AIChE J. 1995, **41**, 2227-2236.

[79] Freund H., Steiner R.; High pressure chemical engineering, P. R. von Rohr, C. Trepp (Eds), Elsevier, Amesterdam, 1996, **211-216**.

[80] Shlichta P.J.; U.S. Patent 4,512, 846, April 23 rd, 1985.

[81] Gross S. M., Roberts G. W., Kiserow D. J., and Desimone J. M; Macromolecules 2000, **33**, 40-45.

[82] Shekunov B. Y., Edwards A. D. and Forbes R.; Proceeding of the 6th International proceeding of SF fluids, Bordeaux, France, 2003.

[83] Upper G., Becke D. L., Zhang W. and Kiran E.; Proceeding of the 6th international proceeding of SF fluids, Bordeaux, France, 2003.

[84] Kiran E.; Supercritical fluids. Fundamental and application, Eds. E.Kiran, J. M. H. Levelt Sengers, Kluwer Academics Publishers, Dordrecht, 1994, pp. **541-588**.

[85] Kiran E., Liu K.; Korean J. Chem. Eng. 2002, **19**, p.153.

[86] Chen K., Adidharma H., Radosz M.; Ind. Eng. Chem. Res. 2000, **39**, 3069.

[87] Weidner E., Weismet V.; 5th conf. on SCF and their application, 1999, **521**.

[88] Handa Y. P., Zhang Z., and Wong B.; Macromolecules, 1997, **30**, 8499.

[89] Zhang Z., and Handa Y. P.; Macromolecules1997, **30**, 8505.

[90] Mizoguchi K., Hirose T., Naito Y., and Kamiya Y.; Polymer 1987, **28**, 1298.

[91] Kalospiros N. S., Astarita G., and Paulaitis M. E.; Chem. Eng. Sci., 1993, **48**, 23.

CHAPTER 3

Precipitation/crystallization behaviour for polyvinylidene fluoride in $scCO_2$*.

3.1 Introduction.

In recent years supercritical carbon dioxide ($scCO_2$) has generated much interest in the polymer community as an attractive alternative medium for polymerizations process.[1] From an (i) industrial perspective CO_2 is inexpensive, non-toxic, non-flammable, and readily available in high purity from a variety of sources. In addition since CO_2 is ambient gas: polymers can be isolated from the reaction mixture by simple depressurization process, resulting in a dry polymer product. This eliminates the necessity for the energy-intensive drying procedures often required in polymer manufacture. And (ii) from a chemical perspective, CO_2 is relatively inert and does not lead to chain transfer in radical based polymerizations.[2,3] Supercritical CO_2 also plasticizes glassy polymers; this makes it easier to remove impurities or residual monomer from the polymer product and can result in increased polymerization rates by the enhanced diffusion of monomer into the growing polymer. [1, 2, 4]

The poor solubility of most polymers and the high solubility of most vinyl monomers in $scCO_2$ have ensured that studies of precipitation and dispersion polymerizations [1] have dominated the literature.

*"Impact of vinylidene fluoride on the solubility and crystallization of PVDF from $scCO_2$"Fahmy S., Beginn U. Ziener U., Moeller M., in preparation.

Poly(vinylidene fluoride) (PVDF) possesses good thermal, chemical, and environmental stabilities and has a variety of industrial applications spanning from pipes, valves, coatings, films to cables as well as being an acceptable biomaterial.[5] In industry the conventional methods for PVDF production are aqueous suspension or emulsion polymerizations. Both of these generate large quantities of wastewater and require substantial quantities of energy to dry the polymer product. [6] There are many publications on the investigation of free radical (co)-polymerization of VDF monomers by aqueous emulsion and suspension techniques. [7-11]
However, fluoropolymers solubility in CO_2 depends on the number of fluorinated side groups and on the molecular weight of the side groups relative to the molecular weight of the hydrocarbon main chain. It has also been suggested that CO_2 either forms a weak complex or preferentially clusters near the fluorine atom of the C-F bonds that are more polar than C-H bonds. [12-17, 19] These studies establish that fluorinating a polymer enhances its solubility several fold in $scCO_2$, but that fluorination alone does not ensure that the polymer will remain soluble in CO_2 at temperatures below 100 °C. [18]

Conventionally, PVDF solubility in highly polar solvents like DMF or DMA is ensured by alternating CH_2 and CF_2 groups. PVDF can be utilized in a temperature range between –40 and +150°C. Most vinylidene units join head to tail, normally only 3.5-6% of the monomer units are linked head to head (CF_2 to CF_2)[20] and tail to tail (CH_2 to CH_2), respectively. The percentage of these missinsertions is increased at elevated polymerization temperature. [21] Crystallinity is between 40-60% with three polymorphs.

Despite of the industrial advantageous of PVDF, McHugh et al. [22] reported that PVDF with a weight average molecular weight (M_w) of 530.000 g/mol did not dissolve in supercritical carbon dioxide up to 300°C and 2750 bar. Although the lack of PVDF solubility in CO_2 was likely due to the presence of highly crosslinked material in the sample that originated from the polymerization process.

Relatively limited data have been reported so far for the solubility of PVDF/CO_2 systems.[23] For a PVDF with Mw = 200 kg/mol a minimum temperature of 130°C at a pressure of 1700 bar was needed to ensure complete solubilization in CO_2. Increasing temperature from 135°C to 215 °C resulted in minor decrease of the cloud point pressure from 1700 to 1600 bar. Below 130°C PVDF was reported to be insoluble in

$scCO_2$ because of crystallization [24] below which it is not possible to obtain a single phase regardless of the pressure. Below crystallization temperature, where turbidity of the solution makes it difficult to determine if the second phase contains solid crystals. However, it was possible to deduce whether crystals are present by measuring the temperature needed to obtain a single phase when the solution is isobarically heated at fixed rate.

In another aspect, during any polymerisation process, polymer is formed in the presence of its own monomer. However, during the course of reaction, the ratio of polymer to monomer decreases continuously, resulting in a distinct change of the solvent quality of the mixture. So that, monomer could be considered as co-solvent that might enhance the solubility of mother polymer in $scCO_2$ and thus expand the single phase region. [18, 26] In addition to favourable interaction of the polymer and the monomer, a liquid co-solvent may increase the density of the CO_2-rich phase and in the meantime reduce the differences in free volume between the polymer and the solvent mixture.

Kirby et al. [24] has demonstrated for a similar like system i.e. PMMA/MMA/CO_2 ternary mixture. Where, they reported PMMA is not soluble in pure CO_2 to temperatures of 255°C and pressures as high as 2550 bar. On another hand, McHugh et al. [26] has investigated the impact of methyl methacrylate (MMA) cosolvent on the solubility of poly methylmethacrylate (PMMA) in supercritical CO_2. Since PMMA is a polar polymer, the addition of polar MMA to CO_2 provides enhanced polar interactions between PMMA and the mixed solvent that is expected to lead to a decrease in cloud-point temperature and pressure. [17,27-28]While addition of 28.9 wt. % MMA in solution the cloud-point pressure remains virtually constant at 900 bar over a temperature range of 20 to 170°C. If 48.4 wt.% MMA is added to the solution, the cloud-point curve exhibits LCST-type phase behavior with a positive slope at very low pressures.

In this work further detailed work on the solubility of PVDF in $scCO_2$ obtained by isothermal depressurization as well as isobaric cooling experiments were investigated so far. The morphology and degree of crystallization of the segregated polymer are examined. Moreover, the impact of free monomer VDF on the precipitation/crystallization boundaries of PVDF in supercritical carbon dioxide has been measured to study its consequences role for polymerisation reactions of VDF in $scCO_2$.

3.2 Experimental Section:

3.2.1 Materials

The polyvinylidene fluoride samples; Solef 1010, was supported from Solvay, Brussels, Belgium and termed as **PVDF 226**. Kynar 741 was donated from Elf Atochem France, and named as **PVDF 323**. Vinylidene fluoride gas was obtained from Solvay Solexis, Italy. Molecular characterizations of the polymers are summarised in Table 3.1. The two polymers were used as received without further modification. Carbon dioxide SFE grade (5.5) was provided from (Linde AG) and used without further purification.

Table 3.1: *Molecular and physical characteristics of PVDF samples used in this study.*

Polymer	Mn[a] [Kg/mol]	M_w/M_n [Kg/mol]	Tm (°C)	ΔH_m (J/g) (2 run)	Powder density (mg/ml)[c]	Head/ head fraction %	Degree of crystallinity %[b]
PVDF 323	98.00	3.29	168	56.98	0.41	5.5±2	55±5
PVDF 226	72.00	3.14	164.3	52.84	0.40	3.5±2	53±5

[a] GPC values against PMMA standards
[b] Calculated from DSC value
[c] Measured by weighing out samples in fixed volume.

3.2.2 Methods:

3.2.2.1 Differential Scanning Calorimetry (DSC):

Thermal transitions as well as the degree of crystallinity of polyvinylidene fluoride were measured using a DSC 204 Phoenix unit (NETZSCH); the instrument was calibrated with ultra pure indium. All measurements were performed under a nitrogen atmosphere. For both untreated and treated (i.e. samples collected from high pressure autoclave after CO_2 treatment) PVDF samples the heating protocol was as follow; polymer sample (ca. 3-5 mg) were heated to 200°C with a heating rate of 10 K/min. Subsequently, samples were annealed at 200°C for 3 min. and followed by cooling to -60°C with a cooling rate of 10K/min. Degree of crystallinity was calculated according to ($crystallinity = \Delta H / 105$) with the implementation that 100% crystalline PVDF offers ΔH of 6.50 kJ per mol of repeating unit.

3.2.2.2 Size Exclusion Chromatography (SEC):

Size Exclusion Chromatography (SEC) was performed in DMF/0.1M LiBr as solvent with Waters μ-Styragel columns with pore sizes of 10^5, 10^4, 10^3 Å, a guard column. A Waters 410 differential refractometer was used as a detector. Narrow PMMA standards

(PSS) were used for calibration and molecular weights were evaluated by means of SEC-WIN version 2.54 from PSS.

3.2.2.3 Nuclear Magnetic resonance spectroscopy (^{13}C-NMR):

^{13}C-NMR spectra were performed in deutrated DMF (99.8%, Aldrich) on a Brucker DRX 400 spectrometer at 50 MHz, chemical shifts refer to the signal at 77ppm, ^{13}CNMR (δ in ppm, DMF: 32 ($-CF_2-CH_2-$), 116 ($-CH_2-\underline{CF_2}-\underline{CF_2}-CH_2-$) and 121 ($-CF_2-\underline{CH_2}-\underline{CH_2}-CF_2-$). Degree of head-head or tail-tail connections for PVDF 323 was calculated to be 5.5%. While, for PVDF 226 were approximately 3.5 %.

3.2.2.4 High pressure setup*:*

The experimental setup consists of a high-pressure variable volume autoclave (Sitec AG) with an internal working volume 5.6 mL (see Figure 3.1). Schematic diagram of the high pressure cell based on the designs of Buback/Franck and McHugh [26, 29] are illustrated. The high pressure view cell was equipped with (i) an electric heating jacket capable of working at temperature (25-200°C), (ii) two sapphire windows (1.0 cm thick, 3/4 inch in diameter) to monitor the reaction condition, (iii) a digital pressure gauge (KGT GmbH) with an accuracy of ± 1.0 bar, and (iv) a high pressure thermocouple (Sitec AG) to measure the internal autoclave temperature. The system temperature was controlled by a Pt 100 thermocouple (Temperature Product GmbH) with an accuracy of ± 0.1°C. For a purpose of changing pressure at constant composition; the view cell was connected to a thermostated manual spindle pump having a metallic O-ring (Sitec AG) that allowed increasing the internal volume of the system up to 13.6 mL. The system conditions were capable to operate at maximum pressure of 3.000 bar and a maximum temperature of 200°C. In order to determine the accurate volume and volume changes of variable volume autoclave; the real volume of the high pressure reactor was calculated by means of NIST (National Institute of Standards) equation for pure carbon dioxide at following temperatures of 30, 50, 75, 100, 150, 190°C at constant pressure of 200 bar. Figure 3.2 shows the correlation diagram between actual real volumes of autoclave versus measured volume calculated from NIST values.

3.2.2.4.1 Determination of cloud point for PVDF/CO_2 mixture (Isothermal Expansion):

In a typical experiment, pre-weight amount of solid polymer (ca. 0.3-0.7± 0.02 g) was inserted in the view cell prior to pressurization. Then CO_2 was purged at 3-6 bar to

remove any entrapped air right before conducting the experiment. Isothermal depressurization measurements were carried out generally by increasing the system volume using the spindle pump to a situation where a hazy (cloud point) solution can be distinguished in the cell. All cloud point determinations were repeated at least three times. Reproducibility was within an accuracy range of ± 1.0°C and ± 5-10 bar. Cloud points were determined either visually, as defined as the condition where the magnetic stirring bar could no longer be seen inside the cell [27] or photometrically. In the latter case a halogen lamp (Tech 5, GmbH) illuminated the view cell from the rear, while the front window was connected to an online diode array UV/VIS spectrometer (Zeiss AG). The cloud point pressure was obtained by extrapolation of the light intensity/pressure curve to zero transmission. Subsequent to the cloud point observations the view cell was cooled down to ambient temperature and followed by slow venting of carbon dioxide. As a selective example at 100°C (Figure 3.3), a depressurization rate was determined for pure CO_2 from the following equation $\log P = (2.5 \pm 0.01) - (0.017 \pm 0.0004)t \min^{-1}$. It's worthy to mention that slow depressurization is an essential parameter to avoid any morphological change during venting process. In a last step the polymer was collected from high pressure cell for further characterization by DSC and electron microscopy techniques.

3.2.2.4.2 Determination of cloud point for PVDF/VDF/CO_2 mixture (Isothermal expansion):

For the injection of gaseous monomers (VDF), the setup was modified by two high pressure needle valves connected to the spindle pump (Figure 3.1, named as V_1 and V_2 HIP GmbH). For accurate transferring of VDF, the spindle pump was first opened to maximum volume, and then the injection unit and the cell were carefully evacuated prior to adding monomer via valve V_2. Then vinylidene fluoride was charged to the variable volume autoclave through valve V_1 using a ¼" high pressure flexible tubing from a pre-weight storage tank that was originally placed on a balance (Ohaus I1L 210, precision: ±0.1 g). When the desired amount of monomer was transferred, valve V_1 was closed and the cells content was compressed by moving the piston of the spindle pump inward to the minimum volume position (i.e. 5.6 mL). Finally CO_2 was injected by a diaphragm membrane pump (Nova Swiss AG) and the system was allowed to equilibrate at the start temperature for about 30min., while solution was stirred continuously by means of a magnetic bar. The system was heated to the start temperature well above the cloud point (i.e. clear homogenous solution).

3.2.2.4.3 Determination of cloud point (isobaric cooling):

A clear solution was prepared above the cloud point value. Isobaric cooling experiments were operated by lowering the temperature at constant pressure. While the temperature decreased the pressure in the view cell was continuously adjusted by moving the piston of the spindle pump inward to compensate for pressure changes. Turbidity was observed in the vicinity of the cloud point (so-called crystallization) region. At the condition where 90% drop occurs for the transmitted light, temperature was recorded. Then the cell was heated again to acquire the clear solution. Approximately it took around 4-5°C to have clear PVDF in CO_2 solution again. In a second attempt, same policy was performed to determine the cloud point value followed by cooling…heating etc. The crystallization pressure, temperature average values were taken.

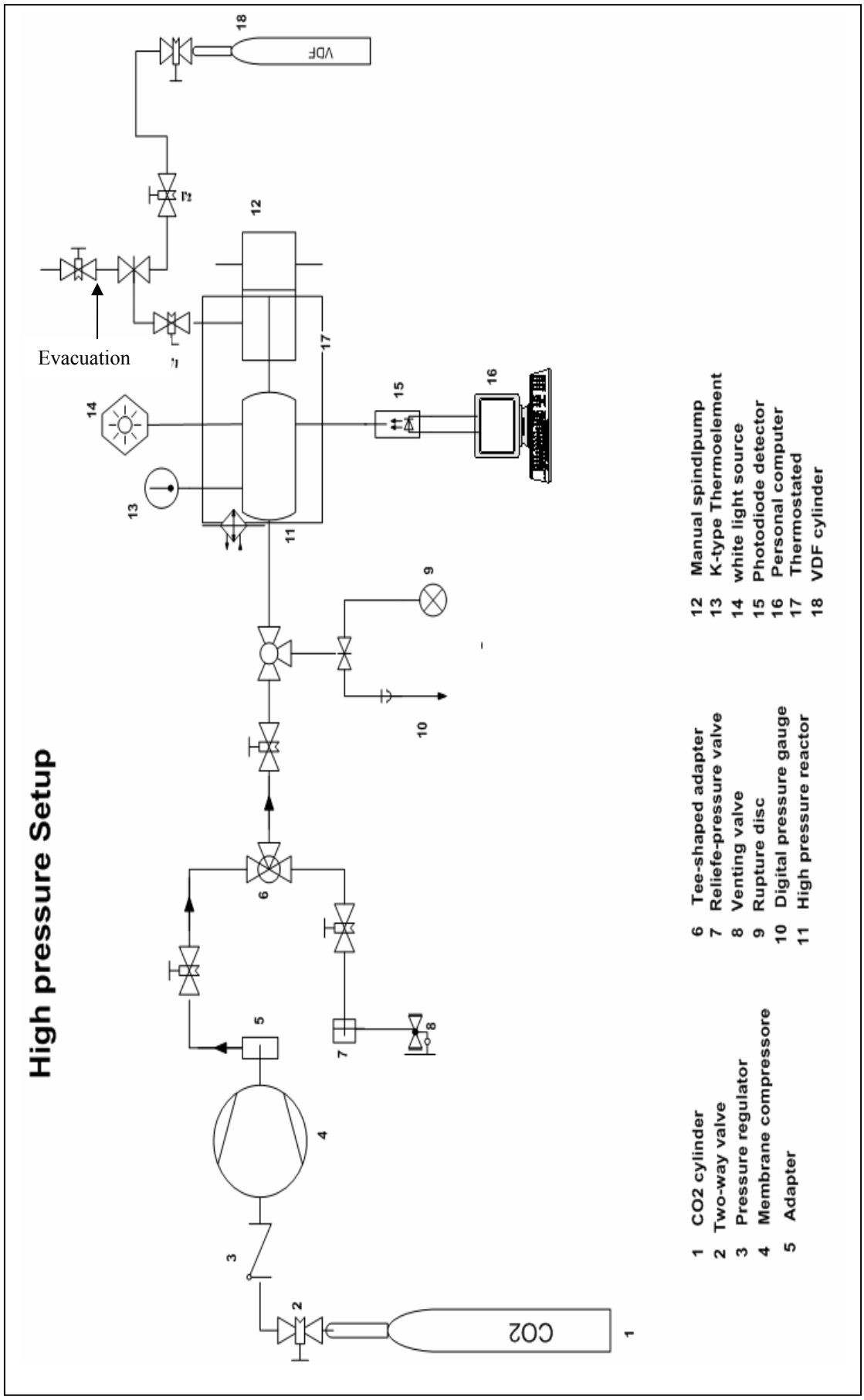
High pressure Setup
Evacuation
CO2
VDF
1 CO2 cylinder
2 Two-way valve
3 Pressure regulator
4 Membrane compressore
5 Adapter
6 Tee-shaped adapter
7 Reliefe-pressure valve
8 Venting valve
9 Rupture disc
10 Digital pressure gauge
11 High pressure reactor
12 Manual spindlpump
13 K-type Thermoelement
14 white light source
15 Photodiode detector
16 Personal computer
17 Thermostated
18 VDF cylinder

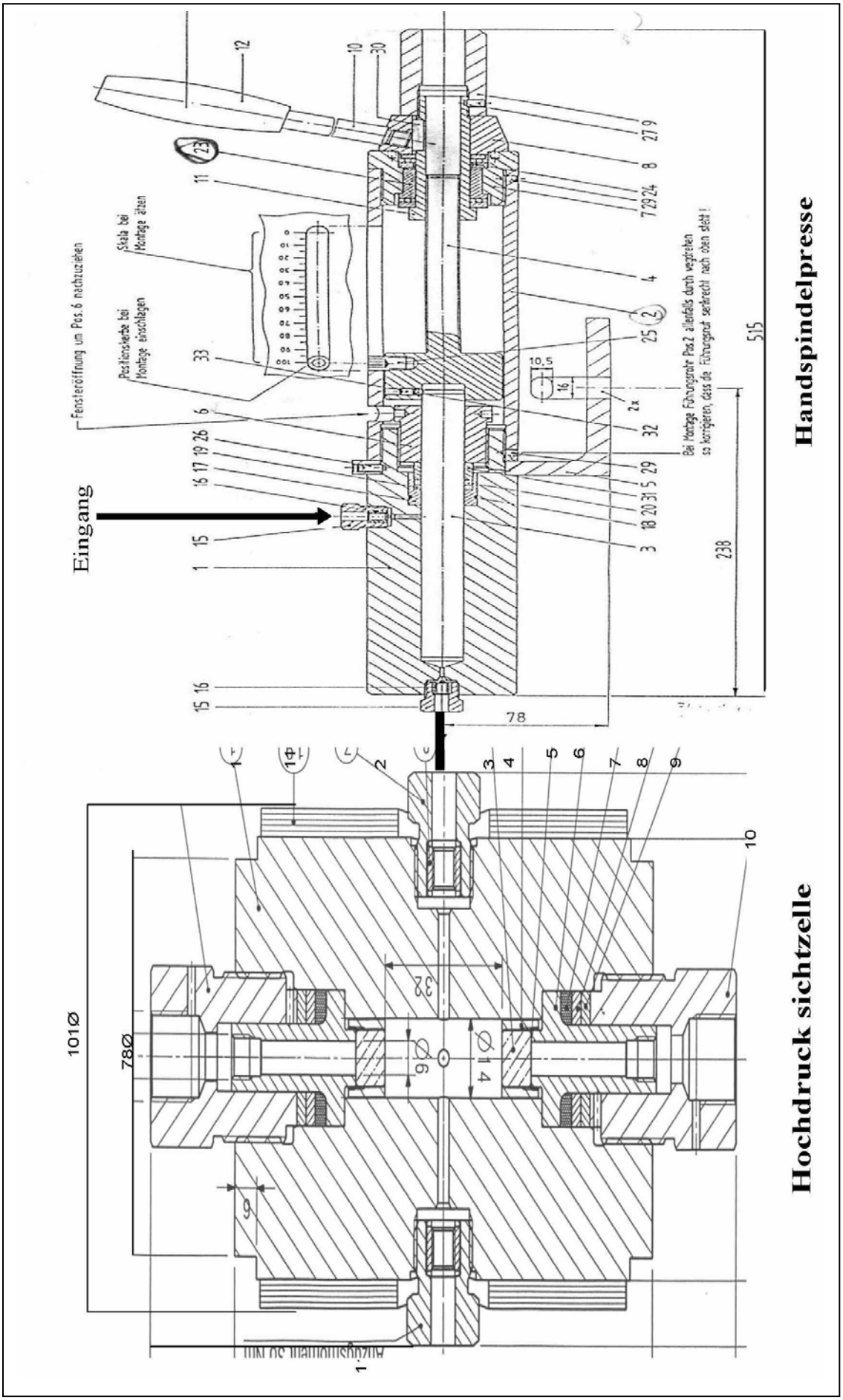
Eingang
Fensteröffnung um Pos. 6 nachzuziehen
Skala bei Montage ätzen
Positionsscheibe bei Montage einschlagen
Bei Montage Führungsnute Pos.2 allenfalls durch wegstreichen so korrigieren, dass die Führungsnut senkrecht nach oben steht !
515
238
78
Handspindelpresse
101Ø
78Ø
32
Ø 6
Ø 14
Hochdruck sichtzelle

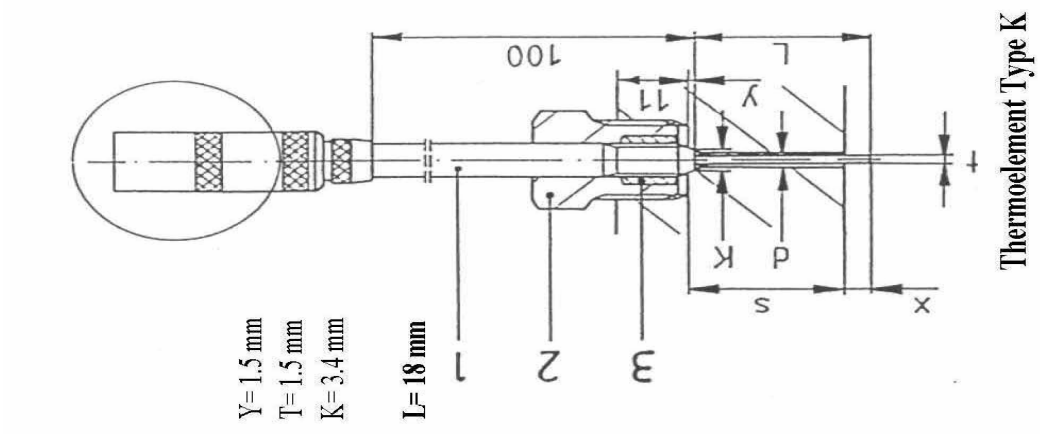

Hochdruck Sichtzelle (3000 bar & 400°C):

1- Zellenköper
2- Druckschraube ¼ HP
3- Schaluglas
4- Kappe
5- Dichtfolie
6- Fensterstopfen
7- Dichtung (Silber)
8- Dichtung (Graphit)
9- Ring
10- Druckschraube
11- Heizmental elektrisch

Thermoelement Type K ¼ HP (4000bar & 500°C):

1- Thermoelement Type K- Ni/Cr-Ni
2- Druckschraube ¼ HP
3- Druckring ¼ HP

Handspindelpresse (4000 bar & 220°C):

1- Zylinder
2- Führungsrohr
3- Spindel
4- Antriebsspindel
5- Befestigungsfuss
6- Druckschraube
7- Flanschbüschse
8- Ring
9- Abschlusskappe
10- Hebel
11- Gewindebuchse
12- Griff
13- Druckschraube
14- Druckring ¼ HP
15- Buchse
16- O-Ring Ø 14x2
17- Dichtung (PTFE)
18- Dichtung (Nylon)
19- Nadal Axialkugellager Ø 25x/42x30
20- Nadelrillen Kugellager Ø 25x/42x11
21- Arretierbolzen
22- Gewindestift mit Zapfen M6x12
23- Gewindestift mit Zapfen M6x6
24- Gewindestift mit Zapfen M5x8
25- Federkeil 8h9x25x7
26- Druckstück
27- Kugel Ø4
28- Gewindestift mit Ringschneide M5x6

Figure 3.1: *Schematic technical drawing of high pressure setup.*

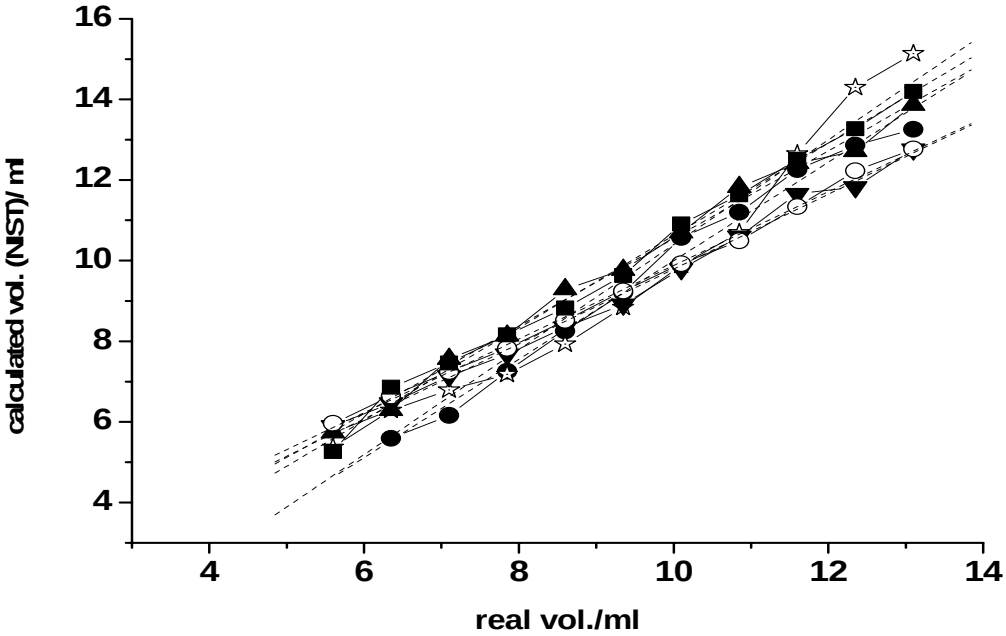

Figure 3.2: *Correlation diagram between real volumes of high pressure reactor filled with pure carbon dioxide at 30°C(●)50°C(*),75°C(▲),100°C(▼),150°C(○), and 190°C(■) at 250 bar vs. calculated volume from NIST equation at the same conditions. (—)Is the linear fitting for calculated volume from NIST equation.*

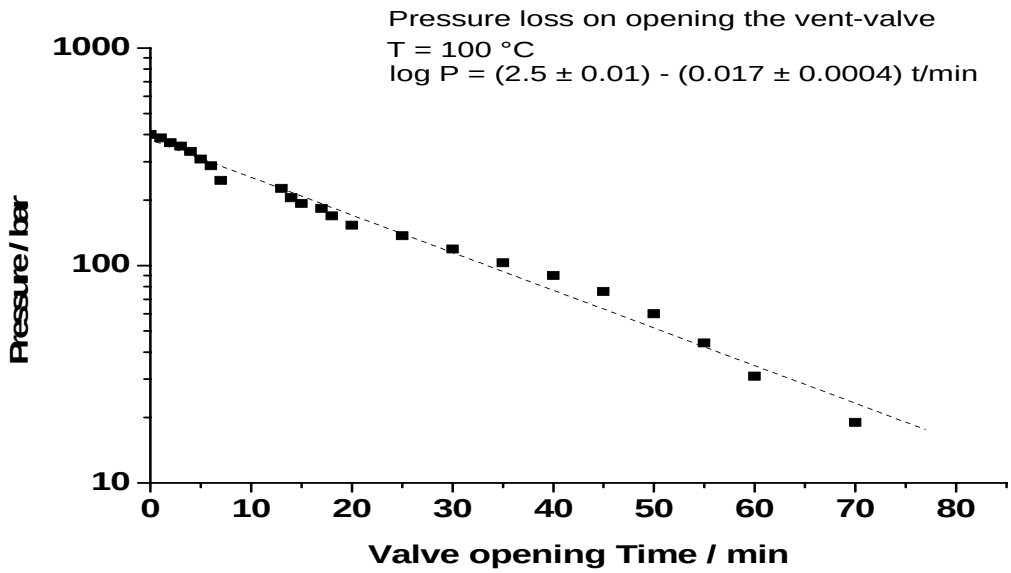

Figure 3.3*: Pressure/time profile of the variable volume autoclave upon opening venting valve.*

3. 3 Results and discussion:

In a variable volume view cell the mixture of PVDF and CO_2 was equilibrated under stirring condition. Starting temperature and pressure were always selected to obtain clear homogeneous solutions (i.e. at T= 160°C & P= 1800 bar). Cloud point lines separating the one homogenous phase region from the area of phase segregation measured by (i) isothermal depressurization in the high temperature range, and (ii) isobaric cooling in the low temperature regime were determined (cf. experimental part).

3.3.1 Phase behaviour diagram of PVDF/CO_2 binary mixture:

As a major drawback of dispersion polymerization of PVDF in $scCO_2$ is a bimodal molecular weight distribution of the resulting polymer. Where, aggregation of closely spaced polymer chains results in the formation of primary nuclei. Upon formation of primary polymer particles, polymerization proceeds in two phases; namely in the polymer-rich phase and in continuous monomer-CO_2 phase. It is assumed that, during this polymerization stage, the rate of mass transfer of monomer and CO_2 from continuous phase to the polymer particles is very fast so that the latter is kept at any time saturated with monomer and CO_2, subsequently the rate of polymerization, which depends on the sum of rate at both phases, becomes insignificant. Proposed precipitation way of PVDF may occur either by liquid-liquid demixing as illustrated in Figure 3.4, resulting in an amorphous precipitate or liquid-liquid demixing interfered with vitrification or by crystallization itself . Berghamns et al [25] have reported on precipitation of semicrystalline polymer with UCST behaviour from melt. Where, polymer is supposed to be monodisperse so that the binodal coincide with cloud point curve. For a formation of porous material by L+L demixing and vitrification; a polymer solution with composition X will demix into two coexisting solutions with composition $\phi_2^{'}$ and $\phi_2^{''}$ when cooled from T_1 to T_2. This demixing will proceed when cooling is continued and the concentrations of the coexisting phases $\phi_2^{'}$ and $\phi_2^{''}$ will follow the binodal on both side of X until T_g^d is reached and the concentrated phase (ϕ_2^d) vitrifies. In the initial stages of the demixing a phase-separated situation composed of many small domains of high and low polymer content will exist. At low polymer concentration, droplets of the concentrate will be dispersed in dilute matrix. At intermediate concentrations, interesting discontinuous structure can be generated such a multi-domain, two phase system has to evolve towards its final equilibrium situation: a system composed of only two layers with different polymer content. When, this non-

equilibrium stage is frozen by vitrification and the solvent is eliminated, a porous material is obtained.

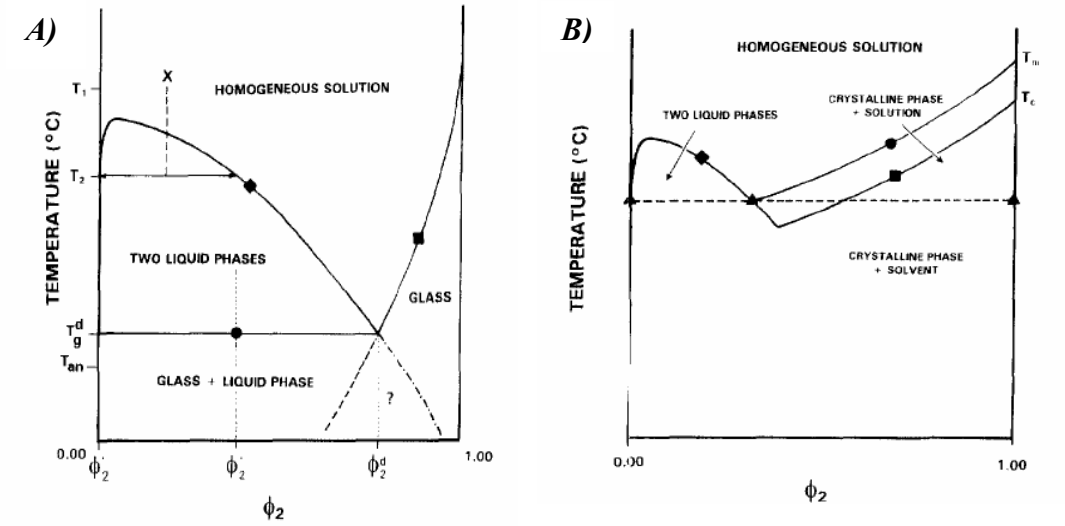

Figure 3.4: *Schematic representation of the interference between L+L demixing and (A) glass transition temperature; -♦-, binodal -■-, T_g-concentration relation; -●-,(B) Melting and crystallization process, -♦-, binodal; -■-,T_c-concentration relation; -●-,T_m-concentration under the binodal; ▲, invariant three phase equilibrium.* [25, 30]

On other hand, precipitation of PVDF by direct crystallization from homogenous solution is shown in figure 3.4 (b). Where, polymer crystallization proceeds at a certain degree of undercooling so that the interference between demixing and crystallization will take place at the temperature and concentration that correspond to this intersection point between the crystallization line (concentration dependence of the crystallization temperature) and the binodal. At given polymer content, increasing T_m will be observed under miscibility gap for polydisperse polymers. In general, cooling rate plays a crucial role during crystallization process, where at slow cooling rate only crystallization can take place, while, at higher rate crystallization can interfere with L+L demixing resulting in crystalline porous material.

Since McHugh et al,[22] has reported on the effect of a different molecular weight samples of PVDF on the location of L+L demixing cloud point pressure in $scCO_2$ (cf. Figure 3.5). To the best of our knowledge up to now, no attempt was made to determine the pressure/temperature trace of the crystallized PVDF.

3.3.1.1 Isothermal depressurization:

Figure 3.6 compares the solubility data of the two technical PVDF samples (PVDF 323 and PVDF 226). The different positions of the cloud point lines were attributed to differences in molecular weight and molecular weight distributions. Where, weight average molecular weight of PVDF 323 is Mw = 323 Kg/mol, while for PVDF 226 is Mw = 226 Kg/mol. From the first glance, one can observe that polymer molecular weight in the range investigated in this study has a minor effect on the pressure and temperature needed to obtain a single phase homogenous solution regime, a similar comparative study has been reported by McHugh et al. [27]

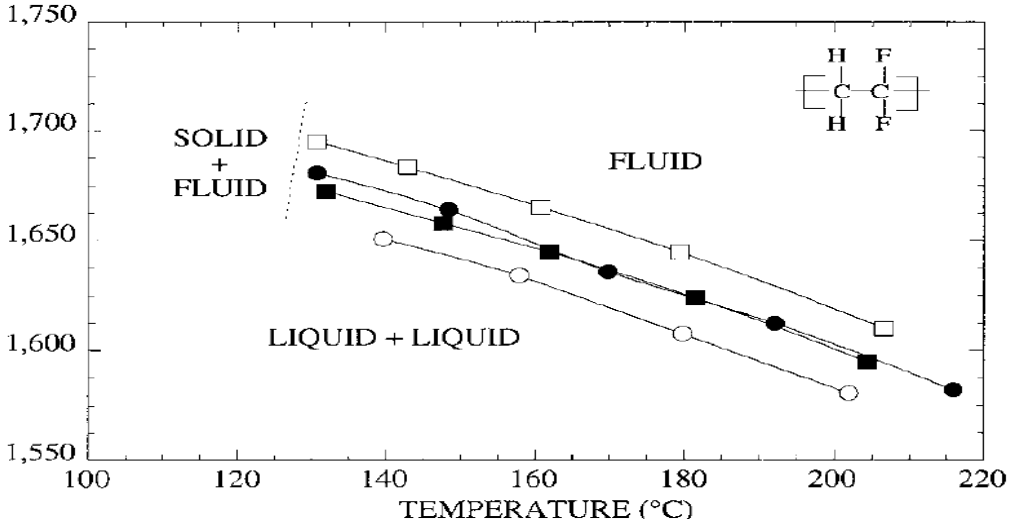

Figure 3.5: *Molecular weight effect on the solubility of PVDF in $scCO_2$: PVDF (Kynar-741) (●), PVDF-181(○), PVDF-275 (■), and PVDF-329(□). (ref. 22)*

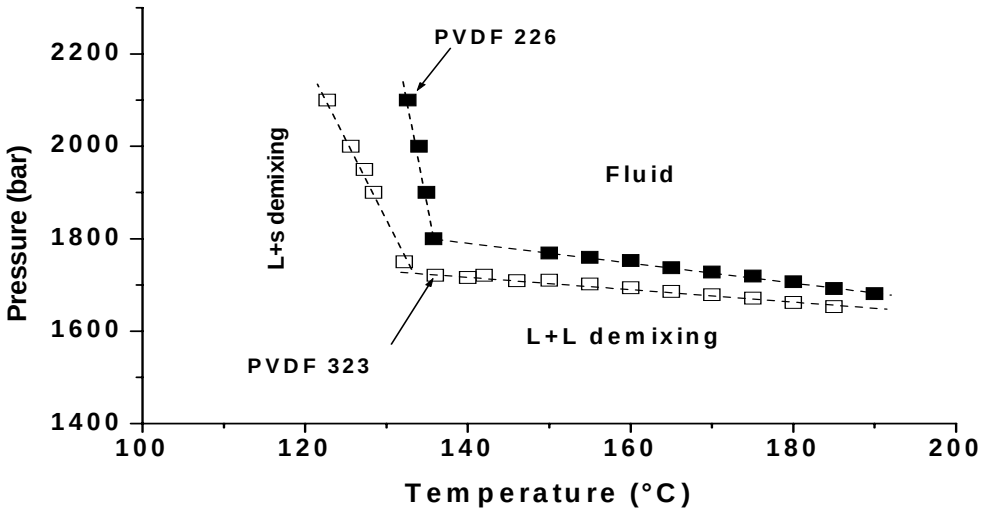

Figure 3.6: *A P-T diagram showing liquid/liquid (precipitation)and liquid/solid (crystallization) for 2wt % PVDF/$scCO_2$ system. PVDFs Mwt (□: Mw = 323 Kg/mol, ■: M_w = 226 Kg/mol).*

The reason for the slightly difference L+L segregation cloud points and L+S crystallization point between PVDF226 and PVDF323, could be either due to degree of crystallinity or microstructure dissimilarities. However, for two PVDF samples degree of crystallinity as calculated from DSC measurement was almost identical (i.e. PVDF 323: 55 ± 5%, and PVDF 226: 53 ± 5%). On another hand, the microstructure of the polymeric chains with respect to the infrastructure of head-to-head or tail-to-tail connections determined from ^{13}C-NMR spectroscopy (i.e. PVDF 323: 5.5 ±3 %, PVDF 226: 3.0 ± 2%) did not shows a considerable differences. Subsequently, one can conclude that infrastructure dissimilarities are not the reason for slightly difference between L+L and L+S segregation lines value between two polymers under current investigation study.

Figure 3.7, depicts SEM micrographs of PVDF 323 samples that were obtained from dissolution/precipitation experiments after carbon dioxide treatment. Pressure release (isothermal expansion) caused the precipitation of polyvinylidene fluoride with sponge-like morphologies. The pores diameter of the interconnected chains contains a large number of spherical voids between 5 and 20 μm as seen in Figure 3.7 a, b. On other hand slow cooling at constant pressure yielded precipitated powders with larger particles than observed with the untreated polymer (i.e. pure PVDF). The particles exhibited a lamellar structure as its typical for chain folded crystal (Figure 3.7 c, d).

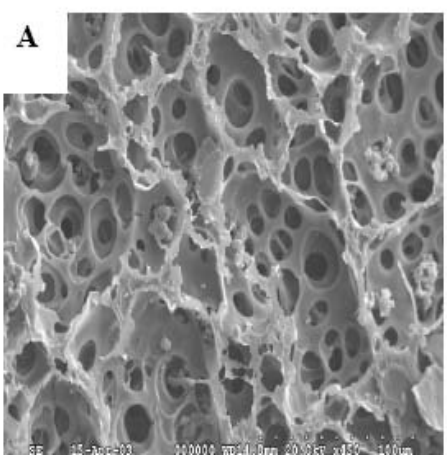

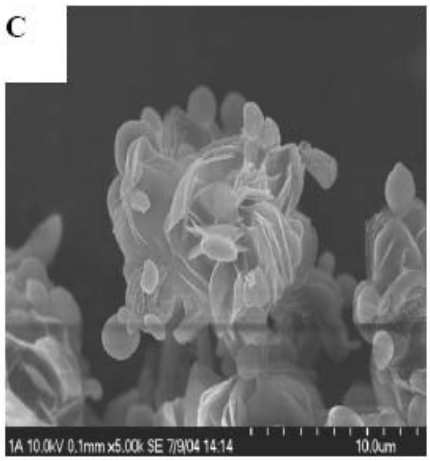

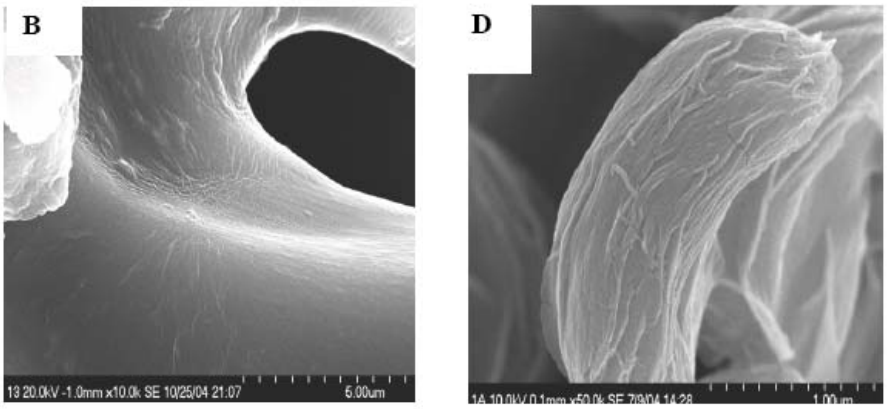

Figure 3.7: *SEM micrograph of PVDF (PVDF 323) collected from high pressure cell. PVDF was precipitated by isothermal depressurisation, at 160°C and 1800 bar; (a) 100µm magnification resolution, (b) 5.0 µm magnification resolution, while PVDF 323crystallized by isobaric cooling from $scCO_2$ at 160°C at 1900 bar, (c) 10.0 µm magnification resolution (D) 1.00 µm resolution, respectively.*

The concentration dependence of the measured cloud point curves of PVDF 323 either on isothermal expansion or isobaric cooling is summarized in Figure 3.8. Quite high pressures above 1800 bar were needed to keep the PVDF dissolved at temperatures between 125°C and 132°C (crystallized PVDF). While, at high temperatures the cloud point pressures varied a little with temperatures, i.e. the respective slope was dP/dT = -1.5 bar/K (precipitation). This observation may be due to high polarity of carbon dioxide at high temperature; which enhances polar-polar interaction between CO_2 and polar repeating unit of PVDF sample. Also it's worthwhile to mention that in this region; cloud points were weakly concentration dependent and increased slightly when the polymer concentration was increased. For more than 5wt% PVDF in CO_2, the higher weight concentration of PVDF the slightly dependence of the cloud point pressure was observed, which in contrast to what other reported. [27, 28, 31-32] Where they reported on the cloud point data of PVDF at 5 wt % only corresponding to maxima in the pressure-composition isotherm (cf. Figure 3.9). This phenomenon may be attributed to the higher temperature of the solution; at which dipole-dipole interaction becomes small and polar polymer (i.e. PVDF) behaves as non-polar polymer which can solubilize easily in sc fluid. Consequently, this behaviour reflects the higher magnitude of polymer segment-solvent segment interaction which overcomes the polymer-polymer segment interaction value.

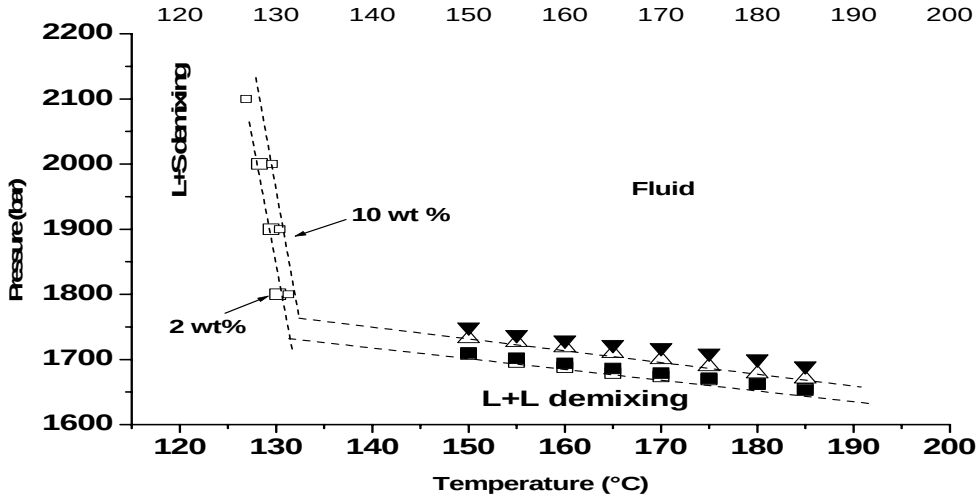

Figure 3.8: *Cloud points curves for 2 w % (□), 5 wt% (■), 10 wt% (Δ) and 15 wt % (▼) PVDF 323 in scCO₂.*

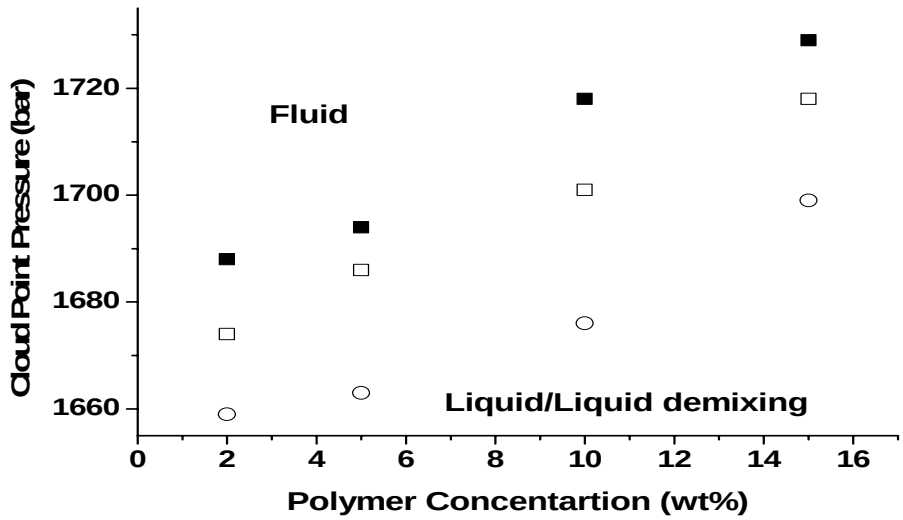

Figure 3.9: *Cloud pressure vs. composition correlation of PVDF323 in scCO₂ at (■) 160°C, (□) 170°C and (O) 180°C.*

3.3.1.2 Phase behaviour diagram for PVDF/CO_2 binary mixture (Isobaric cooling):

It should be noticed that the origin of the P-T behaviour of PVDF/CO_2 binary system has crystallization boundary limited at ~35°C below the normal melting point of the polymer ($T_{m,\ PVDF}$ = 168°C). Where, strong opalescence was observed for the cloud point transitions of the PVDF/CO_2 system (i.e. at liquid/solid border). Obviously, the slightly negative slope of the P-T trace of the cloud point is similar to what has been

observed by Ehrlich and Kurpen [33] and Condo [34] for the polyethylene-propane system. Rätzsch, Findeisen, and Sernow [35] found also the same negative slope trend for the polyethylene-ethylene system. Where, they reported in the two mentioned cases that when SCF has a relatively low solubility in the molten heavy component (i.e. polymeric material), the S-L-V curve (cf. Figure 3.10) might have a negative dP/dT slope. [35, 37]

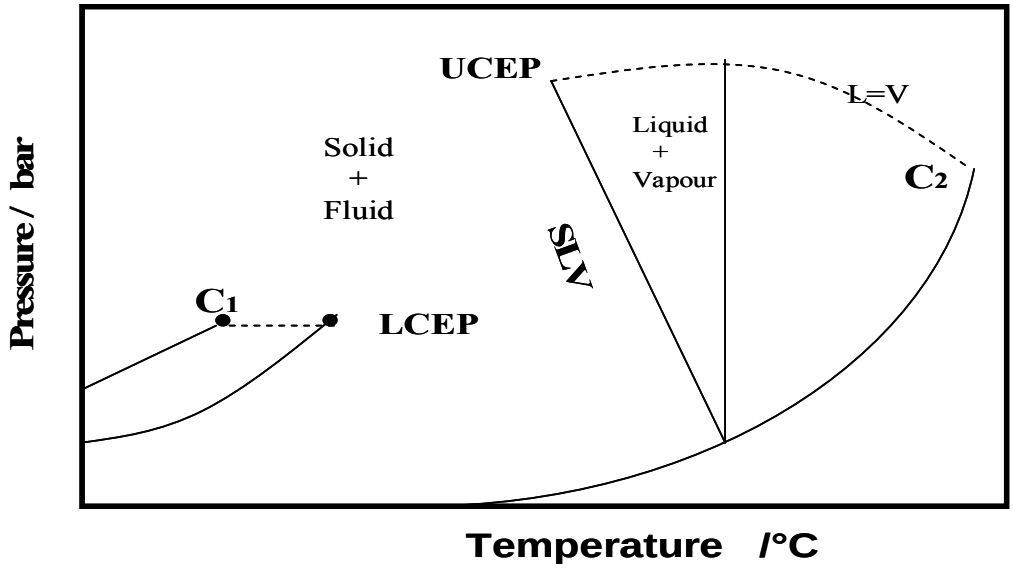

Figure 3.10: *Schematic pressure-temperature diagram for a mixture consisting of a heavy non-volatile solid and a low molecular weight solvent; the lower (LCEP) and Upper critical end points (UCEP) occur at the intersections of the critical mixtures curve designated L=V, and the solid-liquid-vapour (SLV) line; the two critical points are designated C_1 and C_2. (Redrawn from ref. 36)*

Figure 3.10, shows the critical mixture (L=V) curve is intersected at two locations by the solid-liquid-vapor (SLV) line. The SLV line in the pressure-temperature (P-T) diagram represents the melting point depression that occurs as low molecular weight supercritical solvent (ex. CO_2) dissolves in the solute-rich liquid phase which exists when the solid (i.e. polymer) melts. Meanwhile, Solid-fluid phase behaviour occurs in the P-T region between the two branches of the SLV line regardless of the system pressure. [19] Another theoretical explanation for the slightly negative behaviour for L+S border comes from Arrhenius law. It's well known that, solubility of a compressed gas in a given polymer (equation 3.1) is related to the temperature and the heat of the solution according to:

$$S = S_o \exp(-\Delta H / RT) \qquad (3.1)$$

Where S_o is the solubility coefficient, ΔH is the heat of solution, R is the gas constant, and T is the absolute temperature. Since the heat of solution is commonly negative in polymer-CO_2 system, so the solubility of CO_2 in polymer-rich phase will be decreased with an increase in temperature. In another approach, explaining the negative nature of L+S border, the pressure was observed to increases as the amount of sorbed CO_2 inside PVDF-rich phase increases. Subsequently the degree of swelling of PVDF and the solubility of CO_2 in polymer rich-phase increase several fold as shown in Figure 3.11. From previously mentioned information (i.e. solubility of sorbed CO_2 in polymer rich phase with respect to degree of polymer swelling and origin of SLV line), an important result could be driven, as the slope of L+S line for pressure/temperature curve of PVDF in CO_2 must be apparently with negative value.

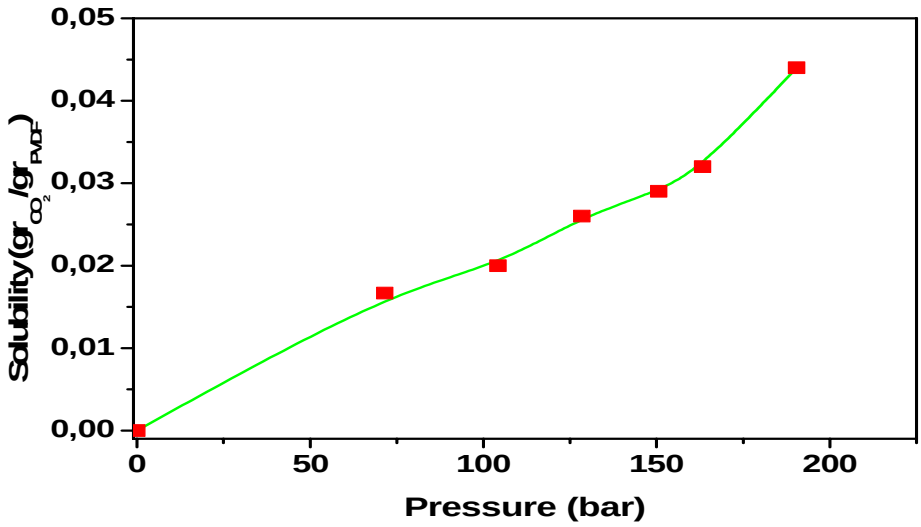

Figure 3.11: *Solubility data of carbon dioxide in PVDF(gr_{CO2}/gr_{PVDF}) as function of pressure at 40°C.* [38]

On crossing the solid-fluid border, it was observed that turbidity of the solution makes it difficult to determine if the second phase contains solid crystals in solution or not. However, it was possible experimentally to deduce whether crystals are present by measuring the temperature needed to obtain a single homogenous solution when the solution is isobarically heated at a fixed rate, i.e. formation of a clear single phase. When polymer crystals were visualized, the solution was heated isobarically at heating rate of 10 K/min back to a situation where homogenous solution was attained. It took approximately 2-5°C until a transparent system was formed again.

As can be seen from Figure 3.12, for 2 wt % PVDF 323 in $scCO_2$, we have got two kinds of crystallization curves with different negative slopes. The difference in the cooling rate could be the reason for these different slopes. Where, at lower cooling rate (0.2 K/min) the onset of crystallization appears at higher temperature (i.e.140°C), while the onset of crystallization is shifted to lower temperature (i.e. 136°C) at higher cooling rate (1.0 K/min). A negative slope was observed as a common trend for both of them. For Future work regarding crystallization kinetics study, the experimental condition should be controlled to the degree necessary to follow up this process. The data however clearly distinguish between the crystallization line and the liquid+liquid demixing and demonstrate the negative slope for L+S segregation line.

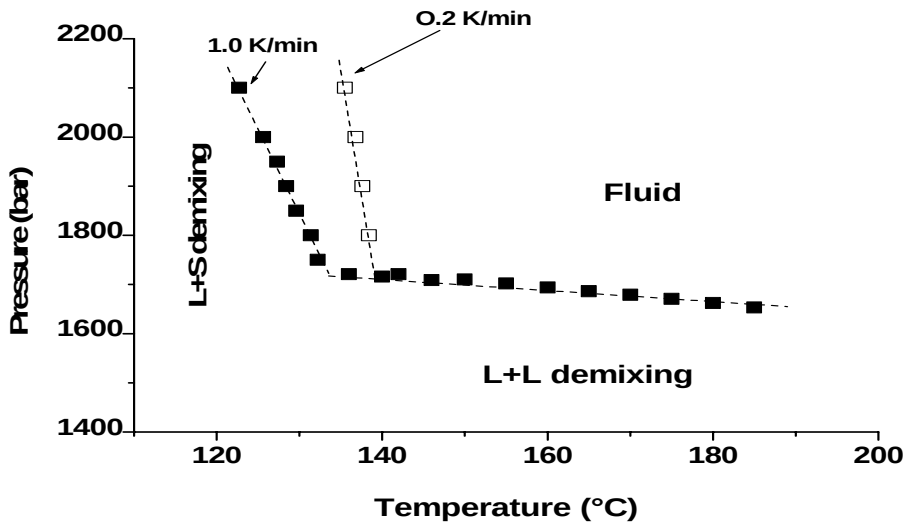

Figure 3.12: *Different crystallisation line for 2 wt% PVDF323 isobarically crystallized from $scCO_2$ (■: dP/dt= -33bar/min, cooling rate 0.2 K/min,□: dP/dt=-100 bar/min, cooling rate 1.0 K/min).*

At this stage, two different kind of crystallization protocol may occur for PVDF. Crystallization can be induced either by; (i) crystals are formed after precipitation through liquid-liquid demixing followed by vitrification or (ii) crossing the solid-fluid border that means crystals are formed directly from homogenous solution. (cf. Figure 3.13)

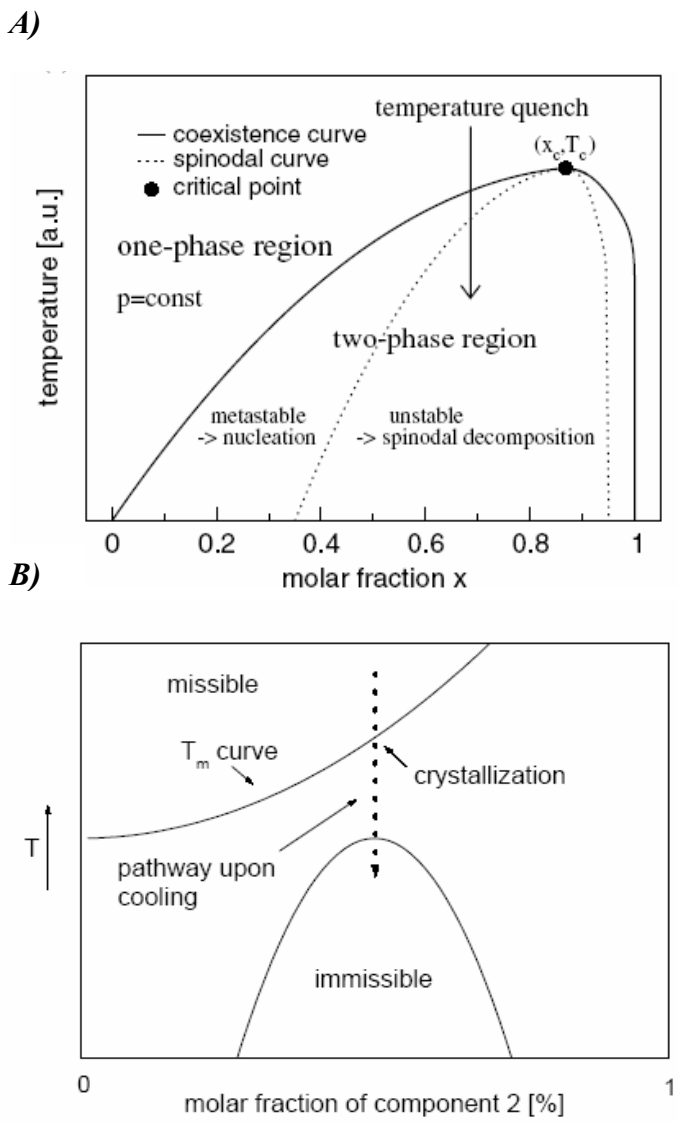

Figure 3.13: *(A) Schematic phase diagram of a compressible polymer solution. Temperature T and molar fraction x of the solvent are variables while, pressure p is constant. The position of the critical point is shown by ●, (B) Schematic representation of possible PVDF crystallization at constant system density.* [39]

After performing isobaric cooling experiments, polymers were collected from the high pressure view cell and the effect of the CO_2 precipitation approach (i.e. crystallization) on the degree of crystallinity and powder density of polymer was investigated (c.f. Table 3.2). Table 3.2 shows that the change in melting temperature of PVDF 226 (ΔT_m = - 2.8°C) was less affected than PVDF 323 (ΔT_m = - 15.4°C), while the degree of crystallinity decreased by the same order of magnitude (ca. 12-13%) for both kind of polymer. Note that, the powder density of PVDF226 & 323 remained almost unaltered within an experimental error. [24, 40]

Basically, from sponge like morphology of the PVDF samples (cf. Figure 3.7a) obtained on isothermal depressurisation. We might conclude that for polymer to segregate from solution via a spontaneous (liquid+liquid) demixing process, as an unstable regime (metastable nucleation = nucleation and growth regime) of a polymers phase diagram. In this process, interdiffusion of the nonsolvent and the solvent brings the composition of the homogeneous polymer solution into the miscibility gap. Hence, the polymer solution is decomposed into a polymer-rich phase and a polymer-poor phase. At a certain stage during phase demixing, the polymer-rich phase is solidified into a solid matrix, while the polymer-poor phase develops into the pores. (Spinodal decomposition proposed by Cahn/Hilliard equation). [41] On subsequent cooling to ambient temperature the polymer crystallises in the polymer enriched region and the bicontinuous structure becomes permanently arrested.

Table 3.2*: Melting transition, degree of crystallinity and powder density of PVDF samples crystallized from carbon dioxide.*

Polymer	Tm [°C]	ΔHm [J/g]	Crystallinity[a] [%]	Powder Density [b][g/ml]
Untreated PVDF 323	168.0	53.6	55.2	0.41
PVDF 323	152.6	44.1	43.4 (-11.87)	0.40
Untreated PVDF 226	169.1	52.7	53.0	0.38
PVDF 226	166.2	40.1	39.4 (-13.60)	0.43

(a) Calculation based on ΔHm = 6.50 kJ / mol per repeating unit for 100% crystalline PVDF.
(b) Calculated by weighing out samples in fixed volume.

3.3.2 Phase behaviour for PVDF/VDF/CO_2 ternary mixture:

3.3.2.1 Isothermal depressurization:

In a second series of experiments homogeneous ternary mixtures of PVDF/VDF/CO_2 were depressurised and precipitated either isothermally or isobarically (cf. Figure 3.14). Figure 3.14 shows the effect of increasing weight fractions of VDF on the precipitation curves of a PVDF/CO_2 binary mixture. In all cases the precipitation line (L+L demixing) exhibited a negative slope (LCST characteristics), which is in accordance with cloud point data reported for a polar fluoropolymer in supercritical fluid. As a general trend,[42,43,44] the cloud point curve exhibits a negative slope in the pressure-temperature diagram for a mixture consisting of a polar- and much less polar component

because the interchange energy characterising the balance of polymer segment-CO_2 cross-interactions relative to polymer segment-segment and CO_2-CO_2 self interactions is very temperature sensitive. At low temperatures the polar interactions between the polymer segments dominate the phase behaviour. While, at high temperature entropic effects are expected to dominate. The location of the cloud point is more a reflection of the free-volume difference between the dense polymer and the expanded CO_2 rather than the balance of intermolecular interactions.

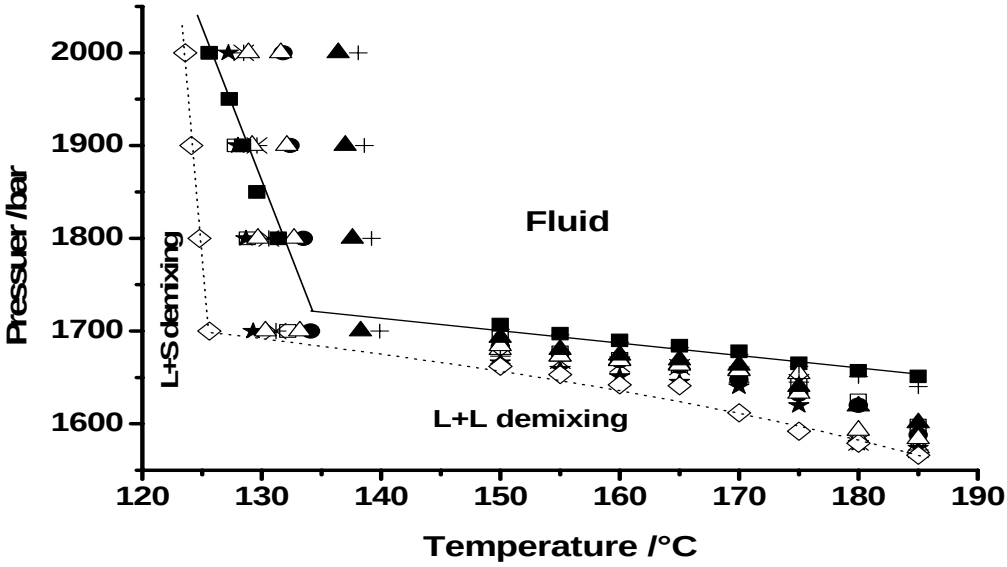

Figure 3.14: *Impact of VDF on the crystallization/ precipitation curves of 2 wt% PVDF in $scCO_2$ (■ = 0 wt%, □ = 14.2 wt%, ● = 17.8 wt%, Δ = 24.7 wt%, ✳ = 28.5 wt%, ★= 34.6 wt%, ◇ = 42 wt%, ▲ = 63.8 wt%, + = 76 wt% VDF). Solid line represents the interconnection between L+L and L+S demixing lines for 2 wt% PVDF323 in $scCO_2$.*

For example, at 150 °C adding ~14.2 wt% VDF monomer to the mixture of PVDF/CO_2 reduced the cloud point pressure by ca. 20 bar from 1710 bar (pure PVDF) to 1690 bar. While, with 17.8 wt% VDF the cloud point pressure dropped to 1683 bar (-47 bar). At about 42 wt% VDF concentration the cloud point pressure was dropped to 1660 bar (-48 bar). Commonly observed, on increasing the added amount of VDF to the system; cloud points pressure decreased as long as the VDF content was below 42 wt% (reference to CO_2).

However, on further increasing content of VDF gas the effect became reversed, as the pressure required reaching the single phase region in the PVDF/CO_2/VDF ternary mixture increased to higher values compared to the other situation (< 42 wt% VDF) effect. At 150 °C the addition of 52 wt% VDF to PVDF/CO_2 yielded a cloud point pressure of 1688 bar. This value is still 22 bar lower than observed in binary PVDF/CO_2 mixtures, but its 26 bar larger than cloud point value for PVDF/42wt%VDF/CO_2 mixture. With a VDF fraction of 76% the cloud point pressure is 1701 bar which in vicinity of situation of monomer free solutions.

The surprising decrease of the cloud point curves at low monomer concentration is still questionable for a future work, on other hand the increase of cloud point at high VDF concentrations is well supported by simulation study.

In the frame of EU project a similar comprehensive simulation studies has been performed by Kiparissides et al [38] using Statistical Associating Fluid Theory (SAFT) to model phase behavior for PVDF/VDF/CO_2 system, data are shown in Figure 3.15. Where, they show that for PVDF/VDF/CO_2 ternary mixture, pressure-composition diagram exhibit a minima for a system containing ~15wt% VDF gas at 155°C. In spite of different value of VDF weight percent at which minima occurs; these result was in general in accordance with our experimental study.

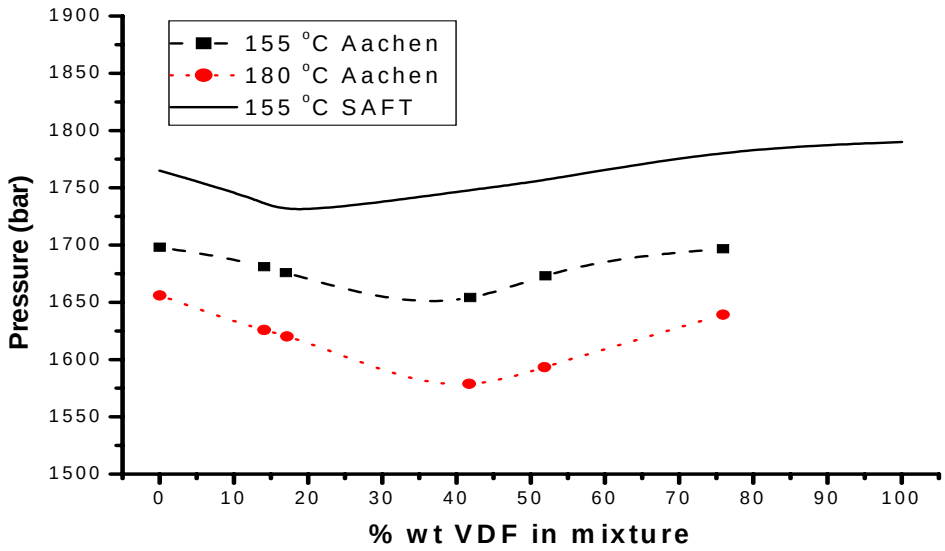

Figure 3.15: *A comparative studies of pressure vs. weight fraction of VDF in CO_2 at (■) 155°C, (●) 185°C, and (-) SAFT predication.* [38]

3.3.2.2 Cloud point curve for PVDF/VDF/CO_2 ternary mixture (Isobaric cooling):

During isobaric cooling experiment, at which L+S transition for PVDF/CO_2/VDF mixture took place in a very narrow temperature range i.e. the crystallization line exists in temperature range between 130-140°C. Crystallization with a cooling rate of 0.2 K/min in presence of 14.2 wt% VDF shifts the precipitation cloud point curve by about 10°C to lower temperatures as compared to the pure PVDF/CO_2 system. Hence, the monomer promoted the crystallization of the polymer. The amount of dissolved CO_2 in the polymer rich-phase increase as the pressure increases. Moreover, the rate of transfer of monomer to polymer particle is very fast. Kiparissides et al have proposed that density of VDF inside polymer particle is also increases at high pressure. Subsequently, the chance collisions of randomly distributed polymeric chain are lowered. So definitely, appearance of onset of crystallization temperature decreased to lower value upon addition of VDF to PVDF/CO_2 binary mixture. (cf. Figure 3.16)

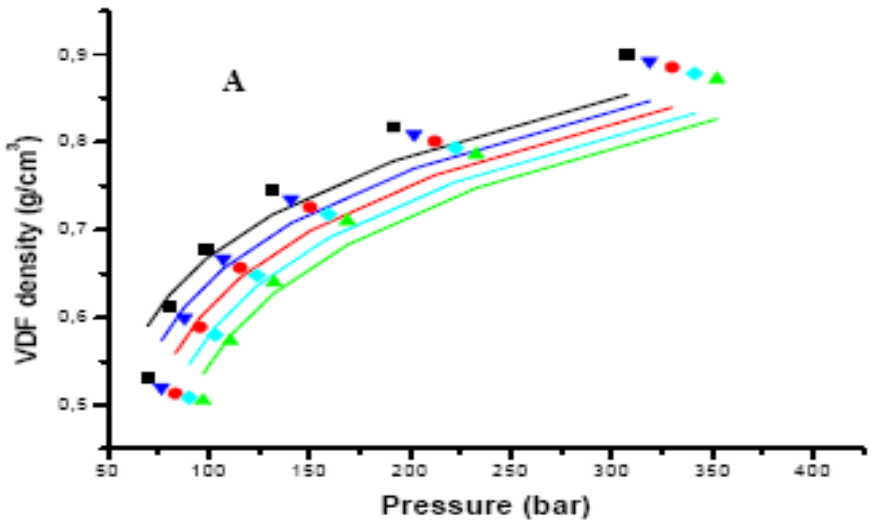

Figure 3.16: *Density vs. -pressure correlation diagram for vinylidene fluoride at (▲)60°C,(♦)55°C,(●)50°C,(▼)45°C,(■)40°C,and(-) SAFT predications; and (-) SAFT predication.*[38] *(SAFT: Statistical Associating Fluid Theory)*

It must be noted that the high-pressure polymer/supercritical fluid/co-solvent studies reported in the literature shows that cloud points monotonically decrease in pressure and temperature with the addition of a polar component, as long as the co-solvent does not form a complex with the polar repeating unit in the polymer.

For many of the arguments invoked to explain the data in this study, it was necessary to have an estimate of solvent density at the cloud point pressure conditions. (cf. Table 3). Where, the density data for the mixture of PVDF/xwt%VDF/CO_2 at 155°C, and 185°C are shown (x=0, 14.2, 17.8, 24.33, 28.51, 34.51, 42, 63.3, and 76 wt% VDF, respectively). With millimetric scale etched on the guide tube, swept volume of the hand pump can be recorded. From knowledge of the initial mass of solution loaded into the cell, and the volume as calculated from the piston position; it was possible to calculate densities directly from Peng Robinson equation of state. Table 3.3, revealed that for an addition of VDF to mixture of PVDF/CO_2: the density decrease as the cloud point pressure decrease for the solution containing VDF up to concentration of ~ 42wt%. We proposed that the higher the concentration of VDF the lower the density of molten polymer in CO_2 turning out in decreasing the entropy penalty paid by carbon dioxide to solvate polymer, this leads to shifting the liquid-liquid demixing points to lower pressure value. At higher concentration of VDF than ~42 wt% (up to 76wt%) the density value increase again resulting in increasing the cloud point pressure again to the situation similar to pure PVDF with 0 wt % VDF monomer unit.

Table 3.3: *Density data at the cloud point pressure at 155°C, and 185°C for the mixture comprising of PVDF/xwt%VDF/CO_2 mixture.*

Polymer	CP (bar), 155°C	ρ(g/ml) 155°C	CP (bar) 185°C	ρ(g/ml) 185°C
PVDF+0wt %VDF	1707	1.0210	1656	0.973
PVDF+14.2wt %VDF	1692	1.018	1598	0.964
PVDF+17.8wt %VDF	1683	1.0176	1588	0.962
PVDF+24.33wt %VDF	1680	1.0172	1584	0.9618
PVDF+28.51wt %VDF	1673	1.016	1580	0.9612
PVDF+34.51wt %VDF	1667	1.015	1580	0.9612
PVDF+42 wt %VDF	1662	1.014	1579	0.9610
PVDF+51wt %VDF	1690	1.0186	1593	0.9630
PVDF+63.3wt %VDF	1693	1.019	1600	0.964
PVDF+76wt %VDF	1702	1.0204	1651	0.973

Effect of adding VDF on the proceeding of polymerization is illustrated in figure 3.17.Where; a schematic ternary phase diagram for PVDF/VDF/CO_2 is showing the effect of the consumption of VDF during polymerisation on the total composition and the resulting phase behaviour. At zero monomer conversion one starts at a given point on the VDF/CO_2 edge of the triangle. With preceding polymerisation, the total system composition follows the dotted arrow, parallel to the VDF/PVDF edge and ends on the PVDF/CO_2 edge at full conversion of the monomer. Along this path, the system will inevitably cross the precipitation line, separating the homogeneous solution of PVDF in the CO_2/VDF mixture and the biphasic system. Until this critical conversion the polymerisation will proceed in a homogeneous solution while in the later stage a heterogeneous polymerisation reaction must occur. Note that the precipitated polymer phase can contain considerable amounts of CO_2 and VDF; hence the precipitated polymer will create new loci of polymerization.

Although the conditions for homogeneous dissolution of a small content of PVDF (P > 1550 bar, T > 140 °C) strongly deviate from realistic technical polymerisation conditions (P < 400 bar, T < 60 °C) the principal items can be transferred. According to the measured cloud point curves the presence of VDF monomer can not be expected to alter the solubility of PVDF significantly under such conditions. This is in accordance to turbidity measurements on polymerising mixtures of VDF / CO_2, demonstrating the onset of turbidity to coincide with the start of the polymerisation reaction, i.e. at monomer conversions well below 0.5 %. [45]

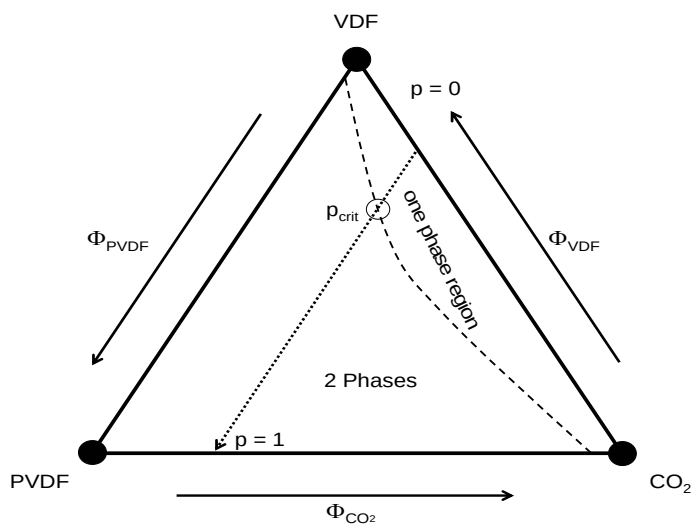

Figure 3.17: *Schematic ternary phase diagram of PVDF/CO_2/VDF mixtures at constant pressure and temperature, showing the precipitation boundary (---) and the changes of composition due to polymerisation of the VDF (……).*

The effect of adding different weight percent of vinylidene fluoride (VDF) on the morphology of precipitated PVDF by isothermal depressurization is illustrated in Figure 3. 18.

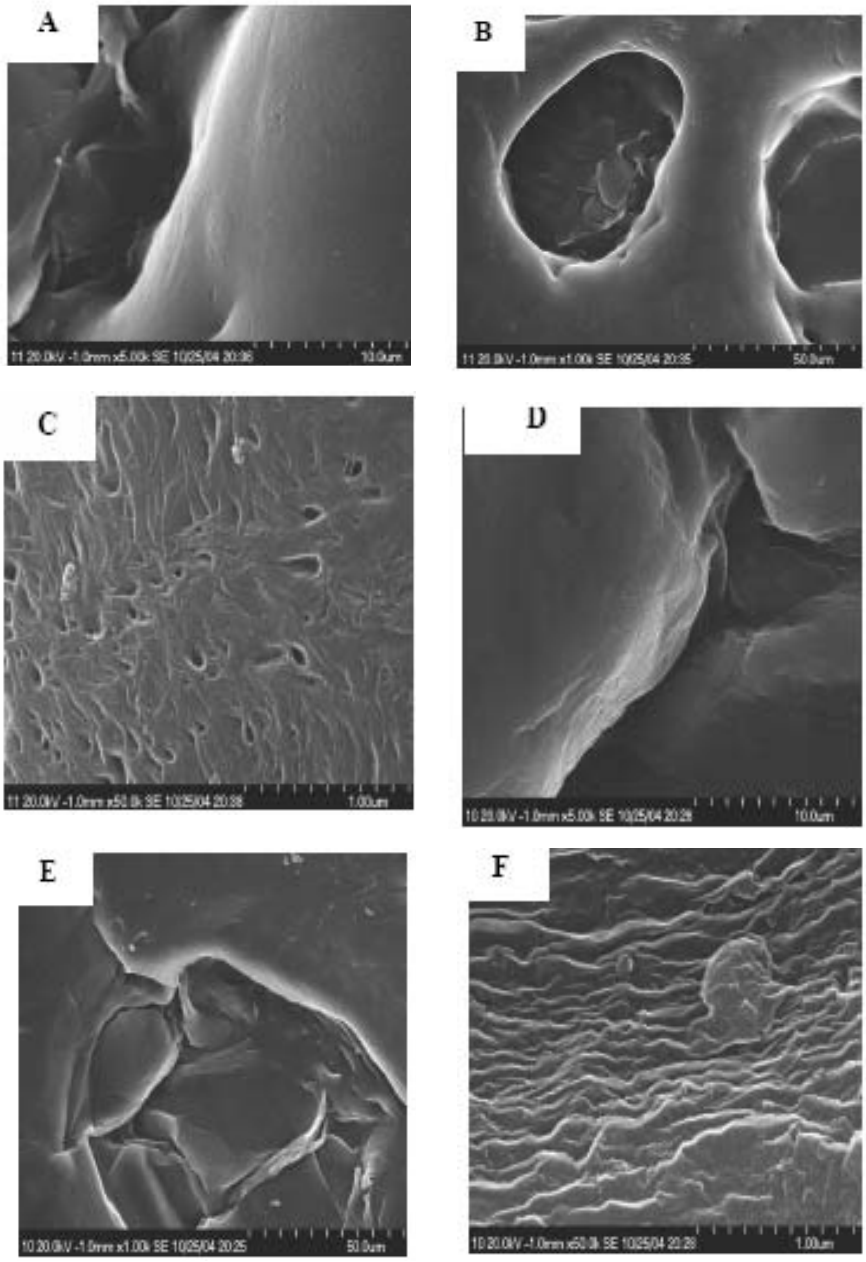

Figure 3.18: *Transmission electron micrograph for PVDF323/34.51 wt% VDF precipitated from $scCO_2$ by isothermal depressurization at 160°C and 1800 bar with depressurization rate 10±2 bar, where (A) 10µm, (B) 50 µm, (C) 1µm scale par, and PVDF323/76 wt% VDF precipitated from $scCO_2$ at same condition where (D) 50 µm, (E) 10 µm,, and (F) 1 µm scale bar.*

Figure 3.18 reveals great effect of adding VDF on the morphological structure of polyvinylidene fluoride precipitated isothermally from $scCO_2$. For example, at 34.51 wt% VDF, a sponge structure of PVDF precipitated at 160°C & 1800 bar were obtained

as seen from top view. At this VDF concentration, a larger pore of macrovoids was formed having diameters estimated to be larger than 20 µm of the interconnected chain. This macroviods were almost spherical in shape like one obtained from isothermally precipitated PVDF from $scCO_2$ with 0 wt% VDF (cf. Figure 3.18 a, b, c). The internal surface of these macrovoids was smooth just like the top of the skin. This suggested that very amorphous boundary layer was formed surrounding the liquid undefined structure of molten polymeric chains during phase separation. As the structure grew to form macrovoids, it crystallizes upon releasing pressure followed by cooling down into a crystalline porous structure. On other hand, for a mixtures containing PVDF/76wt%VDF/CO_2 the pores were small (~1-2 µm), compact and independent, as shown in Figure 3.18.d, e, and f. The internal surface was almost rough. The reason for compact structure of PVDF with high VDF concentration was still unknown.

The effect of the cloud point pressure for different PVDF/VDF/CO_2 ternary mixture on the location of onset of crystallization temperature is depicted on Figure 3.19.

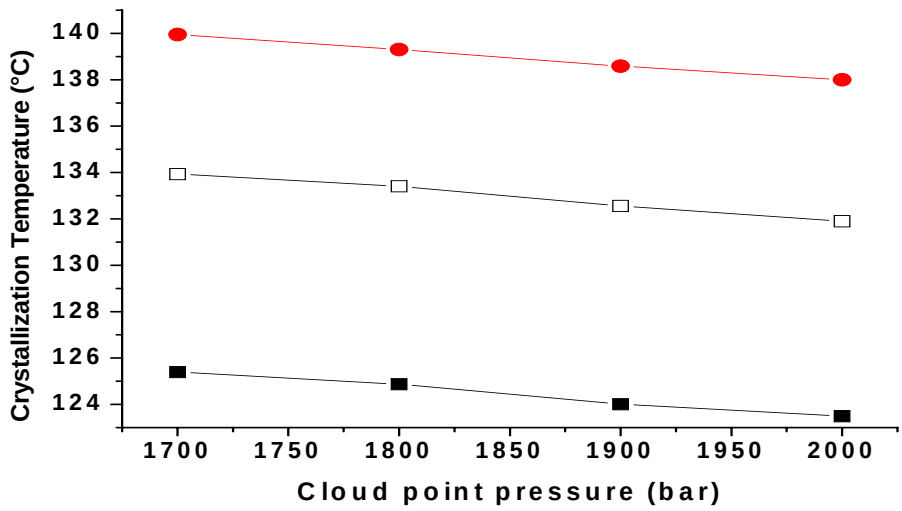

Figure 3.19: *Crystallization temperature (T_c) vs. cloud point pressure for PVDF/xwt%VDF/CO_2mixture, where (■) x=0, (□) x=42and (●) x=76, respectively.*

Once again kiparissides et al [38] has proposed that as the density of carbon dioxide increases at higher pressure; the density of molten PVDF decreases (cf. figure 3.20). These means a lower possibility for the extended polymeric chains to comes together to form a nuclei which grows by crystal growth to form a definite crystallites. Figure 3.19 shows that on increasing the pressure at which the solution expanded from molten state the onset of L+S border shifted to a lower temperature. For example at 1800 bar carbon

dioxide pressure, the onset of turbidity appear at 133.41°C for a mixture of PVDF/CO_2, rather than 132.56°C for the same mixture at 1900 bar. The same trend was observed for all other mixtures containing <42 wt% weight percent of VDF.

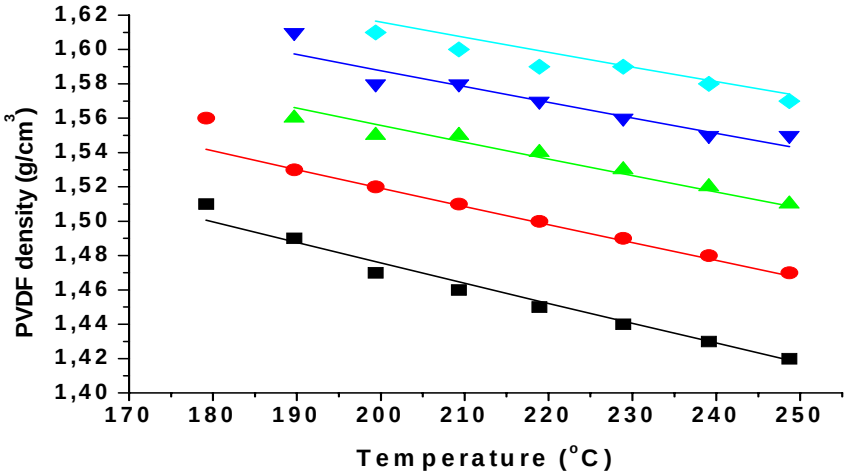

Figure 3.20: *A PVDF density-temperature correlation diagram in $scCO_2$ at (■)1 bar,(●)400 bar,(▲)800bar,(▼)1200bar,and (♦)2000 bar.*[38]

3.4 Conclusion:

The crystallization [46] and L+L-demixing of polyvinylidene fluoride (PVDF) from supercritical carbon dioxide were investigated over a temperature range from 110°C to 190°C at pressures between 1400 to 2100 bar. Isobaric cooling caused the crystallization of the polymer to form a particulate powders, while isothermal expansion yielded PVDF with crystalline sponge like morphologies caused by spinodal liquid/ liquid decomposition followed by polymer crystallization after elimination of CO_2. In the later case first liquid droplets were formed composing of polymer melt swollen by CO_2, i.e. the crystals are formed at high polymer concentration. Hence, the polymer morphology can easily be controlled by selection of the precipitation mode.

Impact of addition of VDF on the location of L+L demixing was determined at low and high VDF concentration. Where, we found that at low concentration the gaseous monomer can decrease the solubility values for PVDF/$scCO_2$ mixture, while at high concentration the situation is reversed; as VDF can act as anti-solvent for polyvinylidene fluoride in carbon dioxide.

Pioneering work regarding crystallization of PVDF from $scCO_2$ was performed; the cloud point data demonstrate that the L+S demixing lines were observed to have a distinguished negative slope. While, for a future work regarding crystallization kinetics should be done to determine effect of experimental conditions (ex. cooling protocol, and presence of nucleating agent) on the value of crystallization temperature and thickness of lamellar structure.

3.5 References:

[1] Kendall J. L., Canelas D. A., Young J. L., DeSimone J. M.; Chem. Rev. 1999, **99**, 543-563.

[2] Cooper A. I.; J. Mater. Chem. 2000, **10**, 207-234.

[3] Woods H. M., Silva M. M. C. G., Nouvel C., Shakesheff K.M., Howdle S. M.; J. Mater. Chem. 2004, **14**, 1663-1678.

[4] Jessop, P. G., Leitner W.; Chemical Synthesis Using Supercritical Fluids; Wiley-VCH: Weinheim, Germany, **1999**.

[5] Klinge U., Klosterhalfen B., Ottinger A. P., Junge K., Schumpelick V.; Biomaterials 2002, **23**, 3487-3493.

[6 Howe-Grant; M. Fluorine Chemistry: A Comprehensive Treatment; Wiley: New York, **1995**.

[7] Ameduri B., Boutevin B., Kostov G. K., Petrova P.; Des. Monomers Polym. 1999, **2**, 267-285.

[8] McCarthy T. F., Williams R., Bitay J. F., Zero K. Yang M. S., Mares F.; J. Appl. Polym. Sci. 1998, **70**, 2211-2225.

[9] Apostolo M., Albano M., Storti G., Morbidelli M.; Macromol. Symp. 2000, **150**, 65-71.

[10] Ameduri B., Boutevin B.; J. Fluorine Chem. 2000, **104**, 53-62.

[11] Barber, L. A. In Eur. Pat. Appl., Pennwalt Corp., Ep, 1986; p 27.

[12] Adamsky F. A., Beckman E.; J. Macromolecules 1994, **27**, 312.

[13] Hoefling T. A., Newman D. A., Enick R. M., Beckman E. J.; J. Supercrit. fluids 1993, **6,** 165.

[14] Newman D. A., Hoefling T. A., Beitle R. R., Beckman, E. J., Enick R. M.; J. Supercrit. Fluids 1993, **5**, 205.

[15] Kazarian S. G., Vincent M. F., Bright F. V., Liotta C. L., Eckert C. A.; J. Am. Chem. Soc. 1996, **118**, 1729.

[16] Shah V. M., Hardy B. J., Stern S. A.; J. Polym. Sci. Polym. Phys. Ed.1993, **31**, 313.

[17] Patterson D.; Polym. Eng. Sci. 1982, **22**, 64.

[18] Mertdogan C. A., Byun H.-S., McHugh M. A., Tuminello W. H.; Macromolecules 1996, **29,** 6548.

[19] Lovinger A.J., Bassett D.C., 2nd Ed., Applied Science Publishers, London (1982)

[20] Wilson C.W.; J. Polym. Sci. A 1963, **1**, 1305

[21] Gorlitz M., Minke R., Trautvetter W., Weisengerber G.; Angew. Makromol. Chem. 1973, **29/30**, 137.

[22] Dinoia T. P., Conway S. E., McHugh M.; J. Polym. Science; Part B; Polymer Physics, 2000, **38**, 2832-2840.

[23] Stejny J., Whitfield A.F., Pritchard G. M., and Hill M. J; Polymer 1998, **39**, No. 17, 4175-4179.

[24] Kirby C.F.; McHugh M. A.; Phase behavior of polymer in supercritical solvents. Chem. Rev. 1999, **99**, 565.

[25] Berghmans H.; De Cooman R.; Koningveld R.; Polymer 1997, **39**, 4621-4629.

[26] Michele L., McHugh M.; Fluid Phase Equilibria 1999, **157**, 285-297.

[27] Meilchen M.A., Hasch B.M., Lee S.-H., McHugh M.A.; Polymer 1992, **33**, 1922–1925.

[28] Lee S.-H., LoStracco M.A., McHugh M.A.; Macromolecules 1996, **29**, 1349–1358.

[29] Irani C. A., Cozewith C.; J. Appl. Polym. Sci. 1986, **31**, 1839.

[30] Lovinger A.J.; Poly (vinylidene fluoride) in developments in crystalline Polymers, Bassett D.C., 1st Ed., Applied Science Publishers, London (1982).

[31] Hasch B.M., Meilchen M.A., Lee S.-H., M.A. McHugh; J. Polym. Sci. Part B, Polym. Phys. Ed. 1993, **31,** 429–439.

[32] O`Shea K.E., Kimse K.M., Fox M.A., Johnston K.P.; J. Phys. Chem. 991, **95**, 7863.

[33] Ehrlich P., Kurpen J. J.; J. Polym. Sci. Part A 1963, **19,** 1481.

[34] Condo P.D., M.Sc.thesis, State University of New York, **1989.**

[35] Rätzsch M. T., Findeisen R., Sernow V. S.Z.; J. Phys. Chem., 1980, **261**, 95.

[36] De Swaan Arons J., Diepen G. A. M.; Trav. Chim. Pays-Bas 1963, **249**, 82.

[37] Shaffer K.A., Desimone J.M.; Trends Polym. Sci. 1995, **3**, 146.

[38] Scientific group of Prof. Dr. C. Kiparissides, Chemical Process Engineering Institute, Technical University of Theesaloniki, Greece.

[39] Verinau P., Müller M., and Binder K.; New Journal of Physics 2004, **6,** 7.

[40] Gangal S.V., Encyclopedia of polymer Science and Engineering, 2nd edition, Wiley

Interscience New York 1998, **16**, 577.

[41] Cahn J.W., Hilliard J.E.; J. Chem. Phys. 1958, **28**, 258.

[42] Romack T.J., Kipp B.E., and Desimone J. M.; Macromolecules, 1995**, 28**, 8432-8434.

[43] Romack T. J., Combes J. R., Desimone J. M; Macromolecules 1995, **28**, 1724.

[44] Romack T.J., Combes J. R., and DeSimone J. M.; Polymer Preprint, **36**, number 1, April 1995**.**

[45] J. Ellmann, Ph.D thesis, Ulm, 2001.

[46] Kiran E., Crystallization of polyethylene from supercritical fluids, proceeding of 6th international symposium in supercritical fluid, France **2003**.

CHAPTER 4

Phase behavior of novel molecularly designed macromolecular stabilizers in $scCO_2$*.

4.1 Introduction.

Unlike conventional organic solvents, supercritical CO_2 is non-toxic, non-flammable, inexpensive and environmentally beginn. However, it has an extremely weak Van der Waals attraction forces, and its polarizability/volume ratio is less than that of all alkanes except methane. Also, it has no dipole moment (sometimes it has a neglectable dipole moment value due to vibrational mode of C-O bond). Basically, few high molecular weights polymers like poly (fluoroacrylates), poly (dimethyl siloxane) and poly (ether carbonate) are soluble in CO_2. [1-4]

Polymers in general have very limited solubility in $scCO_2$ at temperatures below 80°C. [1, 3,5-10] Although, solubilities in $scCO_2$ can be increased significantly at higher temperatures at elevated pressure [2, 11, 12]. To date, there has been limited literature data of how to correlate the solubility of amorphous polymers in CO_2 to its molecular structure and relevant physical and chemical interactions between polymer and sc solution. Various ideas have been proposed concerning the balance between the van der Waals interactions, polar interactions particularly quadruple-dipole, quadrupole-quadrupole and Lewis acid-base interactions for various classes of polymers in $scCO_2$.

*"Phase behaviour of novel molecularly designed macromolecular stabilizer in $scCO_2$" Fahmy S., Ellmann J, U.Beginn, and M.Moeller, in preparation.

The solubilities of various poly (ether), poly (acrylate), and poly (siloxane) homopolymers and a variety of commercially available block copolymer were measured in CO_2 at 25 to 65°C and pressures of ca. 70 to 410 bar. [13,14] Almost without exception, polymer solubility increases with decreasing surface tension of the polymer, which can be related to the cohesive energy density of the polymer. Whereas, polymers with low cohesive energy densities are more compatible with CO_2 which has very weak van der Waals attraction forces. In polymer/CO_2 system, solubility is governed primarily by polymer-polymer interactions, while polymer-CO_2 interactions play a much smaller role.

Much work has been done focusing on the use of amphiphilic macromolecules to stabilize dispersions of the growing polymer during the polymerization process in $scCO_2$. These surfactants consist of a 'CO_2-philic' segment, almost a siloxane or fluorocarbon and 'CO_2–phobic' segments that interact with the polymer being synthesized. The three main approaches to developing macromolecular stabilizers for usage in CO_2 are: (i) Use of CO_2-compatible polymers (e.g. poly[1,1-dihydroperfluorooctyl acrylate]), (ii) use of 'CO_2-philic' stabilizers bearing a suitable polymerisable group to be incorporated into the growing polymer chain, forming a graft copolymer in situ, [15-17] or (iii) use of block copolymers with 'CO_2- phobic' and 'CO_2-philic' blocks [18-20] or graft systems with a 'CO_2-phobic' backbone and 'CO_2-philic' grafted chains.[21]

Specifically, one of the most soluble polymers in CO_2 is poly (1,1-dihydroperfluorooctylacrylate) (PFOA). Poly (FOA) with a number average molecular weight, $M_n = 10^6$ g/mol can be produced by free radical homogenous polymerization in CO_2.[1, 14] A recent small angle neutron scattering investigation demonstrated that PFOA has a positive second virial coefficient in CO_2 at moderate pressures indicating that CO_2 is thermodynamically good solvent for this polymer. [22] Poly (FOA) homopolymers and copolymers have been used as stabilizers in dispersion polymerization to produce polystyrene and poly (methylmethacrylate). [23, 24] Poly (FOA) is characterized by a lower critical solution temperature (LCST) phase behavior in CO_2. [25]

In the presented work (i) the effect of the macromolecular architecture on the solubility of random- and block copolymers from 1H, 1H, 2H, 2H-perfluorodecylacrylate and

methyl methacrylate is described, particularly for copolymers exhibiting similar molecular weight and composition ratio. (ii) The effect of molecular architecture on the solubility of selected commercial fluorosiloxane copolymers have been investigated as well, which to our best of knowledge have not been reported in the literature so far.

4.2 Experimental section:

4.2.1 Materials:

2,2´-Azobisisobutyronitrile (AIBN) (Aldrich, >97%) was recrystallized from methanol, perfluorododecyliodide (Clariant, >92%) and from toluene. Toluene was dried over sodium and destilled. 1,3-bis(trifluoro-methyl)benzene (α, α, α, α', α', α'-hexafluoro-m-xylene, HFX, Apollo), 1,1,2-trichlorotrifluoroethane (Freon-113, Merck), $CuBr_2$ (Aldrich) and aluminium-oxide 90 (active, neutral, Merck) were used as received. CuCl und CuBr (both Aldrich) were stirred with conc. acetic acid, filtered, washed with methanol and dried in vacuum. 1H,1H,2H,2H-Perfluorodecylacrylate (Apollo) was purified over aluminium-oxide (neutral). Methyl methacrylate (Merck) were destilled from KOH, CaH_2 and degassed. Toluene-4-sulfonyl chloride (Fluka) was recrystallized from hexane. Anisole (Aldrich) and toluene (techn. grade) were destilled from sodium.

Synthesis [26] of random copolymers: MMA (3g) and F8H2MA (64.5g) and 60mL of HFX were weighed into an argon purged 250 mL flask which was equipped with a reflux condenser. The solution was degassed 3 times and the flask was refilled with argon. After the polymerization temperature (60°C) was reached 248mg (1mol%) AIBN were added and the reaction mixture was purged with argon for additional 10min. The reaction was allowed to continue for 72h. After that the reaction solution was diluted with 50mL of Freon-113, the polymer was precipitated in 2L of methanol and dried over night under vacuum in a petri dish at 45°C. Table 4.1, summarized a molecular characterization of resultant copolymer.

^{1}H-NMR (δ in ppm, Freon 113/$CDCl_3$): 1-2 (6H, $-CH_2-CH-$), 2.4 (2H, $-CF_2-CH_2-$), 4.3 (2H, $-O-CH_2-$). ^{13}C-NMR (δ in ppm, Freon 113/$CDCl_3$): 30 ($-CF_2-CH_2-$), 56 ($-O-CH_2-$), 100-125 (fluorinated carbon region), 165 (>C=O). ^{19}F-NMR (δ in ppm relative to $CFCl_3$, Freon 113/$CDCl_3$):.IR: 2956, 2850 (aliphatic CH); 1741 (C=O); 1245, 1206, 1149 (CF).

Table 4.1: *Molecular characterisation of random copolymers from MMA and perfluorooctylethylacrylate monomers.* [26]

Polymer	MMA:F8H2-A [mol %]	Mn g/mol	Mw g/mol	Mw/Mn
$P[MMA_{0.35}$-co-$F8H2A_{0.65}]$	35:65	15000	24.000	1.6
$P[MMA_{0.35}$-co-$F8H2A_{0.65}]$	35:65	16.900	40.600	2.4
$P[MMA_{0.35}$-co-$F8H2A_{0.65}]$	35:65	10.700	24.800	2.3

Synthesis[27] of block copolymers from methyl methacrylate and perfluorooc-ylethylacrylate were synthesized by Atom transfer radical polymerization (ATRP) technique. [28] In a typical experiment, 1 mol equivalent poly(methyl methacrylate) macroinitiator (equals 1.0 g) was filled in a screw cap vial, 0.8 mol equivalents CuBr and 0.8 mol equivalents $6R_f$-TETA were weighed in. Then 1 mL HFX, 3 mL anisole and 50 mol equivalents 1H,1H,2H,2H-perfluorodecylacrylate were added and the vial was sealed. Additionally 5wt% $CuBr_2$, calculated from the mass of CuBr, was weighed in. The solution was degassed 4 times and filled with argon. Then the reaction vial was put in the shaker at 90°C. After 24 h the reaction was ended by cooling down the solution. The raw product was precipitated in methanol, filtered and dried in vacuum at 45°C (raw yield). Then the polymer was dissolved in THF, filtered over a short aluminum-oxide column and precipitated in methanol. Table 4.2 summarizes the molecular characteristics of the compounds.

^{1}H-NMR (δ in ppm, Freon 113/$CDCl_3$): 1-2 (6H, $-CH_2-CH-$), 2.4 (2H, $-CF_2-CH_2-$), 4.3 (2H, $-O-CH_2-$). ^{13}C-NMR (δ in ppm, Freon 113/$CDCl_3$): 30 ($-CF_2-CH_2-$), 56 ($-O-CH_2-$), 100-125 (fluorinated carbon region), 165 (>C=O). ^{19}F-NMR (δ in ppm relative to $CFCl_3$, Freon 113/$CDCl_3$):): -82.1 (3F, $-CF_3$), -114.7 (2F, $-CH_2-CF_2-$), -122.6 - -127.5 (12F, $-CF_2$). IR: 2956, 2850 (aliphatic CH); 1741 (C=O); 1245, 1206, 1149 (CF).

Table 4.2: *Molecular characterisations of block copolymers composed from MMA and perfluorooctylethylacrylate monomers.* [28]

Block Copolymer	Xn_{MMA}/ Xn_{F8H2A}	M_n g/mol	M_w g/mol	M_w/M_n
$PMMA_{156}$-b-$PF8H2A_{94}$	156 : 94	21.000	23.500	1.1
$PMMA_{80}$-b-$PF8H2A_{74}$	80 : 74	9.000	11.000	1.2

$PMMA_{562}$-b-PF8H2A_{189}	562 : 189	71.200	90.500	1.3
$PMMA_{156}$-b-PF8H2A_{144}	156 : 144	20.600	23.100	1.1
$PMMA_{316}$-b-PF8H2A_{228}	316 : 228	32.400	38.800	1.2
$PMMA_{316}$-b-PF8H2A_{2}	316 : 2	35.400	38.500	1.1
$PMMA_{36}$-b-PF8H2A_{45}	36 : 45	21.600	23.200	1.07
$PMMA_{79}$-b-PF8H2A_{39}	79 : 39	12.000	14.100	1.2
$PMMA_{80}$-b-PF8H2A_{104}	80: 104	61.900	92.850	1.5

Fluorosiloxane copolymers: Siloxane polymers end capped with perfluoroalkyl groups named as ά-ω- Perfluoroalkyl polysiloxanes (*LE4385, LE4388*), and siloxane polymers side grafted with perfluoroalkyl polysiloxane (*LE4386, LE4389*) were obtained from (Degussa AG, Essen, Germany) and used as received without further treatments. Figure 4.1 illustrate the chemical characterization of fluorosiloxane.

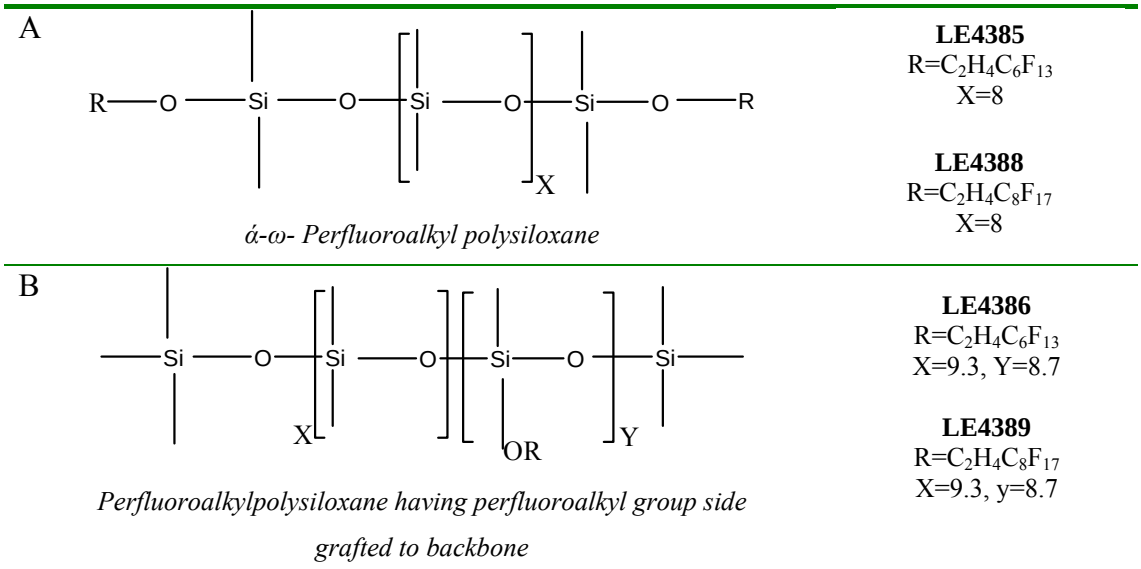

Figure 4.1: *Molecular structure of fluorinated siloxane polymers (A) polysiloxane end capped with perfluoroalkyl group, (B) polysiloxane side grafted with perfluoroalkyl group.*

4.2.2 Methods:

Size Exclusion Chromatography (SEC)***:*** Molecular weights and molecular weight distributions were obtained from SEC runs at 20 °C with tetrahydrofuran (THF) as a solvent. The setup consisted of Waters μ-Styragel columns with nominal pore sizes of

10^5, 10^4 and 10^3 Å and a guard column. Sample detection was done with a Waters 410 differential refractometer. The setup was calibrated with narrow poly (methylmethacrylate) samples from PSS (Mainz). For the calculation of molecular weights, PSS scientific software 3.0 b-61 was used. For a typical run 10 µL of a solution containing 15mg polymer per mL were injected.

Nuclear magnetic resonance: ^{1}H-, ^{13}C- and ^{19}F-NMR spectra were measured in $CDCl_3$ (99.8%, Deutero GmbH) on a Bruker DRX 400 spectrometer at 400 MHz (^{1}H), 50 MHz (^{13}C) and 188 MHz (^{19}F), respectively. Chemical shifts refer to the signal of $CHCl_3$ at 7.24 ppm (^{1}H) and 77 ppm (^{13}C) or to the signal of $CFCl_3$ at 0 ppm (^{19}F).

4.2.3 Phase behavior determination:

The detailed experimental high pressure setup used for determination of the cloud point of polymer-SCF mixture has been described in chapter 3 of this thesis. Typically, turbidity measurement has been performed according to the following manner: a pre-weight amount of solid polymer (ca. 0.3-0.7± 0.02 g) was inserted in the view cell prior to pressurization. Then CO_2 was purged at 3-6 bar to remove any entrapped air right before conducting the experiment. Precipitation measurements were carried out by increasing the system volume using the spindle pump to a situation where a cloudy solution can be distinguished in the cell. All cloud point determinations were repeated at least three times. Reproducibility was within an accuracy range of ± 1.0°C and ± 5-10 bar. Where, cloud-point pressure is defined as the point at which the solution becomes so opaque that it is no longer possible to distinguish the stir bar in solution. Cloud points were determined visually. Subsequent to the cloud point observations the view cell was cooled down to ambient temperature and followed by venting carbon dioxide with a very low depressurization rate. Polymer concentration was chosen to be 2 & 5 wt%. These values should be in vicinity of the maximum in the pressure-composition diagram. [29, 30]

4.3. Result &Discussion:

4.3.1 Cloud point curves for fluoroacrylate copolymers:

Scheme 1 depicts the molecular structure of the macromolecules under investigation in the current study, namely (Scheme 1a) block copolymers from 1H, 2H, 2H-perfluorodecylacrylate and methyl methacrylate as well as random copolymers (Scheme 1b) made up from these monomers. The details on composition and molecular weights are summarised in the experimental part (cf. Table 4.1 and Table 4.2). Both polymer classes were prepared with standard methods, e.g. atom-transfer radical polymerisation (ATRP) for the block- and free radical polymerisation for the random copolymers. [32]

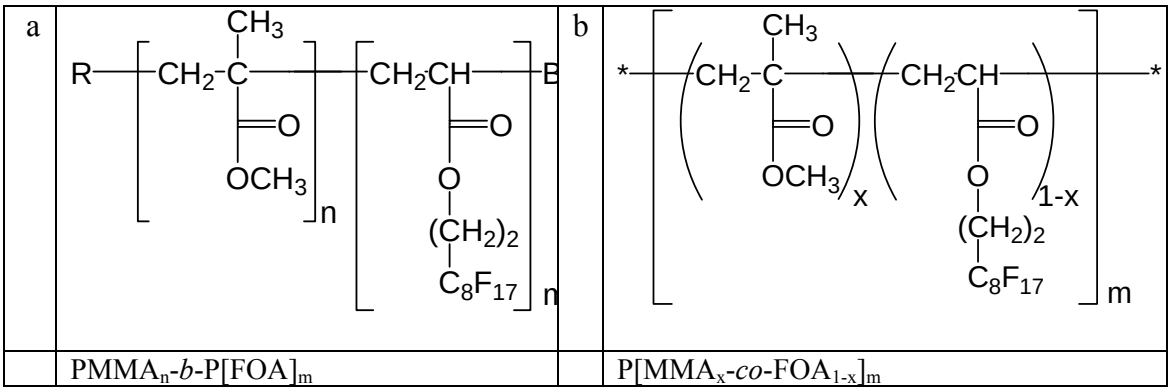

Scheme 1: *Structure formula of (a) block- and (b) random copolymers from 1H, 2H, 2H-perfluorodecylacrylate and methylmethacrylate.*

In a variable volume view cell the mixture of polymer and CO_2 was equilibrated under stirring condition prior to measurement. Cloud point lines separating the regions of solubility from the area of phase segregation in the pressure/temperature diagram were subsequently measured by isothermal depressurization technique experiment with corresponding solution (cf. experimental part). At given temperature, one phase exist at pressure above cloud point pressure.

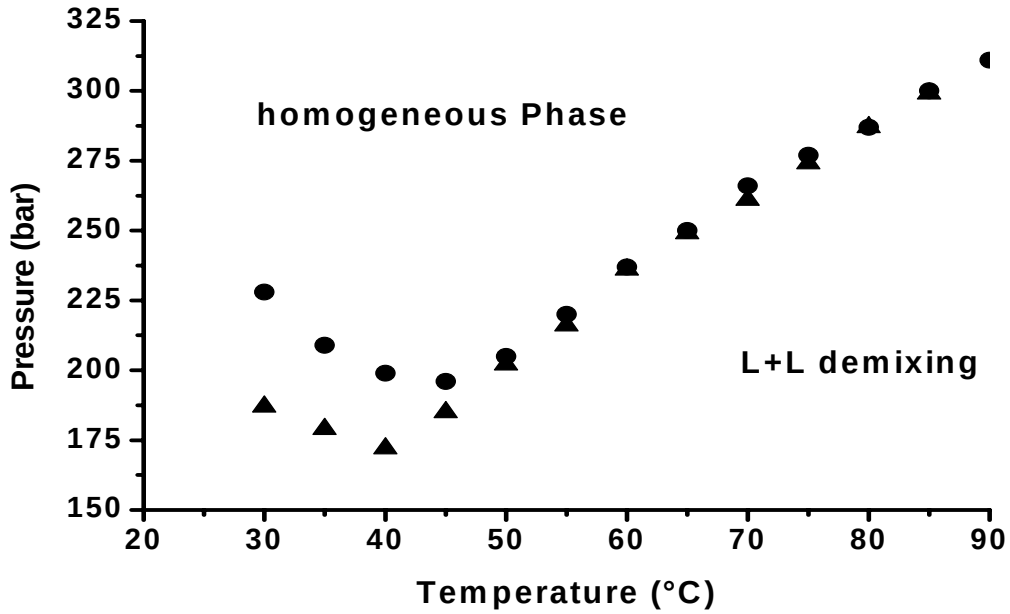

Figure 4.2: *Effect of polymer concentration on the solubility of $P(MMA)_{156}$-b-$P(F8H2A)_{144}$ in $scCO_2$ (● = 2 wt%, ▲ = 5 wt %).*

Figure 4.2 reveals the cloud point curves for $P(MMA)_{156}$-b-$P(F8H2A)_{144}$ at two different concentrations 2wt% and 5 wt%, respectively. The curve consists of two distinct branches below 40°C and above 50°C. The low temperature branches are characterized by negative slopes (2 wt%: -2.9 bar/K, 5 wt%: -1.5 bar/K) as well as concentration dependent L+L border positions. Note that in this regime the solubility is enhanced with increasing concentration. Above 50°C both curves coalesce into a single line of positive slope (dP/dT = 1.8 bar/K). Between 40 and 50°C the cloud point curves pass through a minimum with a concentration dependent position (2 wt%: 44 °C / 194 bar, 5 wt%: 41 °C / 172 bar). Obviously seen at given pressure below 225 bar, block copolymer exhibits a lower critical solution temperature characteristic. A similar trend of the cloud point curve has been reported [31] with poly (dimethylsiloxanes) in $scCO_2$.

The occurrence of LCST (Lower critical solution temperature) for $P(MMA)_{156}$-b-$P(F8H2A)_{144}$ is a consequence of both a large difference in the free volume exerting between solute and solvent (i.e. CO_2), and thermal expansion between fluorinated block copolymers and CO_2. Where in the later case, CO_2 is more compressible than fluorinated block copolymer; it gains a more free volume and entropy during expansion. An increase in temperature or decrease in pressure causes a larger expansion of CO_2 than the polymer. Consequently, phase separation between polymer and CO_2 results in an increase in the block copolymer segmental interactions due to localized densification.

Figure 4.3 shows a comparative pressure/temperature diagram for a series of five block copolymers with different block ratios of P(MMA)/P(F8H2A) covering a molar fraction of PMMA from 0.28 (n=80, m=104) to 0.62 (n=156, m=94). As illustrative example P $(MMA)_{156}$-b-$P(F8H2A)_{144}$ was discussed in detail in Figure 4.2.

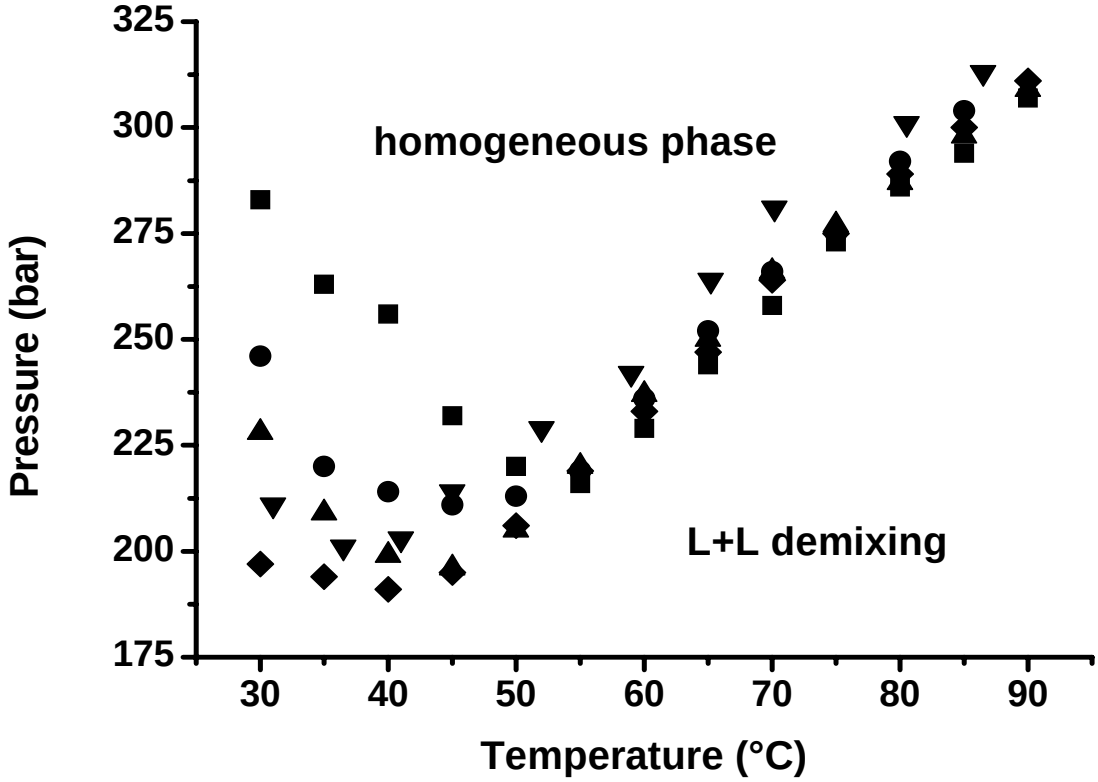

Figure 4.3: *Cloud point diagram for 2 wt% solutions of $P(MMA)_n$-b-$P(F8H2A)_m$ block copolymers (■: n = 80, m = 104, ●: n = 80, m = 74, ▲: n = 156, m = 144, ▼: n = 36, m = 45, , ◆: n = 156, m = 94).*

The shape of the cloud point curves is similar among all other soluble block copolymers, note that the block copolymer of $P(MMA)_{569}$-b-$P(F8H2A)_{189}$, $P(MMA)_{316}$-b-$P(F8H2A)_{228}$ and $P(MMA)_{316}$-b-$P(F8H2A)_2$ were found to be insoluble up to 1100 bar & 85°C; where all this block copolymer contains a higher content of CO_2-phobic group comparing to CO_2-philic moieties. As observed in the above diagram all block copolymer exhibits a minimum with lower solution temperature as can be obviously seen. Only the low temperature branch of the cloud point curve was found to be dependent strongly on the polymers composition, while the high temperature branch showed minor variation in the cloud point position. The best solubility was recorded for P $(MMA)_{156}$-b-$P(F8H2A)_{94}$, while the highest pressure needed to obtain a single phase mixture was recorded for $P(MMA)_{80}$-b-$P(F8H2A)_{104}$.

Based on above mentioned observation, we can conclude that there should be a proper block length ratio balancing the fluorinated and non-fluorinated segments length of block copolymer in order to guarantee a strong interaction between block copolymer and $scCO_2$, subsequently a significant shift in the location of L+L demixing to lower values.

Regarding statistical copolymer, figure 4.4 depicts a synopsis on the cloud point curves of random copolymers from MMA and F8H2A in $scCO_2$. In order to investigate the effect of molecular weight on the position at which phase segregation take place. A serious of random copolymers was intendely synthenthized using a convential free radical polymerization technique. As can be seen in figure 4.4, all random copolymers containing almost 35 mol% MMA and 65 mol% F8H2A (i.e. $P[MMA_{0.35}$-co-$F8H2A_{0.65}]$) with different number average molecular weight values (cf. experimental section). Figure 4.4 compare the cloud point curves of statistical copolymers for two number average molecular weights (M_n=10.700 g/mol and M_n=16.900 g/mol) at two concentrations 2 wt% and 5 wt %, respectively. Where, the cloud point pressures monotonically grow with increasing temperature. The four curves almost run parallel, exhibiting an average slope of 3.6±1 bar/K. With the random copolymers a simple relation can be driven between cloud point, molecular weight and concentration as a follow; with increasing molecular weight and increasing concentration the cloud point pressures grow up.

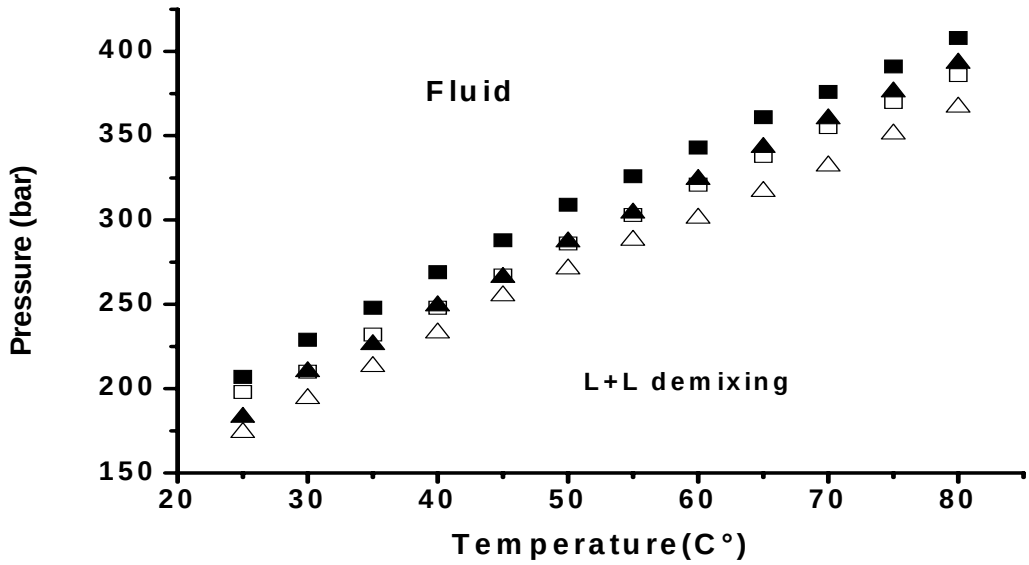

Figure 4.4: *Cloud point curves for random copolymers $P[MMA_{0.35}$-co-$F8H2A_{0.65}]_n$ in $scCO_2$ (M_n = 16.900 g/mol, M_w=40.600 g/mol: □ = 2 wt% ,■= 5 wt% and M_n =10.700 g/mol, M_w=24.800g/mol: △= 2 wt%, ▲ = 5 wt%).*

Figures 4.5 compare the solubility behaviour of random and block copolymers. Although the weight average molecular weight of the block copolymer (M_w = 92.850 g/mol) is almost four times greater than that of the statistical copolymer (M_w = 24.000 g/mol), Moreover block copolymer contains a larger fraction of CO_2 insoluble MMA units (f_{MMA}^{block} = 0.43, f_{MMA}^{random} = 0.35) it exhibits lower cloud point pressured with temperature. Herewithin, the presented data suggests so far that block copolymers could be possible to employ as good stabilizer for dispersion polymerization of PVDF in $scCO_2$ at convential polymerization temperature (ca. 40-50°C) rather than random copolymer do.

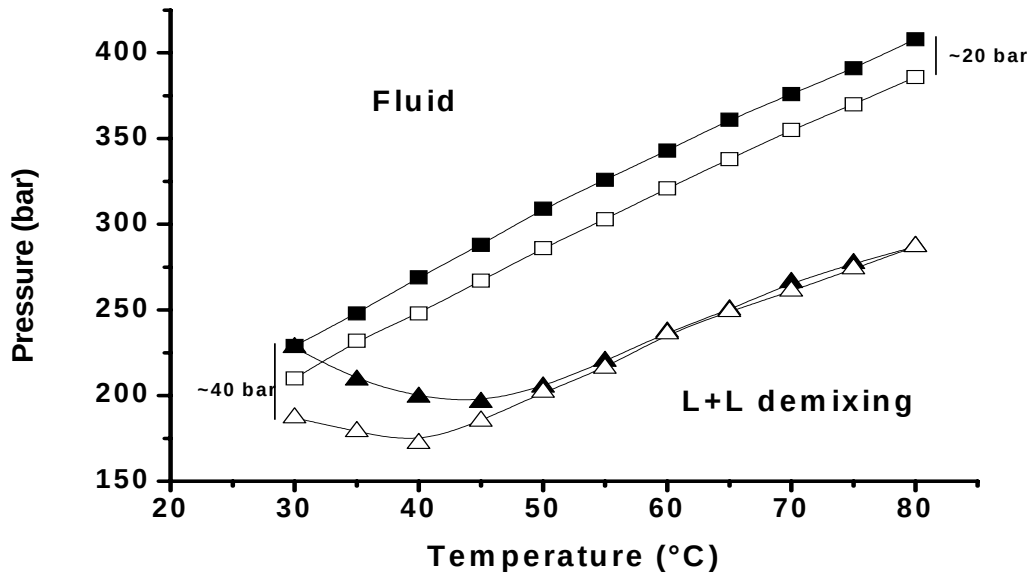

Figure 4.5: *Comparison of cloud point curves from random copolymers $P[MMA_{0.35}$-co-$F8H2A_{0.65}]_n$ (M_w = 24.000 g/mol: □ = 2 wt%, ■= 5 wt%) and block copolymers $P(MMA)_{80}$-b-$P(F8H2A)_{104}$ (M_w = 92.850 g/mol △= 2 wt%, ▲ = 5 wt%).*

4.3.2 Fluorosiloxane copolymer:

As previously mentioned, flourpolymers are the most soluble compounds in CO_2. Due to weak Van der Waals forces between fluorinated moieties, also the high interfacial tension of fluorinated polymer making them highly compatible with carbon dioxide. At the same time, siloxane polymers are highly soluble in carbon dioxide due to large flexibility of polymeric chain. Merging this advantage of both sorts of polymers into a one polymer (named as fluoro-siloxane) will guarantee extremely high miscibility in carbon dioxide. In the following text the phase diagram of fluorosiloxane in $scCO_2$ will be discussed in details.

Referring to above commercial fluorosilioxane, the fluorinated groups are grafted either within main chain (α-ω- Perfluoroalkyl polysiloxanes) or grafted as side chain (perfluoroalkylpolysiloxane) (cf. Figure 4.1). In figure 4.6, there is no significant effect seen upon increasing the fluorinated chain length from $C_2H_4C_6F_{13}$ to $C_2H_4C_8F_{17}$ for α-ω- Perfluoroalkyl polysiloxanes; on the phase diagram in $scCO_2$. Whereas, both polymers show a positive slope relationship as well as linearity in P-T diagram in $scCO_2$, i.e. increasing in temperature necessitates the increase in cloud point pressure to attain enough high solvent density to solvate polymers.

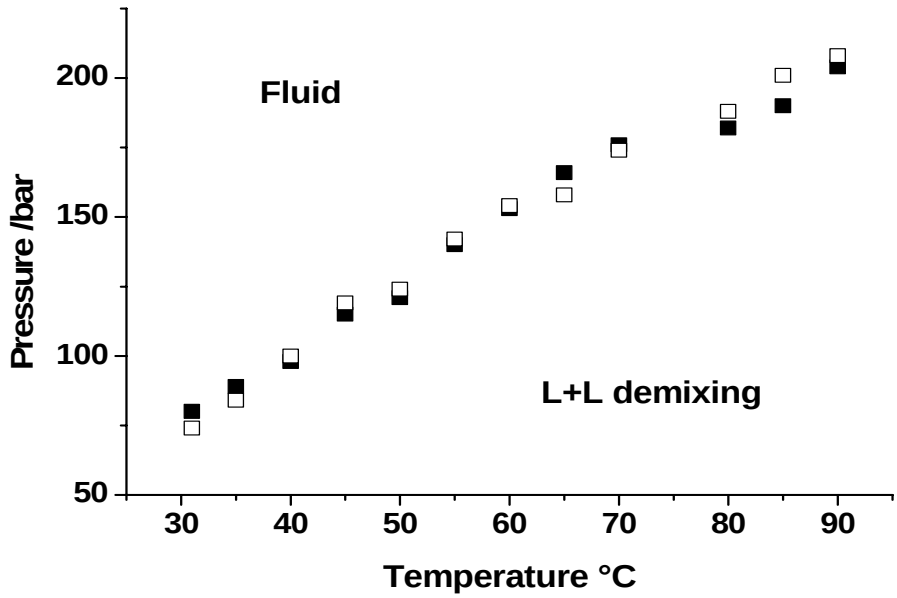

Figure 4.6: *Cloud point curves for (□) 5 wt% and (■) 5 wt %* α-ω- Perfluoroalkyl polysiloxanes *having $C_2H_4C_6F_{13}$ and $C_2H_4C_8F_{17}$ fluorinated end capped group in $scCO_2$, respectively.*

Figure 4.6 reveals that increasing the degree of fluorination from $C_2H_4C_6F_{13}$ to $C_2H_4C_8F_{17}$ for α-ω- Perfluoroalkyl polysiloxanes; the liquid/liquid demixing will not significantly affected. It's interesting to notice that fluoro-siloxane exhibits positive slop in P-T phase behaviour in carbon dioxide which is in contrary to reported literature regarding fluoropolymers behaviour (i.e. decreasing cloud point pressure with increasing temperature) in $scCO_2$. The reseaon of this unusual trend is still unclear. On other hand, siloxane polymers with fluorinated alkyl side chains show lower solution temperature behaviour, as illustrated in Figure 4.7.

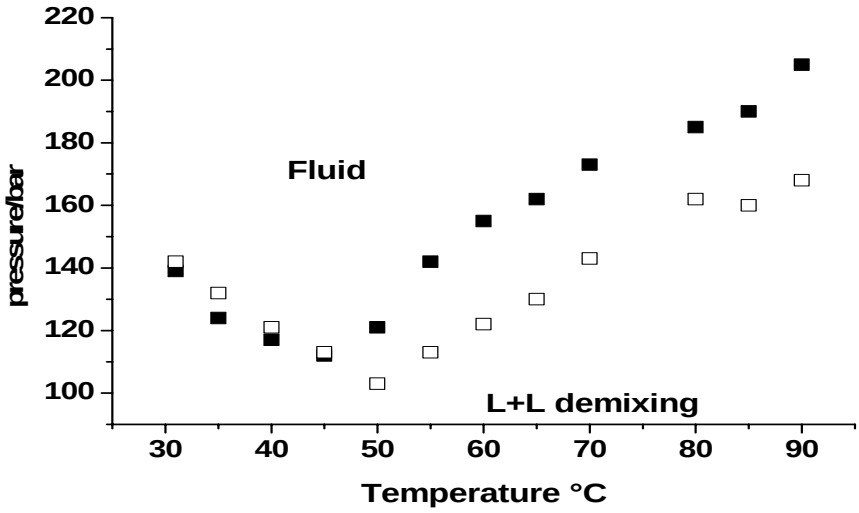

Figure 4.7: *Cloud point curves for (□) 5 wt% and(■) 5 wt %* Perfluoroalkyl polysiloxanes *having* $C_2H_4C_6F_{13}$ *and* $C_2H_4C_8F_{17}$ *fluorinated grafted side group in* $scCO_2$*,, respectively.*

Comparing the cloud point data for the two classes of fluorosiloxane polymer, one can conclude that impact of fluorination is relatively the same for both siloxane polymers at higher temperature (>50°C). Presences of fluoroalkyl- group in the main chain (α-ω-Perfluoroalkyl polysiloxanes) tends to improve solubility (i.e. lower cloud point) rather than grafting at side chain at low temperature regime while the at high temperature both fluorosiloxane polymer exhibit the same cloud points characteristics (cf. Figure 4.8).

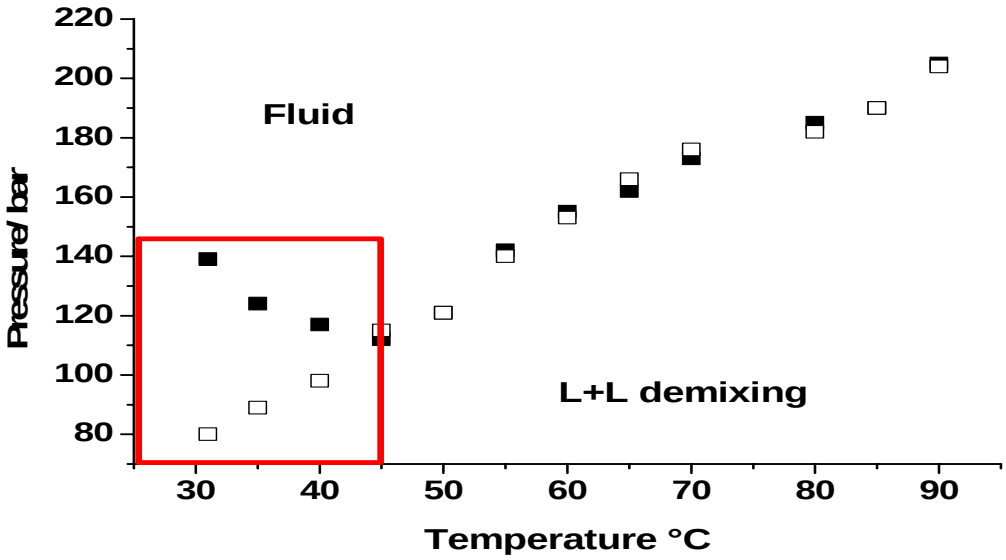

Figure 4.8: *Cloud point curve for (□) 5 wt %* α-ω- Perfluoroalkyl polysiloxanes containing $C_2H_4C_6F_{13}$ *group in the main chain, and (■) 5 wt %* Perfluoroalkyl polysiloxanes having $C_2H_4C_6F_{13}$ *group as side grafts in* $scCO_2$.

4.4. Conclusion

In this work we addressed the effect of the molecular structure on the solubility of statistical and block copolymers of the same constituents i.e. 1H, 1H, 2H, 2H-perfluorodecylacrylate (F8H2A) and methyl methacrylate (MMA). The block copolymers are better soluble than statistical copolymers; as they exhibited lower solution temperature behaviour. Above 50°C the block copolymers solubility was hardly depends on the block length ratio.

In direct comparison, block copolymers constitute from fluorinated acrylate segment and MMA segment exhibit a better solubilities in carbon dioxide even with higher molecular weights and having lower content of CO_2-philic groups in its main chain. The results clearly demonstrate that skilful selection of the polymers architecture is of larger importance for creation of CO_2 soluble macromolecules than the simple selection of the "right" composition. Its worthwhile to emphasis that based on presented cloud point data we have measured; block copolymer of $P[MMA]_x$-b-$P[F8H2A]_y$ can be employed as good stabilizer for PVDF during its synthesis through dispersion polymerization process rather than P[MMA-co-F8H2A] does.

Impact of fluorination is relatively the same for siloxane polymers, whether fluorinated chain exists in the main polymeric chain or as side chain. Only, at lower temperature regime the presence of perfluoroalkane group in main polymeric chain tend to enhance solubility rather than its existence as a side chain of polysiloxane; as a decreasing free volume difference between polymer and CO_2 results in decreasing the pressure needed to obtain a one single phase solution.

4.5 References:

[1] DeSimone J.D., Guan Z., Elsbernd C.S.; Science 1992, **257,** 945-947.

[2] Garg A., Dulari E., Manke C.W.; Macromolecules 1994, **27**, 5643.

[3] Hsiao Y. –L, Maury E. E., DeSimone J.M., Mawson S., Johnston K.P.; Macromolecules 1995, **28**, 8159-8166.

[4] Mawson S.M., Johnston K.P., Combes J.R., DeSimone J.M.; Macromolecules 1995, **28**, 3182-3191.

[5] McHugh M.A., Krukonis V.J.; Supercritical Fluid Extraction Principles and Practice, Butterwotths, Stoneham, MA, 1994.

[6] Danesshvar M., Kim S., Gulari E.; J. Phys. Chem 1990, **94**, 2124.

[7] Hoefling T.A., Enick, R. M. E., Bechman J.; J. Phys. Chem. 1991, **95**, 7127-7129.

[8] Hoefling T.A., Beitle R.R., Enick R.M., Beckman E. J.; Fluid Phase Equilib. 1993, **83**, 203.

[9] Hoefling T.A., Neuman D.A., Enick R.M.; J. Supcrit.Fluids 1993, **6**, 165.

[10] McFann G.J., Johnston K.P., Howdle S.M.; AlChE, 1994, **40**, 543-554.

[11] Mertdogan C.A., Byun H.-S., McHugh M. A., Tuminello W.H.; Macromolecules, 1996.

[12] Takishima S., Johnston K.P., O'Neil M. L.; Ind. Eng. Chem. Res. 1997, **36**, 2821.

[13] O'Neil M.L., Cao Q., Fang M., Johnston K. P., Wilkinson S. P., Smith C. D., Kerschner J.L., Jureller S.H.; J. Supercrit. Fluid, 1997.

[14] DeSimone J.M., Maury E.E., Menceloglu Y.Z., McClain J.B., Romack T.J., Combes J.R.; Science 1994, **265**, 356-9.

[15] Shaffer K.A., Jones T.A., Canelas D.A., DeSimone J.M., Wilkinson S.P.; Macromolecules 1996, **29**, 2704-6.

[16] O'Neil M.L., Yates M.Z., Johnston K.P., Smith C.D., Wilkinson S.P.; Macromolecules 1998, **31**, 2838-47.

[17] O'Neil M.L., Yates M.Z., Johnston K.P., Smith C.D., Wilkinson S.P.; Macromolecules 1998, **31,** 2848-56.

[18] Guan Z., DeSimone J.M.; Macromolecules 1994, **27**, 5527-5532.

[19] Canelas D.A, Desimone J.M.; Macromolecules 1997, **30,** 5673-82.

[20] Hems W.P., Yong t., Van Nunen J.L.M., Cooper A.I., Holmes A.B., Griffen D.A.; J Mater Chem. 1999 , **9**, 1403-7.

[21] Lepilleur C., Beckmann E.J.; Macromolecules 1997, **30**, 745-56.

[22] McClain J .B., London D., Combes J.R., Romack T. J., Canelas D. A., D. E. Betts, Wignal G.D., Samuliski E.T., DeSimone J.M.; J.Am. Chem. Soc. 1996, **118**, 917-918.

[23] Canelas D.A., Betts D.E., DeSimone J. M.; Macromolecules 1996, **29**, 2818.

[24] Peck D.G., Johnston K.P.; Macromolecules 1993, **26**, 1537-1545.

[25] Meilchen M.A., Hasch B.M., McHugh M.A.; Macromolecules 1991, **24**, 4974-4982.

[26] Reza Najjar, Ph.D thesis, RWTH-Aachen, in progress.

[27] Jürgen Ellmann, Ph.D thesis, Ulm, 2001.

[28] Patten T., Xia J., Abernathy T., Matyjaszewski K.; Science 1996, **272**, 866.

[29] LoStracco M. A., Lee S.-H., McHugh M. A.; Polymer 1994, **35**, 3272.

[30] Kirby C. F., McHugh M. A.; Chem. ReV. 1998, **99**, 565-602.

[31] Xiong Y. and Kiran E.; Polymer 1995,**36**, 4817-4826.

[32] Ostu T., Yoshida M. ; Makromol. Rapid Commun. 1982, **3**, 127.

4.6 Appendix

On the miscibility of novel designed siloxane block and statistical copolymers in $scCO_2$

A new molecularly designed block (so-called palm tree) and random copolymers of polydimethylsiloxane-methacrylate macromonemer (molecular weight~ 1000 g/mol), $P[(PDMS\text{-}MA)_{1000}]$-Br and methylmethacrylate (MMA) monomer have been prepared by atom transfer radical (ATRP) polymerization, and controlled free radical polymerization, respectively (cf. Figure 4. 9).

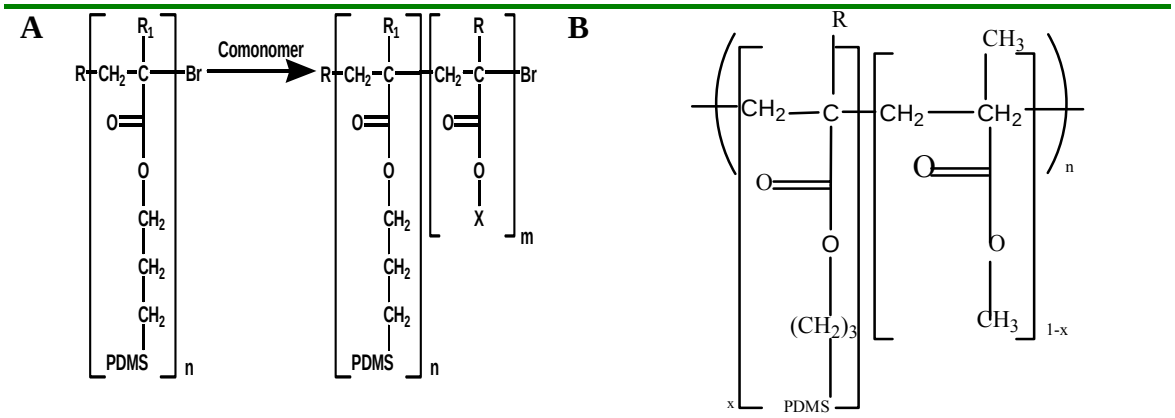

Comonomer: methymethacrylate
X= R_1=R= CH_3

Figure 4.9: *Chemical structure formulas of A) Block copolymers from MMA and $P[PDMS\text{-}MA]_{1000}$ macromomomer, and B) Statistical copolymers from MMA and $P[PDMS\text{-}MA]_{1000}$ macromomomer (Palm tree polymer).*

Polymer synthesis and characterizations. [1]

Material: The molecular weight of poly(dimethylsiloxane) macromer was varied between M_n=1 and 5 kg mol^{-1} (supply by Chisso and Shin-Etsu) the compounds were pre-purified prior to use by filtration over a two-layer column of silica gel (20 cm) and aluminum oxide (Al_2O_3) (20 cm) using absolute chloroform as mobile phase. Methyl methacrylate (Merck, MMA) was distilled over CaH_2 under vacuum, dimethyl-2,2'–azobisisobutyrate (V-601, Wako) was used as received. CuBr (Fluka, 95%) was purified by stirring overnight in glacial acetic acid at room temperature. After filtration it was washed with ethanol several times and then dried for 72 hours at 100°C. $CuBr_2$ (Merck, 98%) and Ethyl-2-bromoisobutyrate (Aldrich, 98%, I_0) were used as received. The ligand 1,1,4,7,10,10-hexamethyltriethylenetetramine (Aldrich, 97%, HMTETA) was used as received and tris[2-(N,N-dimethyl)ethyl]amine (Me_6Tren) was synthesized.

Chlorobenzene (Merck 98%, C_6H_5Cl) was distilled over $LiAlH_2$ under argon atmosphere.

Block copolymer: (1- Macromer M_n=1.000g mol^{-1}):1-mmol (5-grams) of poly (dimethylsiloxane methacrylate), M_n = 1.000 g/mol (= $PDMS_{1.000}$-MA) with was weighed into a 100-mL two-necked flask, 4-mol% of initiator (Wako V-601) was added and dissolved in 12.5-mL of dried benzene. The flask was sealed with a rubber septum, purged with nitrogen, and heated to 60°C after three freeze–thawing cycles. The polymerization of the macromer was carried out during 24 hours of reaction time. Than the excess of solvent was removed at reduced pressure at –70^0C. A 100-mL separation funnel was charged with the mixture of homopolymer / remnant macromer and a mixture of methanol/diethyl-ether (1:1) was added to the funnel. The solution was shaken thoroughly, and the separated light phase contained the unreacted macromer. The unreacted macromer was recuperated by slowly evaporation of the solvent mixture at room temperature to avoid further polymerization of the macromer. (2- Homopolymerization preparation of P[PDMS-$MA_{1.000}$]Br): polymerizations were carried out in a 20-mL glass bottle with PTFE septa coated screw caps. PDMS-$MA_{1.000}$ (macromer) was evacuated overnight and back-filled with nitrogen. CuBr, $CuBr_2$ and the ligand (Me_6Tren or HMTETA) were weighted in the glass bottle Subsequently macromer and the solvent were added. The solutions were degassed with nitrogen several times; the initiator was injected using a microsyringe under nitrogen. Then the mixtures were allowed to stir at 90^0C for 24 hours. The un-reacted macromer was removed by precipitation first in methanol and a second precipitation in a mixture of methanol / diethyl-ether (1:1). The precipitated product was re-dissolved in absolute chloroform and passed through a short column of alumina oxide to remove the copper salts. The products were dried under vacuum overnight at room temperature. (3- Block copolymerization): Polymerizations were carried out in a 20-mL glass bottle with PTFE septa coated screw caps. The macroinitiator poly(PDMS-MA)-Br was evacuated overnight and back-filled with nitrogen. Methyl methcrylate, CuBr and $CuBr_2$ were weighted in the glass bottle. Then same procedure was repeated as mentioned above in homopolymeriaztion of P[PDMS-$MA_{1.000}$]-Br. The samples were characterized by NMR and SEC to exceed a purity of 98%. Table 4.3 summarizes the molecular characteristics of the

Random copolymers from methyl methacrylate and P[(PDMS-MA)$_{1000}$]-Br macromonmer were prepared by conventional free radical polymerisation. After synthesizing of prepolymer (i.e. P[PDMS-MS$_{1000}$]-Br), a free radical copolymerization was carried out by mixing a known amount of prepolymer, Mn = 1.000 g/mol (= PD-MS$_{1.000}$-MA) and MMA (recrystallized from methanol) in a 100-mL two-necked flask, 4-mol% of initiator (Wako V-601) was added and dissolved in 12.5-mL of dried benzene. The flask was sealed with a rubber septum, purged with nitrogen, and heated to 70°C. A polymerization process was carried out for 24 hr and excess solvent was removed at reduced pressure, then a solid polymer powder was collected. Then samples were characterized by SEC.

Table 4.3: *Molecular characterisation of block and random copolymers from MMA and P[(PDMS-MA) $_{1000}$]-Br macromonmer.*

Polymer	M_w kg/mol†	PDI
P [(PDMS-MA) $_{1k}$]$_8$-b-P[MMA]$_{180}$	210.8	2.3
P [(PDMS-MA) $_{1k}$]$_6$-b-P[MMA]$_{58}$	195.0	1.7
P [(PDMS-MA) $_{1k}$]$_{17}$-b-P[MMA]$_{17}$	35.6	1.6
P [((PDMS-MA) $_{1k}$)$_{20}$-co-PMMA$_{80}$]	194.9	2.3
P [((PDMS-MA) $_{1k}$)$_{33.2}$-co-PMMA$_{68.8}$]	197.1	2.4

† determined by measuring GPC in THF solvent standardized against PMMA.

Result & discussion

Figure 4.10 reveals the liquid/liquid segregation lines for different polymer concentration of the random copolymers investigated in this study so far.

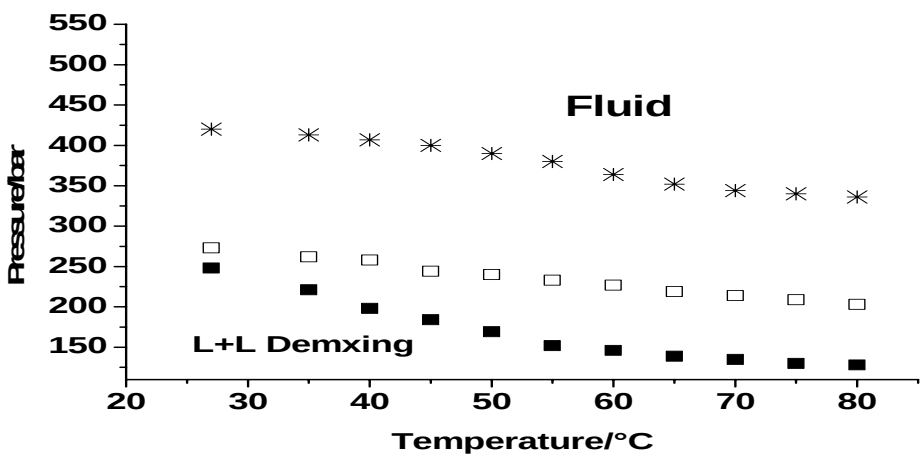

Figure 4.10: *Cloud point curves of (■)0.5 wt% and(□)1.0 wt % of P[((PDMS-MMA)$_{1000}$)$_{33.2}$-co-MMA$_{66.8}$];M_w = 197.1Kg/mol and (∗) 0.1 wt % P[((PDMS-MA)$_{1000}$)$_{20}$-co-MMA$_{80}$] M_w= 194.9 Kg/mol in scCO$_2$.*

Figure 4.10 depicts, for both 0.5 and 1.0 weight percent concentration of $P[((PDMSMA)_{1000})_{33.2}$-co-$MMA_{66.8}]$; the cloud point pressure decreases with increasing temperature. On other hands, increasing the amount of MMA monomer in the polymer backbone from 66.8 to 80% does not show higher miscibility even for the almost similar molecular weight samples. Since PMMA is considered as CO_2 phobic moiety. The difficult miscibility of random copolymer with higher MMA contents in $scCO_2$ may be argued due to increasing the surface tension of polymer with increasing the MMA percentage leading to increasing in the pressure required to solvate copolymer.

On other hand, cloud point curves for block copolymers are shown in Figure 4.11. Where, the pressure for $P[(PDMS\text{-}MA)_{1000}]_8$-b-$P[MMA]_{180}$ was observed to decrease with increasing temperature at constant pressure up to 45°C. But as the solution temperature is further increased the trend is reversed and the demixing pressures increases with temperature. This behaviour might be due to the decrease in solvent density with increasing temperature. Since density not pressure is a natural variable for understanding solvation in supercritical fluids.

It's worthy to note that, the effect of block ratio is a crucial parameter to understand the miscibility of block copolymer in $scCO_2$. By altering the block ratio of MMA and $[(PDMS\text{-}MA)_{1000})]_8$, the cloud point pressure changes significantly in P-T diagram. As an example decreasing MMA block ratio from 180 to 58 in block copolymer, while keeping $P[(PDMS\text{-}MA)_{1000}]_x$ block length and molecular weights almost the same enhance the solubility of the overall copolymer in sc fluid. For example, 1.0 wt% $P[(PDMS\text{-}MA)_{1000}]_8$-b-$P[MMA]_{180}$ (M_w=210.8 kg/mol) at 50°C the cloud point pressure was observed to decrease from 340 bar to 280 bar for $P[(PDMS\text{-}MA)_{1000}]_6$-b-$P[MMA]_{58}$ (M_w=195.0 kg/mol) at the same temperature.

Abetter solubility of copolymer in CO_2 can be achieved by balancing the block length between MMA and $[(PDMS\text{-}MA)_{1000})]_x$ segments. Where, for 1.0 wt % $P[(PDMS\text{-}MA)_{1000}]_{17}$-b-$P[MMA]_{17}$ (M_w=35.6 kg/mol) at 35°C solubility has been increased by ~150 bar rather than 1.0 wt % of $P[(PDMS\text{-}MA)_{1000}]_8$-b-$P[MMA]_{180}$ at the same temperature. This indicates the importance of balancing the block ratio on understanding the miscibility of block copolymer in $scCO_2$. (cf. Figure 4.11)

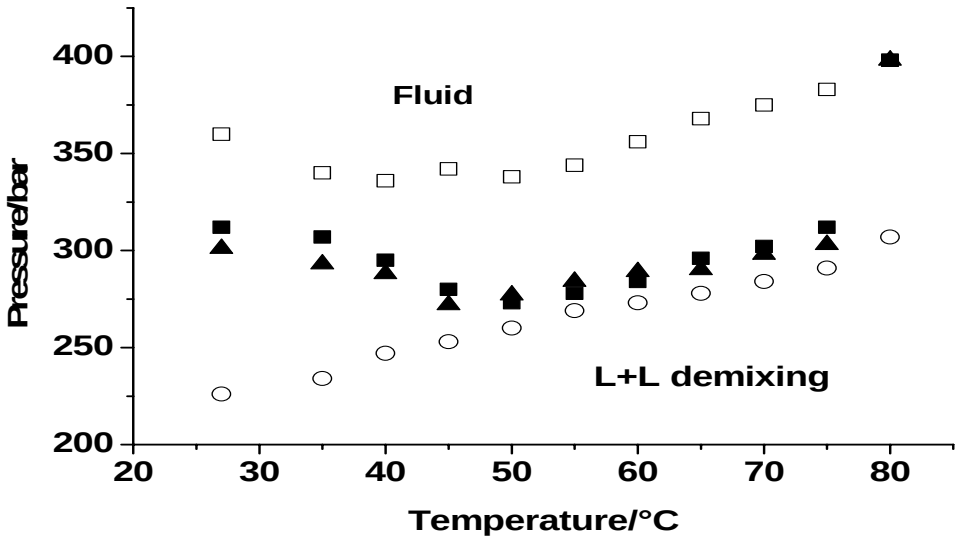

Figure 4.11: *Cloud point curves of (■) 0.5 wt%, and (□) 1.0 wt % of P [(PDMS-MA)* $_{1000}]_8$*-b-P[MMA]*$_{180}$ *,*M_w*=210.8 Kg/mol and (▲) 1.0 wt % P [(PDMS-MA)*$_{1000}]_6$*-b-P[MMA]*$_{58,}$ M_w*=195.0 Kg/mol, and (O) 1.0 wt % P[(PDMS-MA)*$_{1000}]_{17}$*-b-P[MMA]*$_{17}$ *in* $scCO_{2.}$

By comparing random and block copolymer with similar molecular weights (cf. Figure 4.12) it was found that block copolymer exhibits a LCST temperature characteristic, while random copolymer shows a decrease in cloud point pressure with increasing temperature even at temperature up to 80°C. Where, CO_2's density decreases dramatically.

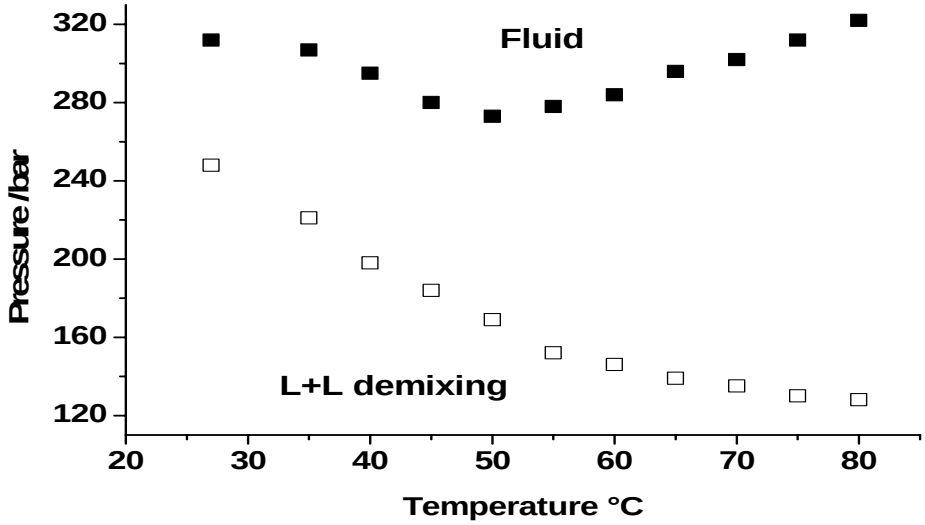

Figure 4.12: *Comparison cloud point curves of (■) 0.5 wt%, of P[(PDMS-MA)* $_{1000}]_6$*-b-P[MMA]*$_{58}$ M_w *=195.0 Kg/mol, and (□) 0.5 wt% P[((PDMS-MA)* $_{1000})_{33.2}$*-co-MMA*$_{68.8}$*]* M_w *= 197.1 Kg/mol in* $scCO_2$*.*

Generally, random copolymer composed from $P[(PDMS\text{-}MA)_{1000}]_x$ and methylmethacrylate (MMA) depicts a higher degree of solubility in carbon dioxide rather than block copolymer of the same composition and molecular weights. For example to form homogenous solution with CO_2 at 40°C, the cloud point pressure required for 0.5 wt % $P[((PDMS\text{-}MA)_{1000})_{33.2}\text{-co-}MMA_{66.8}]$ (M_w = 197.1Kg/mol) is about ~80 bar lower than CP for $P[(PDMS\text{-}MA)_{1000}]_6\text{-b-}MMA]_{58}$ (M_w = 195.0 Kg/mol) at the same temperature. Finally, an observation can be concluded that, the liquid-liquid demixing pressure for random copolymer was found to be about 130 bar lower than that for block copolymer at given temperature.

Conclusion

Newly molecular design random and block macromolecule stabilizers have been successfully prepared either by controlled free radical polymerization between $P[((PDMS\text{-}MMA)_{1000})_x]$-Br and methylmethacrylate (MMA) or atom transfer radical polymerization technique, respectively.

Upon increasing temperature, block copolymer $P[(PDMS\text{-}MMA)_{1k}]_x\text{-b-}P[MMA]_y$ shows a LCST solution behaviour in P-T diagram in $scCO_2$. Since PMMA was reported as $scCO_2$–phobic moiety, increasing weight percent of MMA either in block or random copolymer results in increasing the liquid-liquid demixing pressure to high values i.e. difficult solubility condition.

Random copolymer of $P[((PDMS\text{-}MA)_{1000})_x\text{-co-}MMA_y]$ exhibits a lower cloud point pressure in carbon dioxide rather than block copolymer of approximately same composition. More generally, random copolymer occupy a large free volume than block copolymer which turns out in decreasing the free volume difference between statistical copolymer and CO_2 leading to enhancing solubility.

Reference

[1] Ana Morales, Ph.D Thesis, Ulm, 2004.

CHAPTER 5

Impact of low and high molecular weight additives on the solubility of PVDF in $scCO_2$*.

5.1 Introduction.

Polymer chemists have developed the use of $scCO_2$ as an alternative solvent for polymerization reactions. [1, 2, 4] However, the majority of research work was carried out on polymerization of amorphous MMA and styrene. Because of the significant solubility of amorphous fluoropolymers in CO_2, researchers have explored the use of carbon dioxide as an alternative solvent for the synthesis of fluoropolymers by homogenous solution polymerization. [4, 5]

Particularly, Poly(vinylidene fluoride) (PVDF) and its copolymers exhibit unique electrical, mechanical, and biocompatibility properties and chemical resistance that have promoted their use for coating and liner applications,[6] medical devices,[7] and electronic devices such as transducers and detectors.[8,9]Different crystalline forms of PVDF can be induced by changes in the processing pressure, [8,10,11] temperature,[12] solvent quality,[13] end group type [14,15] and imposed electrical fields. [16] DiNoia et al. [17] have reported on the solubility of PVDF in CO_2. Where, PVDF was found to form a homogenous solution with carbon dioxide at 1500-1700 bar in the temperature regime from 150-200°C. Phase segregation of the polymer from the homogeneous state may be attributed to liquid/liquid demixing (L+L demixing) processes, or termination with the crystallization boundary at about ~130°C. Below crystallization temperature PVDF was

"Impact of low and high molecular weight additives on the solubility of PVDF in $scCO_2$" Fahmy S., Beginn U., and Moeller M. in preparation.

found to undergo crystallization slowly from $scCO_2$ solution. Surprisingly, addition of polar molecules to $scCO_2$ can leads to a dramatic change in the polarity of $scCO_2$, subsequently its solvency power. Lora et al [18] has reported on the effect of adding small amount of polar solvent (ex. DME, Acetone and Ethanol) on the location of cloud point data for PVDF/$scCO_2$ (as seen in Figure 5.1). Where, each of the three co-solvents considered, acetone, DME, and ethanol have a significant dipole moment, although ethanol is the only one of these cosolvents that can self-associate and cross-associate by hydrogen bonding. The addition of these cosolvents to CO_2 is expected to enhance polymer-solvent interactions that will favour the dissolution of polar PVDF.

A

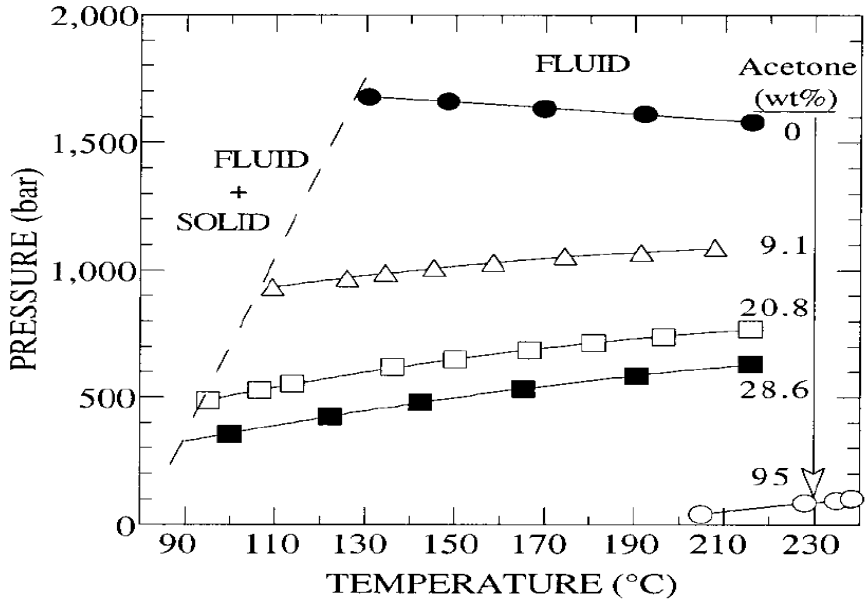

B

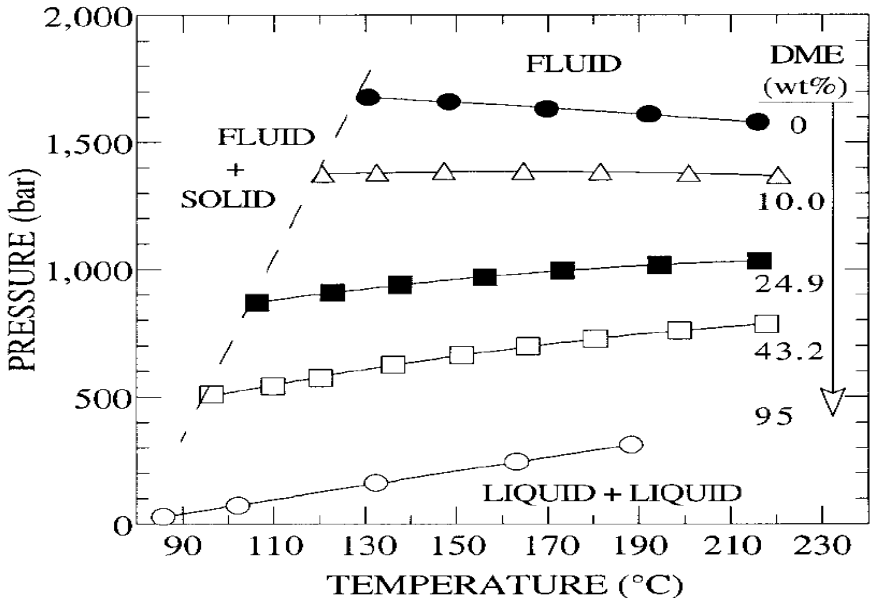

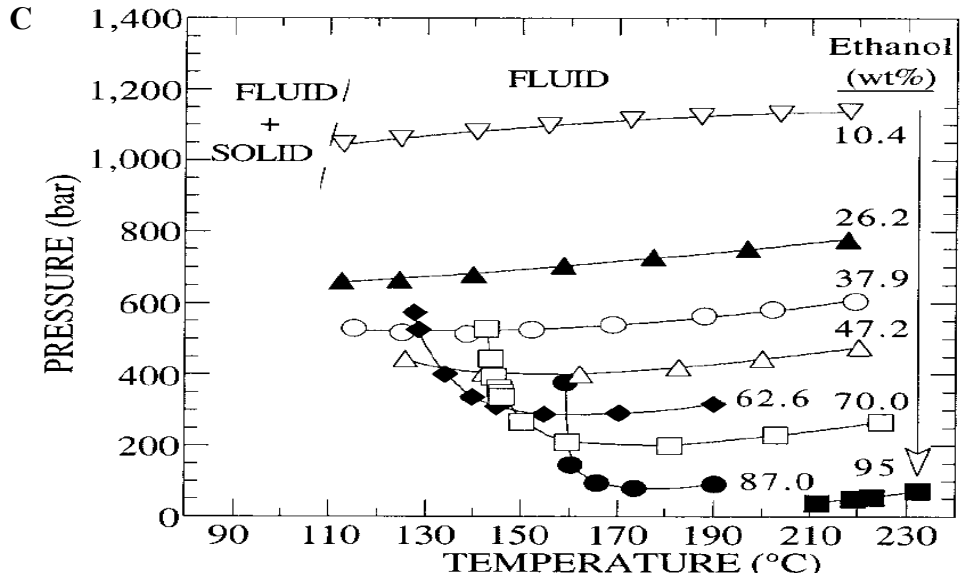

Figure 5.1. *Effect of (A) Acetone, (B) Dimethylether, and (C) ethanol on the phase behaviour of the PVDF/CO_2 system. The PVDF concentration is ~5 wt % in each case.* [18]

McHugh et el have studied the effect of increasing the solvent power of CO_2 for PVDF/scCO_2 mixture as a polar cosolvent is added. Acetone was found to be a better cosolvent for PVDF, compared to DME since acetone is also a better pure component solvent for this fluoropolymers. Although ethanol is a good cosolvent, it self-associates at high solution concentrations and low temperatures, causing it to act as an antisolvent rather than a cosolvent.

The main objective in this chapter is to investigate the extent at which preciously selected low (organic solvent) and high molecular weight (home-made block and statistical copolymer) additives can alter the solubility/crystallization border of PVDF/CO_2 mixtures.

5.2 Experimental:

5.2.1 Materials:

The polyvinylidene fluoride sample Kynar 741, **PVDF323** was supplied from Elf Atochem France. Molecular characterization of the polymer is summarised in Table 5.1, polymer was used as received without any further modification.

Table 5.1: *Molecular characterizations for PVDF 323sample used in this study.*

Polymer	M_n[a] Kg/mol	M_w/M_n	ΔH_m (J/g)	T_m(°C)	Powder Density[b] (mg/ml)	Crystallinity %[c]
Kynar 741	98.00	3.29	53.2	168	0.41	~55

a Determined by GPC in THF.
b Calculated by weighing out samples in fixed volume.
c Determined by DSC calculated based on ΔHm = 6.50 kJ / mol of repeating unit for 100% crystalline PVDF.

SFE grade carbon dioxide (5.5) was provided from (Linde AG) and used without further purification. N, N- dimethyl acetamide (DMAc), N,N-dimethyl formamide (DMF), dimethylsulfoxide (DMSO), methanol, cyclohexanone, 1-4-dioxane, γ-butyrolactone, ethylene carbonate, perfluoropentan-1-ol, N-methylpyrroldidone (NMP), N, N'-dimethyl-N, N'-trimethylene urea, and Krytox methyl ester were purchased from Aldrich (> 99% purity) and used as received. Double distilled water was used through-out as well. Physical properties of some of solvent and cosolvent used in this chapter are shown in Table 5.2.

Table 5.2: *Properties of the solvents and cosolvents used in this study.*[a]

Solvent	Boiling point (°C)	Density g/ml at 25°C	Melting point (°C)	Dipole Moment (D) Debye 20°C	Molecular weight (g/mol)
N, N- dimethyl acetamide	165	0.94	-20	3.72	87.1
N, N-dimethyl formamide	152	0.945	-60	3.86	73.09
Dimethylsulfoxide	189	1.096	19	3.90	78.13
Cyclohexanone	155.6	0.9421	-16.4	2.9	48.16
1,4-Dioxane	101	1.034	12	0.45	88.1
γ-butyrolactone	206	1.13	-43	2.8	86.1
N-methylpyrroldidone	202	1.033	-24	4.1	99.13
H_2O	100	0.998	0	1.82	18
Hexafluoropropene	-29.6	1.31	-156	0.4	150
Carbon dioxide	-78.5	1.977	-55.6	0	44

a references 19, 20.

The high molecular weight additives, poly(fluoro-octylacrylate)-*b*-poly(methylmethacrylate), $P[F8H2A]_{94}$-*block*-$PMMA_{156}$ and poly[dimethylsiloxane-monomethacrylate]-*block*-poly[methylmethacrylate], $P[PDMS\text{-}MA]_6$–*b*-$PMMA_{150}$ were

prepared by the atom transfer radical polymerization (ATRP) technique. Statistical co-polymers composed from MMA and fluoroacrylate or siloxane macromonomer, abbreviated as P[F8H2A-*co*-MMA] and P[PDMS-MA-*co*-MMA] were prepared by conventional free radical polymerization. Table 5.3 summarises the molecular characterization of this additives. The purity of these polymers exceeded 97% as calculated from ^{1}H-NMR and elemental analysis.

Table 5.3: *Molecular properties of high molecular weight block- and statistical copolymers additives used in this study.*

No.	Formula	Mn[(a)] [kg/mol]	Mw/Mn [(a)]	Ref.
1	P[F8H2A]$_{94}$-*b*- PMMA$_{156}$	21.0	1.09	(21)
2	P[F8H2A$_{0.35}$-*co*- PMMA$_{0.65}$]	153.0	2.28	(21)
3	P[PDMS-MA]$_{6}$-*b*- PMMA$_{150}$	135.8	1.86	(22)
4	P[(PDMS-MA)$_{0.66}$-*co*- PMMA$_{0.34}$]	103.5	3.24	(22,23)

(a) Determined from GPC in THF calibrated against standard PS.

5.2.2 Methods:

5.2.2.1 Polymer blends formation:

The effect of additives on the thermal transitions characteristics of PVDF in absence of neat CO_2 were determined by blending of polyvinylidene fluoride with macromolecular additives in form of thin films (ca. 0.1-0.15 mm thickness) by solution casting technique. Where, 10 mL DMF, 0.05 g PVDF and 0.05 g each additive was mixed overnight at 60°C under stirring condition. 2ml of the clear solutions were cast on a Petri dish (diameter = 5 cm). After evaporating the majority of solvent under ambient conditions; the prepared films were dried in a vacuum oven at 130°C for 24 hours to ensure complete removal of solvent.

5.2.2.2 Differential Scanning Calorimetry (DSC):

Thermal transitions as well as the degree of crystallinity of polyvinylidene fluoride were measured on a DSC 204 Phoenix unit (NETZSCH); the instrument was calibrated with ultra pure indium. All measurements were performed under a nitrogen atmosphere.

Polymer samples (ca~3-5 mg) were heated up to 200°C with a heating rate of 10 K/min. In order to eliminate thermal hysteresis, all data were calculated from the second heating peak.

5.2.2.3 Size Exclusion Chromatography (SEC)*:*

Size Exclusion Chromatography (SEC) was performed in DMF/0.1M LiBr as solvent with Waters μ-Styragel columns with pore sizes of 10^5, 10^4, 10^3 Å, a guard column. A Waters 410 differential refractometer was used as a detector. Narrow PMMA standards (PSS) were used for calibration and molecular weights were evaluated by means of SEC-WIN version 2.54 from PSS.

5.2.2.4 Scanning electron microscopy (SEM):

Scanning electron microscopy (SEM) was performed on a Zeiss DSM 962 microscope. The sample surface was covered with a 20nm thin layer of Au/Pt using a Balzers Union SCD 040 sputtering apparatus. The instruments were operated at 80kv accelerating voltage at room temperature.

5.2.2.5 High pressure setup:

In chapter 3 in this thesis, a detailed technical drawing describing the high pressure setup was shown. In a typically experiment, pre-weight amount of polymer (ca. 0.3-0.7± 0.02 g) was inserted in the view cell prior to pressurization. Then CO_2 was purged at 3-6 bar to remove any entrapped air right before conducting the experiment. Cloud point data were recorded by increasing the system volume using the spindle pump to a situation where a hazy solution can be distinguished in the cell. All cloud point determinations were repeated at least three times. Reproducibility was within an accuracy range of ± 1.0°C and ± 5-10 bar. Cloud points were determined either visually, as defined as the condition where the magnetic stirring bar could no longer be seen or photometrically. The cloud point pressure was obtained at condition where 90% drop in the intensity of transmitted light take place. Directly after measuring cloud point pressure, the system was cooled to room temperature followed by slowly venting CO_2 with a very small depressurization rate.

For cloud point investigation of PVDF/HFP/CO_2 ternary mixtures, pre-weight gaseous hexafluoropropene (HFP) was condensed from the storage vessel into maximally opened spindle pump by cooling the pump body with ice. Then the movable piston was

pushed inward to minimum value (i.e. cell volume =5.6 ml). Subsequent to filling polymer and HFP in the cell; CO_2 was injected and the system was allowed to equilibrate at the start temperature for about 30 min under continuous stirring by a magnetic stirring bar. Starting pressure and temperature were chosen sufficiently high to ensure complete dissolution of the PVDF in CO_2. On another hand, isobaric cooling experiments were performed by lowering the temperature at a very small rate. While, the temperature decreased down the pressure in the view cell was continuously adjusted by moving the piston of the spindle pump inward to compensate for pressure loss. After detecting of the respective cloud point the cell was heated isobarically to the start temperature and the experiment was repeated. (cf. experimental section in chapter 3 of this thesis)

5.3 Results & discussion:

5.3.1 Effect of low molecular weight additives on precipitation-crystallization boundaries:

The addition of carbon dioxide into a binary polymer/solvent mixture changes the system to ternary one and hence changes the system's behaviour. (cf. Figure 5.2)

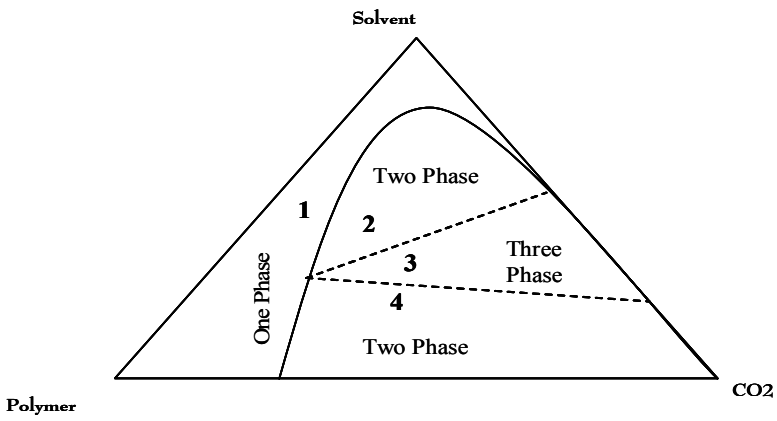

Figure 5.2: *Schematic polymer-solvent-C0$_2$ ternary diagram. Addition of carbon dioxide (at constant T and P) can cause the system to go from one phase to two phases and then in to three phases.*

Figure 5.2 shows schematically the phase behaviour of a ternary mixture when the pressure and the temperature remain the same and the compositions of the three components changes. For low polymer concentrations, adding a supercritical fluid

moves the mixture from the single phase region (point 1) into the liquid-liquid region (point 2). Further increase of the SCF brings the system into the three-phase region (liquid / liquid / vapor or liquid-liquid-fluid) (point 3). In such mixtures the vapor phase typically contains more than 90%$C0_2$ and very little polymer. At medium to high polymer concentrations, the addition of $C0_2$ brings the system into a liquid-vapor area (point 4).

Regarding polyvinylidene fluoride, the effect of adding small portions of inert polar low molecular weight compounds on the precipitation/crystallization lines of PVDF 323 was investigated by dissolving mixtures of the 0.4 wt% (referred to CO_2) additives and 0.2 wt% PVDF in CO_2 and subsequently performing either isothermal depressurisation or isobaric cooling procedure, respectively. Figure 5.3 depicts the effect of adding different low molecular weight organic solvents on the liquid/liquid demixing and the solid/fluid segregation lines, respectively.

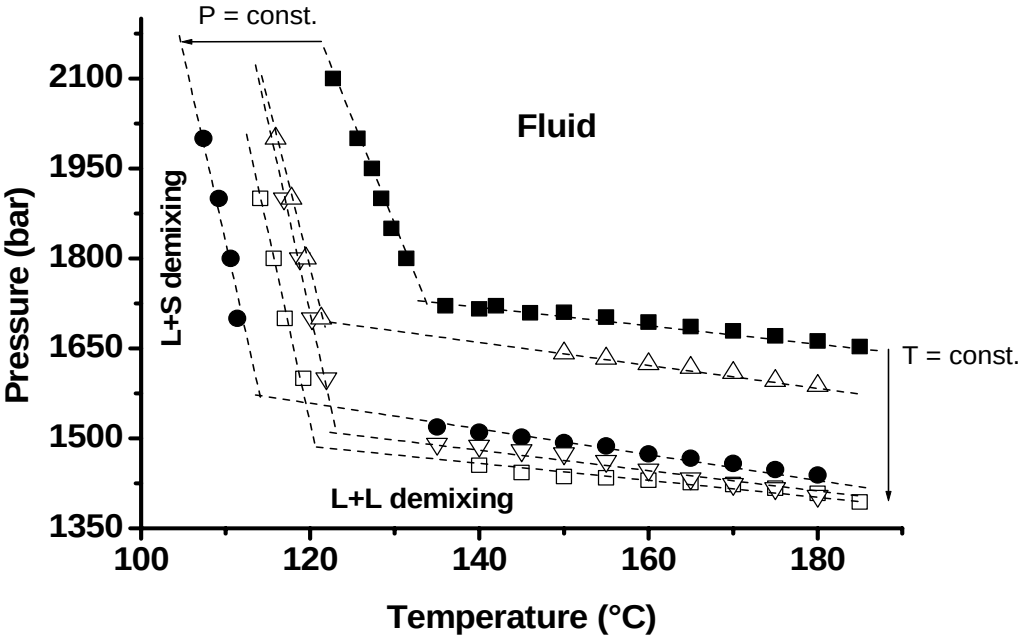

Figure 5.3: *Effect of addition of low molecular weight organic solvents on the L+L demixing/crystallization lines for 2 wt% solutions of PVDF 323 in CO_2 where; pure PVDF 323 (■), PVDF 323 + 0.4 wt% DMAc (□), PVDF323+ 0.4 wt% cyclohexanone (△) PVDF323+0.4 wt% DMSO (●),PVDF323+0.4 wt% γ-butyrolactone (▽).*

So far three types of additives were distinguished, namely as (i) compounds that alter the position of the L+L demixing as well as the crystallization cloud point lines (L+S), (ii) substances that shift the L+Ldemixing line, while the crystallization line was hardly

affected and (iii) additives that have virtually no effect. Additives that selectively shift the crystallization line have not been identified so far. Figure 5.3 depicts the change of the cloud point curves of 2 wt% PVDF 323 in CO_2 on adding 0.4 wt% DMAc, cyclohexanone and γ-butyrolactone. The highest shift in L+L demixing curve was measured to be about -274 bar (-16%) in the presence of DMAc. Since, dipole moment value (D) is a measure of degree of self association among solvent molecules. Where, DMAc is a polar solvent with the lowest D value (i.e. 3.72), while DMF and DMSO have a slightly higher D values; D=3.86 and D= 3.90, respectively. However, all of them are good solvents for PVDF. The dipole moment value is apparently an indicator of strong interaction occurs between DMAc and PVDF polar repeating units. Surprisingly, the dramatic decrease in the cloud point pressure of PVDF with increasing the DMAc concentration is described in Figure 5.4. Other solvents like γ-butyrolactone are considered as effective cosolvent like DMAc and DMSO; where the most effective additives to lower the crystallisation temperatures was γ-butyrolactone (ΔT = - 20 K).

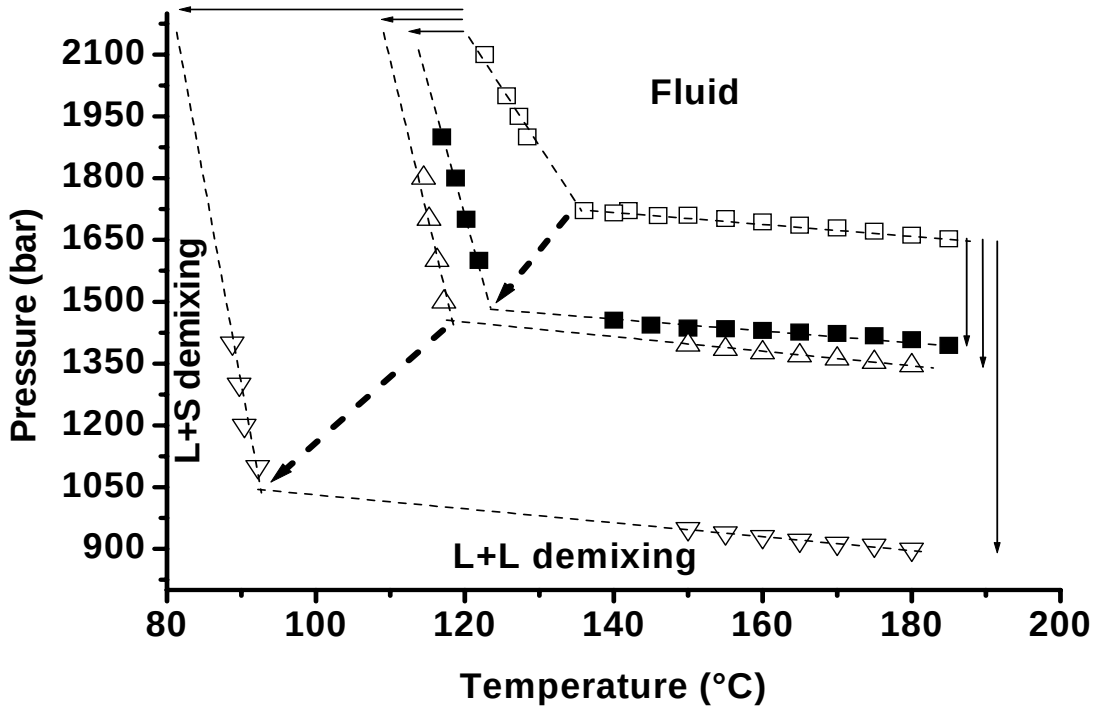

Figure 5.4: *Effect of different DMAc concentrations on the L+L and L+S demixing lines for 2 wt% solutions of PVDF 323 in CO_2: 0 wt% (□), 0.4 wt % (■), 1.0 wt % (Δ), and 8 wt % (▽) DMAc.(cooling rate: was 0.2 K/min)*

As shown in Figure 5.4 adding 0.4 wt% DMAc to a mixture of PVDF/scCO_2 lowers the L+L demixing pressure about 274 bar (-16%),while the addition of 8 wt% DMAc further lowering in the L+L demixing value to 949bar (- 44.5%) was observed. Simultaneously the effect of adding DMAc on the onset of crystallisation temperature

was detected as it reduced by -11°C (0.4 wt% DMAc) and surprisingly by -45°C (8 wt% DMAc).

The effect of increasing DMAc concentration on the morphology of polyvinylidene fluoride isothermally precipitated from $scCO_2$ is shown in Figure 5.5. Where, on another hand morphological effects upon isobaric cooling are illustrated in Figure 5.6.

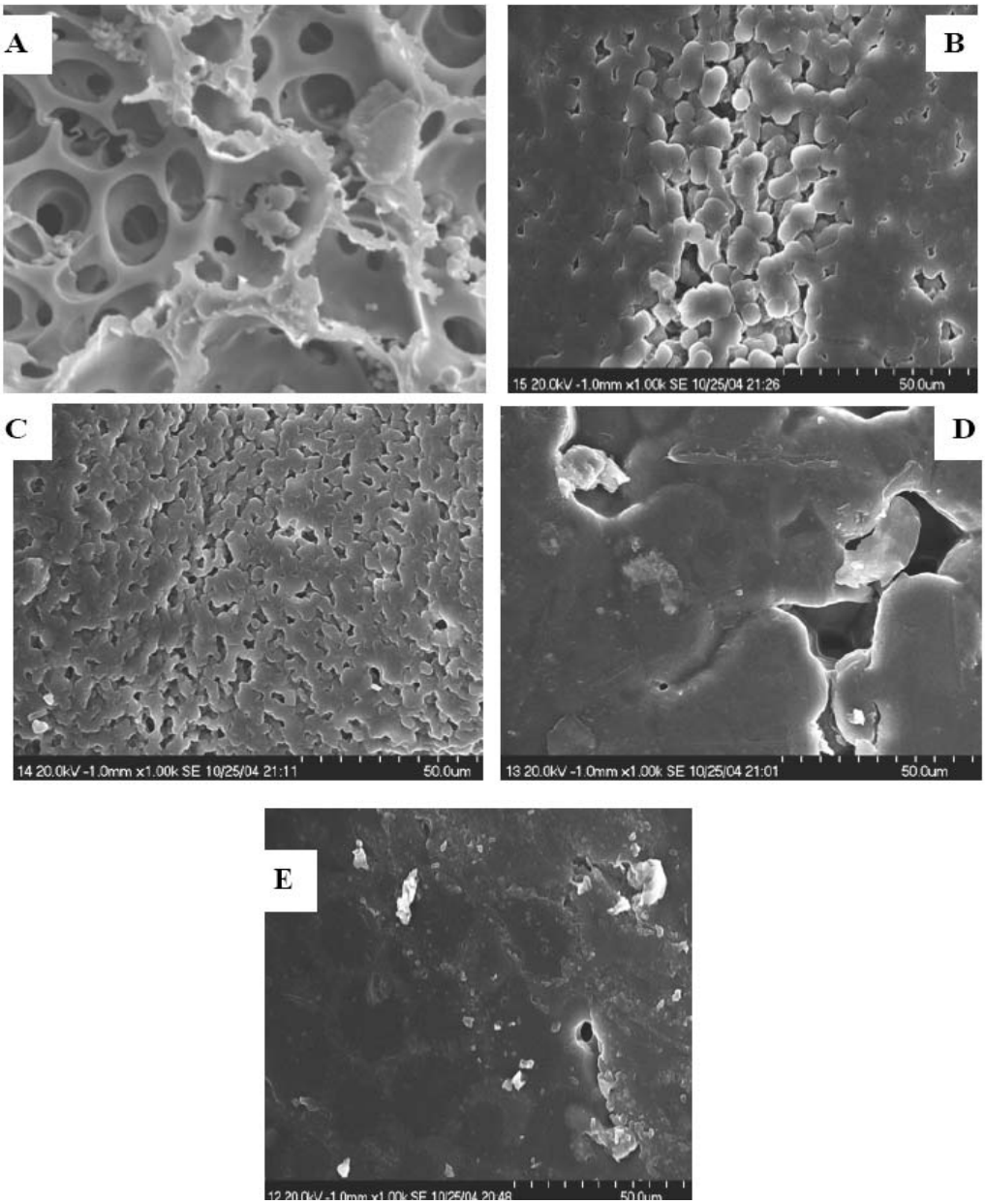

Figure 5.5: *High resolution scanning electron micrograph for 2 wt % PVDF 323 precipitated from $scCO_2$ at 140°C and 1600 bar with (A) 0 wt%, (B) 0.4 wt%, (C) 1.0 wt%, (D) 4.0 wt%, and (E) 8.0 wt% DMA. (50µm, scale bar).*

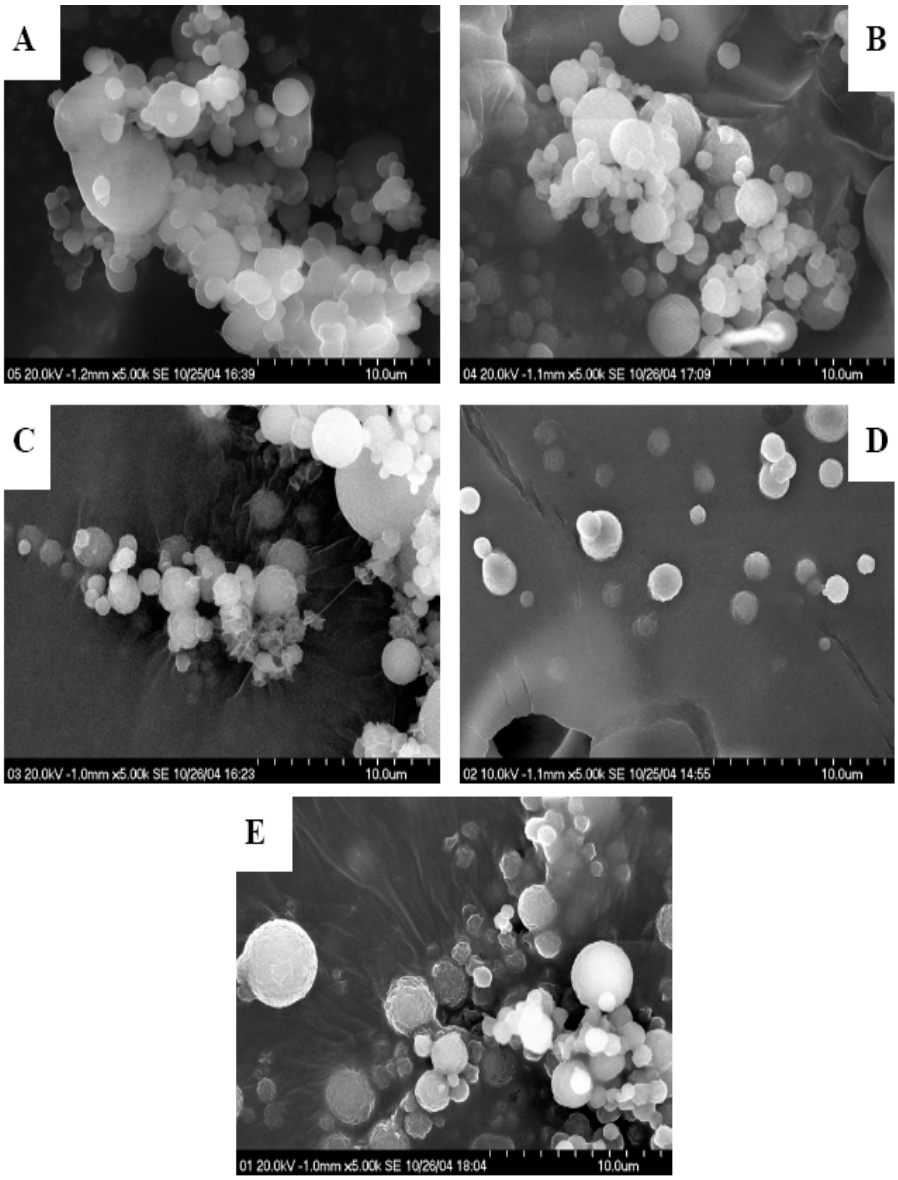

Figure 5.6: *High resolution scanning electron micrograph for 2 wt % PVDF 323 crystallized from $scCO_2$ at 1800 bar and 160°C with (A) 0 wt%, (B) 0.4 wt%, (C) 1.0 wt%, (D) 4.0 wt%, and (E) 8.0 wt% DMAc (10µm, scale bar).*

Polyvinylidene fluoride precipitated isothermally from $scCO_2$ exhibit sponge like structure having microvoids. [24] The pore diameter of these microvoids starts to decrease upon increases the concentration of DMAc added to PVDF/CO_2 mixtures as shown in figure 5.5. The decrease in pore diameter of microvoids of PVDF mirrors the high miscibility (i.e. cosolvency) of DMAc in polymer matrix. This high miscibility is reason lying behind the dramatic decrease in L+L & L+S cloud point curves. For, 2 wt% PVDF 323+0.4 wt% DMAc pressure of 1693 bar at 160°C is required to obtain a clear homogenous solution which is lower than pressure needed for pure PVDF (~1710

bar) to keep it completely soluble at the similar condition. Consequently, the cloud point pressure was found to be sharply decreased by ca. 300, 400, 800 bar upon increasing the amount of added DMAc from 1.0 to 4.0 and 8.0 wt%, respectively. The onset of crystallization temperature of PVDF is also decreased quite significantly with increasing DMAc concentration.

As seen in Figure 5.4, the onset of crystallization temperature of 2 wt% PVDF /0.4 wt% DMAc appears at 136.0 °C when the solution was cooled isobarically at 1800 bar. Meanwhile, onset of crystallization were observed at ca. 122.0°C, 117.6°C, and 92.2 °C for a solution of 2wt% PVDF with 1.0 wt% DMAc, 4.0 wt%, and 8.0 wt% isobarically cooled at 1800 bar, respectively. This sharp shift in the crystallization temperature might be probably due to the increase in the solvent density upon increasing the added amount of DMAc.

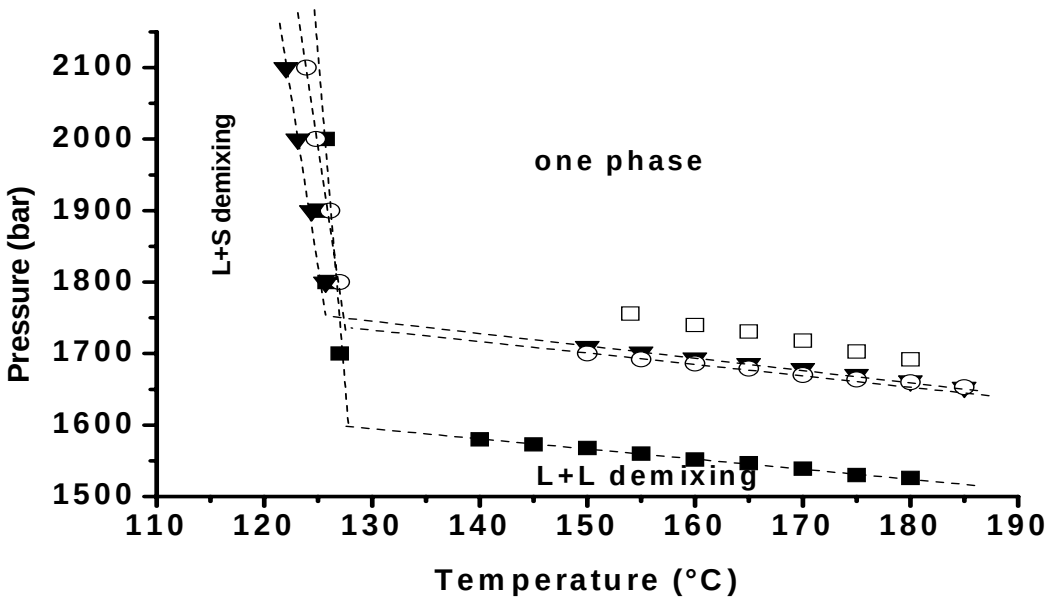

Figure 5.7: *Selective shift of the "L+L demixing" line for 2 wt% of PVDF 323 (□) and PVDF 323/additive/*sc*CO_2 solutions. where, (■) 2 wt % PVDF 323 + 0.4 wt% N-methylpyrrolidone, (○) 2 wt % PVDF 323 + 0.4 wt N, N-dimethyl-N,N-trimethylene urea, (▼) 2 wt % PVDF 323 + 0.4 wt Krytox methyl ester.*

Figure 5.7 shows PVDF 323/additive/CO_2 systems of the second and third type additive effect. N-methylpyrrolidone (NMP) is an additive that strongly shifts the L+L demixing curve, but hardly affects the crystallization line of the polymer, while N,N'-dimethyl-N,N'-trimethylene urea and Krytox methyl ester show minor effects on both kind of cloud point curves. These substances have a minor impact on altering the crystallisation lines, since the temperature shifts were below 5 K. On the other hand the L+L demixing

pressures of the 2 wt% PVDF 323 solutions became lowered by 150 bar (-5.8 %) in the presence of 0.4 wt% NMP.

Table 5.4 compares the slope of the crystallisation curve of PVDF/cosolvent/ CO_2 as calculated in the presence 0.4 wt% (referred to CO_2) for different additives.

Table 5.4: *Effect of added organic solvents on the slope of the crystallisation and L+L demixing lines of PVDF 323/additive /CO_2 mixtures.*

Solvent	$(dP/dT)^{Crystallization}$	$(dP/dT)^{L+L\ demixing}$
Cyclohexanone	-114	-2.21
γ-Butyrolactone	-59	-2.19
N,N-Dimethylacetamide	-43	-2.17
Dimethylsulfoxyde	-125	-2.31
N-Methyl-pyrrolidone	-100	-2.75
N,N'-dimethyl-N,N'-trimethylene urea	-125	-1.40

5.3.2 Effect of hexafluoropropene (HFP) additive:

Copolymers from VDF and hexafluoropropene (HFP) are commercially produced polymers and are of great interest in industry. [25-28] So far, it's worthwhile to investigate the effect of the adding HFP monomer on the solubility of PVDF in CO_2. Where, addition of HFP gas can affect the copolymerization progress of PVDF in carbon dioxide. Figure 5.8 depicts the cloud point lines of 2 wt% PVDF 323 in CO_2 in the presence of increasing fractions of HFP. It can be clearly seen that, HFP can strongly altered either solvent or solute quality towards each other. Small additions of HFP (up to 12 wt %) reduce the pressures of precipitation lines approximately 700 bar (-41%) compared to pure PVDF value, on further increase (up to 43.8 wt% in the current study) of the HFP content a little effect on the cloud point pressure can be detected.

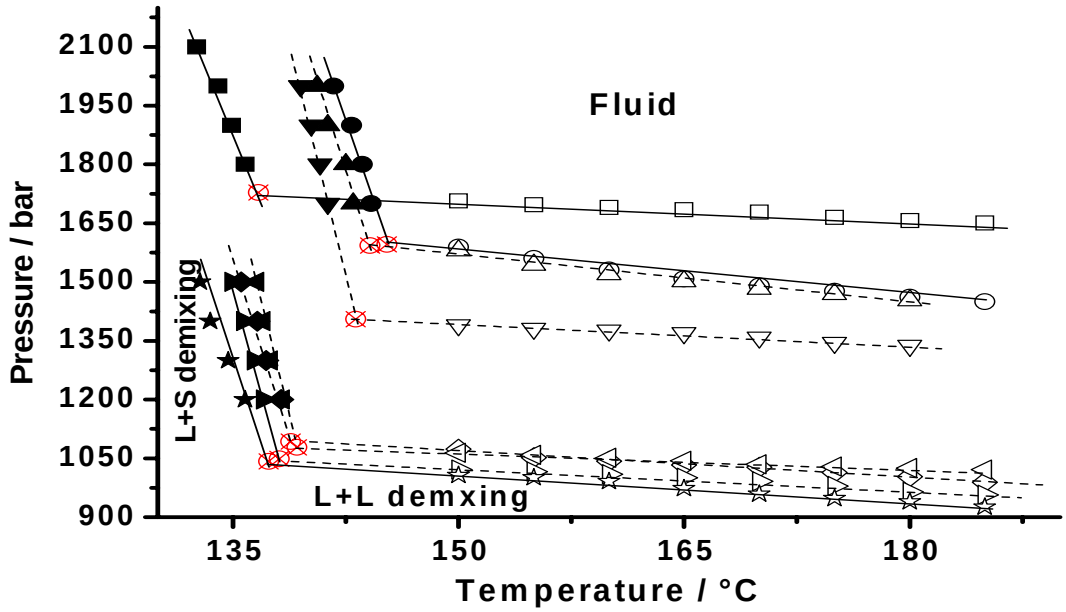

Figure 5.8: *Impact of HFP on the precipitation/crystallization lines of 2 wt% PVDF in $scCO_2$ (closed symbols: crystallization, open symbols: precipitation, ■,□ = 0 wt%, ●,○ = 0.7 wt%, ▲,△ = 2.1 wt%, ▼,▽ = 6.3 wt%, ◆,◇ = 11.3 wt%, ◀,◁ = 19.7 wt%, ▶,▷ = 27.8, ★,☆ = 43.8 wt% HFP).*

For a PVDF/CO_2 containing up to 12 wt% HPF, the slope of the curve is -54 bar / wt%, while the slope is -2.9 bar/wt% between 15 wt% and 44 wt% HFP. These values are fairly constant between 160 and 180 °C (cf. Figure 5.9).

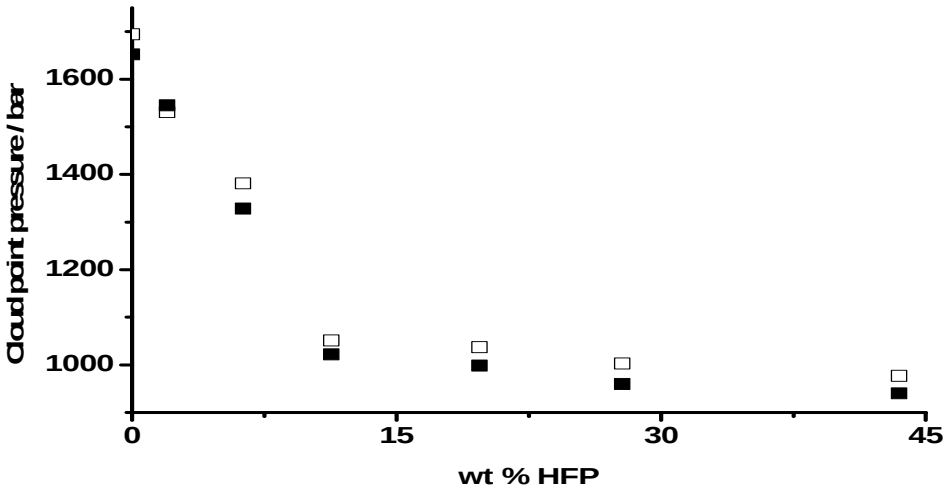

Figure 5.9: *Dependence of the precipitation pressure on the HFP weight percent for PVDF / CO_2 / HFP ternary mixture at 160°C (□), and 180 °C (■).*

The effect of the HFP on the crystallization of PVDF is more complex process. While on other hand, for up to 12 wt% HFP content the precipitation curve becomes shifted to larger temperatures (i.e. good solubility of PVDF in $scCO_2$). But on exceeding 12 - 15 wt% HFP the trend is inversed and the crystallization curves are shifted towards lower temperatures. Figure 5.10 illustrates this effect with the dependence of the intersection point on the HFP content of the mixture. P^* continuously decreases from 1728 bar (pure PVDF) to 1077 bar on adding 11 wt% HFP ($dP^*/d\mu_{HFP}$ = -53 ± 5 bar/wt%$_{HFP}$), at larger HFP contents the slope reduces to -1.4 ± 0.7 bar / wt%$_{HFP}$.

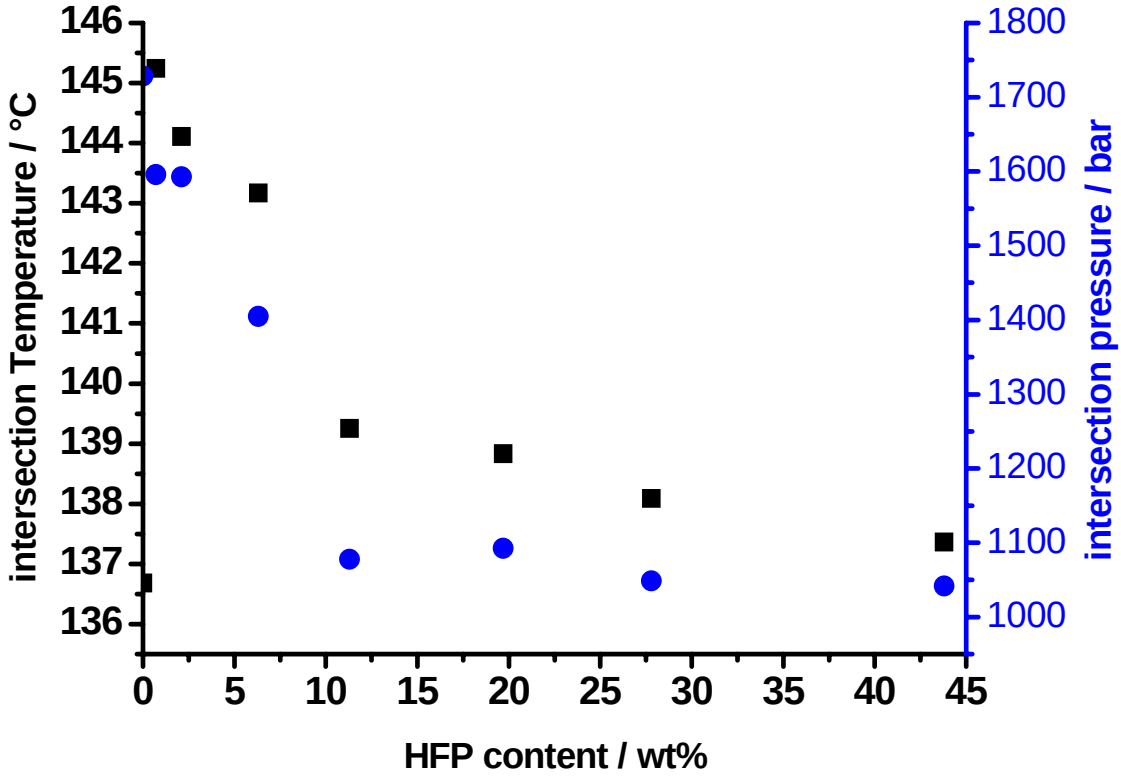

Figure 5.10: *Dependence of the "intersection pressure", P^*, on the HFP content in a 2 wt% solution of PVDF 323 in CO_2/HFP (● = intersection pressure P^*, ■ = intersection temperature T^*).*

The T^* /μ_{HFP} runs through a maximum at approximately 0.7 wt% HFP, i.e. small quantities of HFP increase the crystallization temperature considerably (+8.5°C). Increasing the HFP concentration reduces the effect, but the crystallisation temperature remains larger then with pure CO_2. Note that around 12 wt% HFP content (molar fraction: X_{HFP} = 0.32, X_{CO2} = 0.68) distinct changes in the slopes of the "intersection coordinates" (T^*, P^*) as well as the precipitation pressures occur (cf. Figure 5.8 and Figure 5.9). The reason for these peculiarities is not yet clear. However, HFP is classified as an additive that affects both precipitation and crystallization cloud point

curves. The magnitude of the effect is most pronounced at low HFP additions with the crystallization and at higher HFP contents with the precipitation lines.

The high cosolvency of HFP on the solubility of PVDF might be due to known fact which is CO_2 is nonpolar solvent with low dipole moment and polarizability value (D=0 Debye & 28.6 cm^3 x 10^{-25}, respectively). At higher temperature and pressure a polar interaction between polar polymer and solvent segments will favour the dissolution of polymer in SCF. These suggest that addition of polar component HFP (D=0.4 Debye & 60.4 28.6 cm^3 x 10^{-25}) will increase the polarity of CO_2 in a way to enhance the polymer-solvent interaction at higher pressure and temperature as well.

5.3.3 Effect of high molecular weight additives on precipitation-crystallization boundaries:

The effect of high molecular weight additives on the crystallization and precipitation demixing cloud points of polyvinylidene fluoride has been investigated with ternary mixtures composed from 2 wt% PVDF 323, 0.4 wt% additive and 97.4 wt% CO_2. A given macromolecular additives P[PDMS-MA]$_6$-*b*-PMMA$_{150}$, P[F8H2A]$_{94}$-*b*-PMMA$_{156}$, P[(DMS-MA)$_{0.66}$-*co*-MMA$_{0.34}$] and P[F8H2A$_{0.35}$-*co*-MMA$_{0.65}$] were previously selected in the way that they may be used a detergents during dispersion polymerization in sc fluid. All the materials combine the property of being CO_2-philic (siloxanes or perfluoroalkanes) and CO_2-phobic (PMMA) units in their molecular structure. Care was taken to select block copolymers and statistical polymers similar in composition and molecular weight. As seen in Figure 5.11, adding the macromolecular additives enhance the solubility of PVDF 323, but they were not as effective as the low molecular weight compounds. In order to investigate the effect of the macromolecular additives on the melting behaviour of polyvinylidene fluoride with respect to melting temperature (T_m) and melting enthalpy (ΔH_m), PVDF 323 was blended with this macromolecular additives.

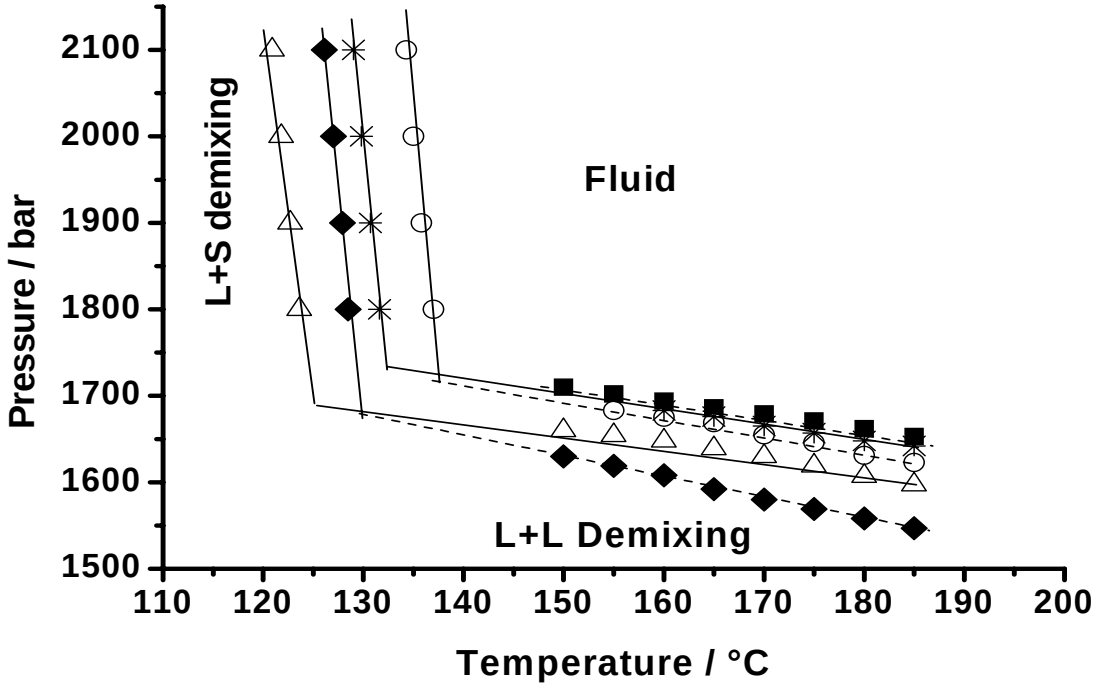

Figure 5.10: *Effect of different polymeric additives on the solubility of 2 wt% PVDF 323 in CO_2. (■ = pure Kynar 741, 2 wt% Kynar 741+ 0.4 wt% P[(DMS-MA)$_{0.66}$-co-MMA$_{0.34}$] (○),PVDF323+0.4 wt% P[F8H2A]$_{94}$-b-PMMA$_{156}$ (✳),PVDF323+0.4 wt% P[(F8H2A)$_{66}$-co-MMA$_{0.35}$] (◆), and PVDF323+0.4 wt% P[DMS-MA]$_6$-b-MMA$_{150}$ (△).*

A film cast from solutions of PVDF 323 and 20 wt% of the macromolecular additives with respect to amount of the PVDF was prepared by solution casting technique. After drying in vacuum followed by annealing at 130°C for 24 hours the polymer blends were characterized by means of DSC measurements. A typical DSC data for polymer blend are summarized in Table 5.5.

High molecular weight additives reduced the degree of crystallinity for 20–38% compared to pure Kynar 741. Block- and statistical copolymer exhibited similar effects and it was concluded that certain miscibility between polymer sample and additives may exist.

Table 5.5: *Melting transition and degree of crystallinity of PVDF 323 in the presence of macromolecular additives.*

Polymer Blend	Tm [°C]	ΔHm [J/g]	Crystallinity[a] [%]
PVDF 323	168.0	53.6	53.2
PVDF 323 + 20 wt% P[PDMS-MA]$_6$-*b*-PMMA$_{150}$	167.1	33.3	32.7 (-20.5%)

PVDF 323 + 20 wt% P[F8H2A]$_{94}$-*b*-PMMA$_{156}$	166.1	17.2	17.0 (-36.2%)
PVDF 323 + 20 wt% P[(PDMS-MA)$_{0.66}$-*co*-MMA$_{0.34}$]	164.7	22.6	22.3 (-31.0%)
PVDF 323 + 20 wt% P[F8H2A$_{0.35}$-*co*-MMA$_{0.65}$]	167.9	15.4	15.1 (-38.2%)

[(a)]Calculation based on ΔHm = 6.50 kJ / mol repeating unit for 100% crystalline PVDF.

5.4 Conclusion:

The crystallization and L+L demixing of polyvinylidene fluoride (PVDF) in the presence of various classes of high and low molecular weight cosolvents in supercritical carbon dioxide were investigated over a temperature range from 110°C to 190°C at pressures between 1400 to 2100 bar. Where, we observe that low molecular weight additives can considerably influence the solubility of PVDF in CO_2. Moreover, based on the type of additive it is possible to selectively lower the L+L demixing pressure and keep the L+S demixing temperature fairly constant or lowering both at same time.

The addition of N,N-Dimethyl acetamide (DMAc) has fantastic effect on decreasing both precipitation and crystallization lines of polyvinylidene fluoride in carbon dioxide. Obviously seen, that addition of 8 wt% DMAc can depress the onset of precipitation as well as crystallization by about 900 bar and 45°C, respectively. This observation can be fairly transferred to dispersion polymerization process of PVDF in $scCO_2$. Probably a challenging question could arise as DMAc can affect the molecular weight of the resulting polymer by transfer of growing active species to solvent.

Amphiphilic block- and random copolymers were observed to retain the cloud point lines to lower value, also degree of crystallinity of the PVDF can be reduced to 38% from its original value. In no case the additives were able to shift the cloud point lines below 300-400 bar, the present pressure limit for large scale industrial PVDF polymerization reactions. However, the results demonstrate that by proper combination of additives and dissolution / L+L demixing conditions the morphology and crystallinity of PVDF can be controlled over a wide range.

Generally speaking, low molecular weight additives have a powerful influence on the solubility and crystallization of PVDF in $scCO_2$ as compared to high molecular weight additives effect. While, high molecular weight macromolecules being under investigation which could be used as detergent during dispersion polymerization of PVDF in CO_2 have a minor effect in altering the precipitation and crystallization behaviour of the growing polymeric chains.

5.5 References:

[1] Kendall, J. L., Canelas, D. A., Young, J. L., DeSimone, J. M.; Chem. Rev. 1999, **99**, 543-563.

[2] Cooper, A. I.; J. Mater. Chem. 2000, **10**, 207-234.

[3] Woods, H. M., Silva, M. M. C. G., Nouvel, C., Shakesheff, K.M., Howdle, S. M. ;J. Mater. Chem. 2004, **14**, 1663-1678.

[4] US patent; 5,981,673.

[5] Jessop P. G., Leitner W.; Chemical Synthesis Using Supercriticalfluid Wiley-VCH: Weinheim, Germany, 1999.

[6] Briscoe B. J., Lorge O., Wajs A., Dang P.; J Polym Sci Part B: Polym Phys 1998, **36**, 2435.

[7] Laroche G., Lafrance C.-P., Prud'homme R. E., Guidoin R., J Biomed Mater Res 1998, **39**, 184.

[8] Samara G. A.; J Polym Sci Part B: Polym Phys1989, **27**, 39.

[9] Samara G. A.; J Polym Sci Part B: Polym Phys 1992, **30**, 669.

[10] Newman B. A., Yoon C. H., Pae K. D.; J Mater Sci 1979, **14**, 2391.

[11] Scheinbeim J. I., Chung K. T., Pae K. D., Newman B. A.; J Appl Phys 1980, **51**, 5106.

[12] Latour M., Anis K., Faria R. M.; J. Phys D: Appl. Phys 1989, **22**, 806.

[13] Gregorio R. Jr., Cestari M.; J. Polym Sci Part B: Polym Phys 1994, **32**, 859.

[14] Madorskaya L. Y., Loginova N. N., Panshin Y. A., Lobanov A. M.; Polym Sci USSR. 1983, **25**, 2490.

[15] Herman Uno T., Kubono A., Umemeto, S., Kikutani T., Okui N.; Polymer 1997, **38**, 1677.

[16] DeSimone J. M., Zhibin G., Elsbernd C. S; Science 1992, **257**, 945.

[17] DiNoia T. P., Conway S.E., Lim J.S., McHugh M.A.; J. Polym. Sci. B, 2000, **38**, 2832-2840.

[18] Lora M., McHugh Mark A..; J. of Phys. Chem B.: 1999, **103**, 2818-2827.

[19] Prausnitz J. M., Lichtenthaler R. N., de Azevedo E. G.; "Molecular thermodynamics of Fluid-Phase Equilibria" 2nd ed.; Prentice Hall: NJ, 1986.

[20] McClellan A. L.; Tables of Experimental Dipole Moments; W. H. Freeman and Company: San Francisco, 1963.

[21] Juergen Ellmann "Polymerization and Reactive Coating in Supercritical Carbon Dioxide", Ph.D thesis, Ulm, Germany, 2001.

[22] Ana Morales, Ph. D thesis, University of Ulm, Germany, 2004.

[23] Matyjaszewski K., Ed. Controlled radical Polymerization, American Chemical Society, Washington, DC, 1997.

[24] Chapter 3 in this thesis.

[25] LoStracco M. A., Lee S.-H., McHugh M. A.; Polymer 1994, **35**, 3272.

[26] McHugh M. A., Krukonis V.; J. Supercritical Fluid extraction: Principles and Practice, 2nd ed.; Butterworth: Stoneham, MA, 1994.

[27] Kirby C. F., McHugh M. A.; Chem. Rev. 1998, **99**, 565-602.

[28] Scheirs J., "Modern Fluoropolymers: High Performance Polymers for Diverse Applications", Wiley Series in Polymer Science, Chichester England; New York , John Wiley & Sons, Ltd. (UK), 1997.

CHAPTER 6

Effect of molecular weight of PVDF on precipitation/crystallization boundaries in $scCO_2$*.

6.1 Introduction:

Nowadays, there is a growing interest in polymer crystallization process assisted by supercritical carbon dioxide, either due to concern for green technologies, or for intrinsic process performances. Another advantage of supercritical CO_2, as a crystallization solvent is that their pressure and solvent power can be changed much faster than the solvent power of single conventional solvents; where the change is obtained by altering the temperature only. This advantage makes it possible to achieve very high supersaturation of the solute in $scCO_2$.

Carbon dioxide dissolved in polymer affects polymer properties in both molten and solid states. For example, Gendron et al. [(1)] and Lee et al. [(2)] reported that CO_2 dissolved into the polymer causes a reduction of its viscosity. Where, they explained the viscosity reduction by the depression of the glass transition temperature, T_g. The dissolution of CO_2 into the polymer also changes the crystallization temperature, T_c, and the crystallization behaviour.[(3-17)] PVDF has a high dipole moment, high dielectric constant, and can form crystals that offer piezoelectric properties. Most vinylidene fluoride units join head to tail, normally only 3.5-6% of the monomer units are linked head to head (CF_2 to CF_2)[(18)] and tail to tail (CH_2 to CH_2), respectively. The percentage of these missinsertions is increased at elevated polymerization temperature. [(19)] Degree of crystallinity is between 40- 60% with three polymorphs.

*"Effect of molecular weight of PVDF on the crystallization/precipitation boundaries in $scCO_2$" Fahmy S., Beginn U., Moeller M., in preparation.

The most common phase is the α-form (*cis-trans confirmation*), where the fluorine atoms and the hydrogen, respectively are placed alternately on both sides of the chain. This is thermodynamically the most stable form which shows a T_g at –40°C and a T_m at 170°C. [20] PVDF is processable by extrusion and injection molding above 215°C.[21] Melt extrusion process can generally result in formation of β–form due to the mechanical deformation of the chain.[22] The β–modification places all the fluorine atoms on one side of the chain and all the hydrogen atoms on the other side (all-*trans*). This structure is also the key to the piezoelectric activity and to a strong dipole moment normal to the chain direction.

The present chapter reports briefly on the preliminary experiments of the effect of different molecular weight upon crystallization process of polyvinylidene fluoride from a solution of $scCO_2$. Moreover, prediction of polymer molecular weight effects on structural changes (lamellar thickness) was investigated by means of high resolution scanning electron microscopy (HRSEM).

6.2 Experimental

6.2.1 Material

Polyvinylidene fluoride with different molecular weight have been employed kynar 741 (**PVDF 323**) was obtained from elf Atochem, France. A detail description of PVDF323 molecular characterization is shown in chapter 5 in this thesis. Other PVDF samples like; **PVDF 26** (M_w= 26 kg/mol, M_n=11.5 kg/mol), **PVDF 51** (M_w= 51 kg/mol, M_n= 39 kg/mol), **PVDF 15** [23] (M_w= 15 kg/mol, M_n=12 kg/mol), **PVDF 181**(M_w= 181 kg/mol, M_n=18.85 kg/mol), **PVDF 207** (M_w= 207 kg/mol, M_n=96 kg/mol) were synthesized by free precipitation polymerization of vinylidene fluoride in supercritical carbon dioxide using diethylperoxydicarbonate (DEPC, purity >97%) as free radical initiator at 70°C.[24] Carbon dioxide SFE grade (5.5) was provided from (Linde AG) and used without further purification. Semi-crystalline PVDF generally has a T_g of approximately -40°C and T_m of approximately 168-172°C.

6.2.2 Experimental Methods:

6.2.2.1 Size Exclusion Chromatography (SEC)*:*

Size Exclusion Chromatography (SEC) was performed in DMF/0.1M LiBr as solvent with Waters μ-Styragel columns with pore sizes of 10^5, 10^4, 10^3 Å, a guard column. A

Waters 410 differential refractometer was used as a detector. Narrow PMMA standards (PSS) were used for calibration and molecular weights were evaluated by means of SEC-WIN version 2.54 from PSS.

6.2.2.2 Scanning electron microscopy (SEM):

Scanning electron microscopy (SEM) was performed on a Zeiss DSM 962 microscope at Section for electron microscope, University of Ulm, Germany. The sample surface was covered with a 20nm thin layer of Au/Pt using a Balzers Union SCD 040 sputtering apparatus. The instruments were operated at 80kv accelerating voltage at room temperature. The instrument is capable of working at lower temperature using cryogenic cooling system.

6.2.2.3 Phase behaviour Setup& Experimental cloud point determination:

In chapter 3 in this thesis, a detailed technical drawing of high pressure setup was shown. Generally, pre-weight amount of solid polymer (ca. 0.3-0.7±0.02 g) was placed in the view cell. CO_2 was purged at 3-6 bar to remove any entrapped air. Cloud point data were recorded by increasing the system volume using the spindle pump to a situation where a cloudy solution can be distinguished in the cell. All cloud point determinations were repeated at least three times. Cloud points were determined either visually, as defined as the condition where the magnetic stirring bar could no longer be seen or photometrically. In the latter case a halogen lamp (Tech 5, GmbH) illuminated the view cell from the rear, while the front window was connected to an online diode array UV/VIS spectrometer (Zeiss AG). The cloud point pressure was obtained by extrapolation of the light intensity/pressure curve to zero transmission. After measuring cloud point, the system was cooled to room temperature followed by slowly venting CO_2 with a very small depressurization rate.

Isobaric cooling experiments were performed by lowering the temperature at a rate of 0.2 K/min. While the temperature decreased the pressure in the view cell was continuously adjusted by moving the piston of the spindle pump to compensate for pressure drops. The light intensity was found to sharply decrease right after formation of crystals inside the reactor which were dispersed in the cell by magnetic stir bar (i.e. cloud point condition). Once we got a hazy solution, the system was heated at constant heating rate ca.10°C/min to one homogenous phase (clear solution) again. It took around 5-10 deg to

achieve a complete dissolution of crystal again. This heating/cooling protocol was repeated twicely. Reproducibility was within an accuracy range of ± 0.2 °C and ± 5-10 bar.

6.3 Result & Discussion.

6.3.1 Effect of molecular weight:

Figure 6.1 reveals the effect of molecular weight of different PVDF sample on the location of L+L demixing (precipitation), and L+S demixing (crystallization) lines as well.

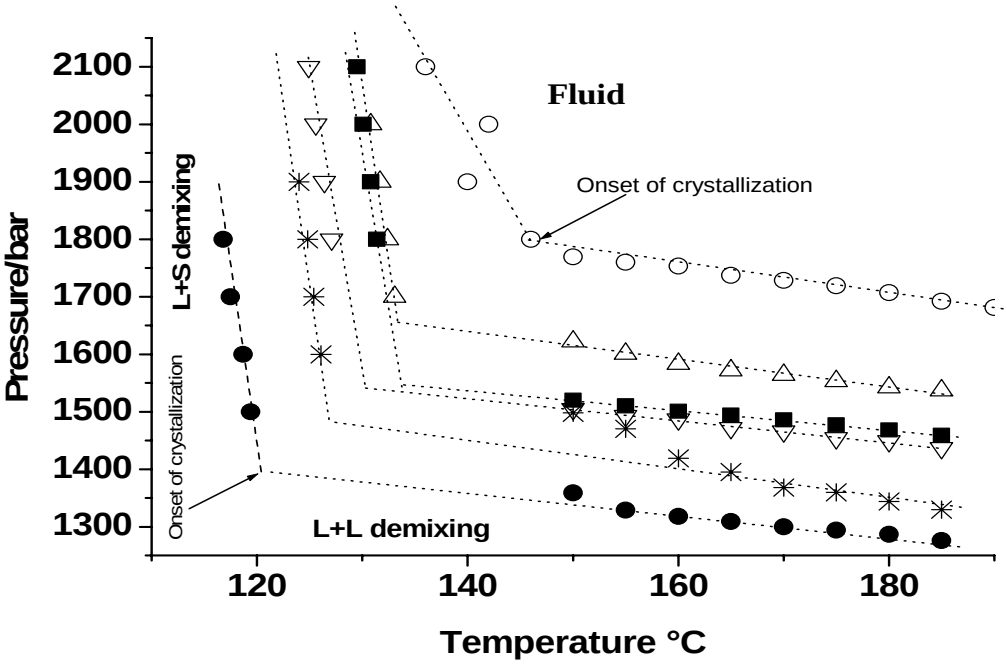

Figure 6.1: *Molecular weight effect on the position of L+L demixing (precipitation) and L+S demixing (crystallization) of PVDF in $scCO_2$: PVDF 323 (o), PVDF 207 (Δ), PVDF 181 (■), PVDF 51 (∇), PVDF 26 (*), and PVDF15 (●). Polymer concentration was 2 wt% for all measurements. (Cooling rate: 0.2 K/min was employed in all measurements)*

Thermodynamically, there are proposed different strategic crystallization processes that may occur for polyvinylidene fluoride in supercritical carbon dioxide. First, crystallization [25] occurs upon crossing the liquid/solid border, which means crystals are formed directly from homogenous solution. And secondly, crystals are formed after

liquid-liquid demixing. In the latter process, liquid droplets are formed consisting of polymer melt swollen by CO_2, i.e. the crystals are formed at high polymer concentration. (Fig.6.2)

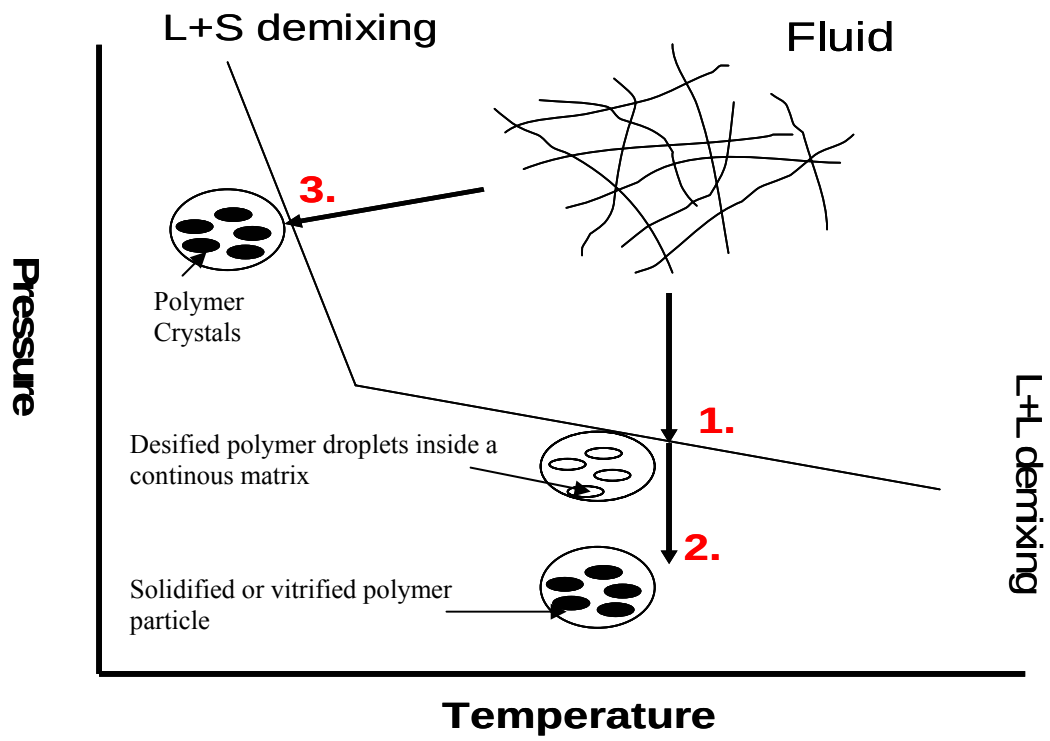

Figure 6.2. *Schematic drawing representing a possible precipitation strategies of PVDF from $scCO_2$, where (1) liquid-liquid demixing, followed by (2) crystallization after L+L demixing, (3) crystal formation from solution..*

Noteworthy to mention that, we realized for a large variation of molecular weights are of great effect on shifting both crytsallization and precipitation lines of PVDF in CO_2 as seen in Fig. 6.1. Where, decreasing in molecular weights of PVDF has a major effect in decreasing both precipitation and crystallization lines in $scCO_2$. As an example for isothermal precipitation at 155°C of 2 wt% PVDF 323, PVDF 181, and PVDF26; the liquid-Liquid segregation boundaries were recorded at 1760, 1510, and 1470 bar, respectively. At same time, the liquid/solid lines for those 3 sorts of PVDFs were shifted to a lower temperature as well. Also, the onset of the crystallization temperature, T_c, for a 2 wt% PVDF 323, 181, 26 isobarically cooled from CO_2 at 160°C and 1800 bar, were 146.0, 131.4, and 124.8°C respectively. (cf. Figure 6.3).

The observed variation in the precipitation must be considered to vary in a systematic manner because of high polydispersity of PVDF samples being investigated so far. Suggesting the presence of different molecular weight fractions, i.e., the lower molecular weight fraction of the polymer remains in the dissolved state while the higher molecular weight chains first undergo liquid/liquid transition and then crystallization. The chains that remain in the solution are then forced to phase separate and rapidly crystallize in the second stage during depressurization of the cell.

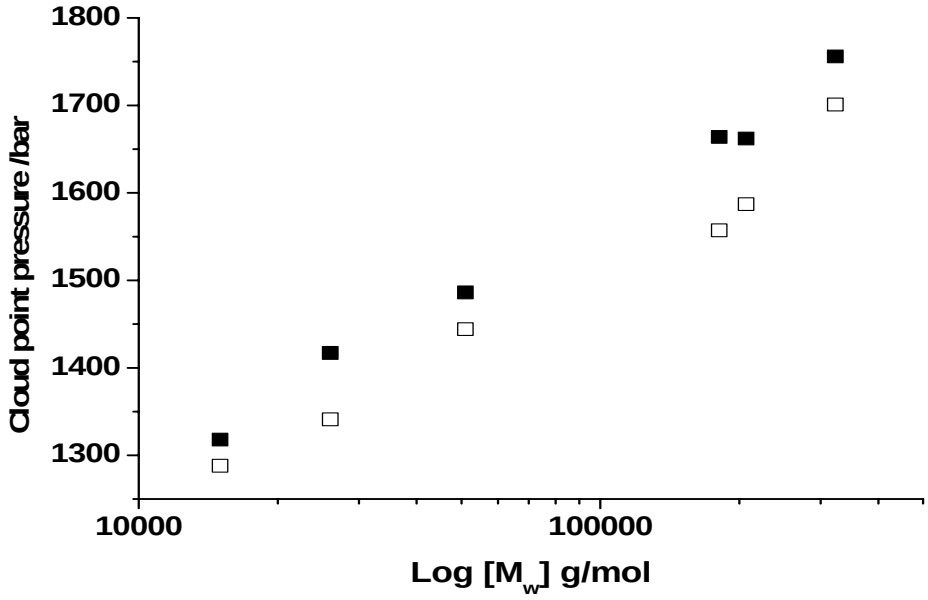

Figure 6.3: *Dependence of cloud point pressure (precipitation) of PVDF in $scCO_2$ as a function of* logarithmic *values of weight average molecular weight of polymer at (■) 160°C and (□) 180°C. Polymer concentration was 2 wt% for all measurements.*

Gibbs Ensemble Monte Carlo calculation method [26] predicts a linear relationship between the cloud point pressure and the logarithmic value of weight average molecular weight of semicrystalline polyvinylidene fluoride. (Figure 6.4) This simulation studies were found to be in accordance with our cloud point data (Fig. 6.3).

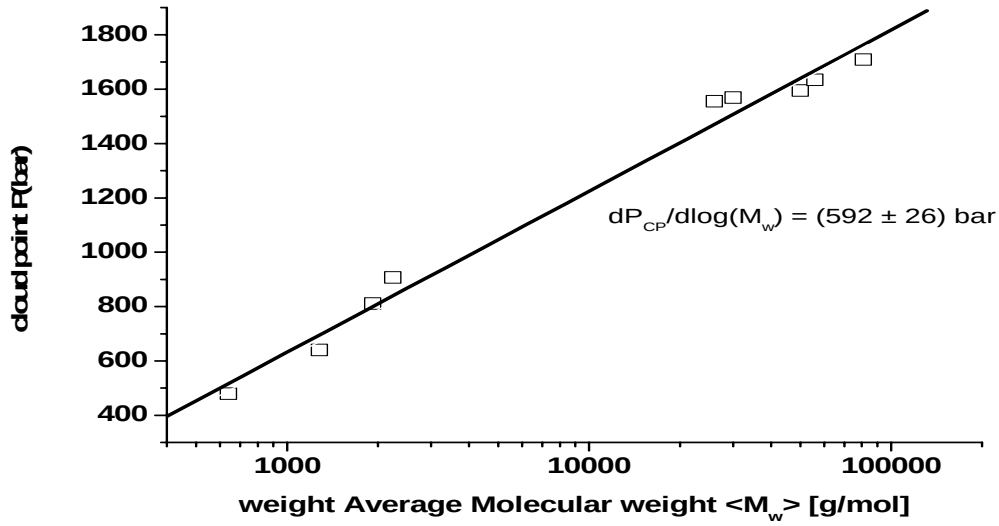

Figure 6.4: *Predication of impact of molecular weight on the position of L+L demixing (solubility) of PVDF in $scCO_2$ at 185°C, using Gibbs Ensemble Monte Carlo method. Open symbol is the experimental data done at CPREI (first 4 point from downward), and RWTH-Aachen data (first 5 point from upward), while solid line represents the simulation data.* [26]

Decreasing the molecular weight of polyvinylidene fluoride has a significant effect in ramification of liquid/solid boundary line (crystallization). However, decreasing the molecular weight of PVDF turns out in shifting the crystallization temperature to lower value as well (cf. figure 6.5).

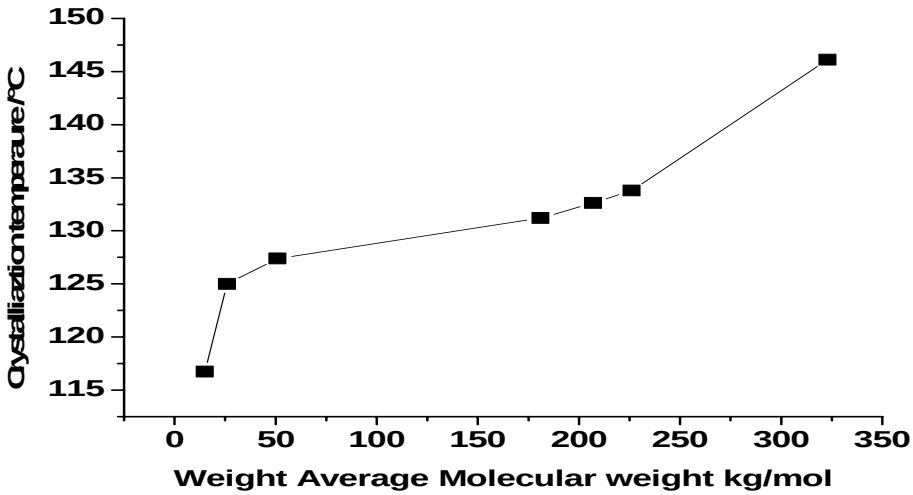

Figure 6.5: *Correlation diagram between weight average molecular weight of different PVDF's samples isobarically cooled at 1800 bar as function of crystallization temperature, T_c, , polymer concentration was 2 wt% for all measurements.(cooling rate was 0.2 K/min)*

Morphological effect of PVDF different molecular weight has been studied using high resolution scanning electron microscopy (HRSEM), Figure 6.6. Where PVDF 323 can undergo either liquid-liquid demixing precipitation before crystallization (roundish-like droplet features, Fig.6.6 a), or can be directly crystallized (Fig. 6.6b). While other low molecular weight samples a well developed lamellar structure. (Fig.6.6, c,d,e, and f).

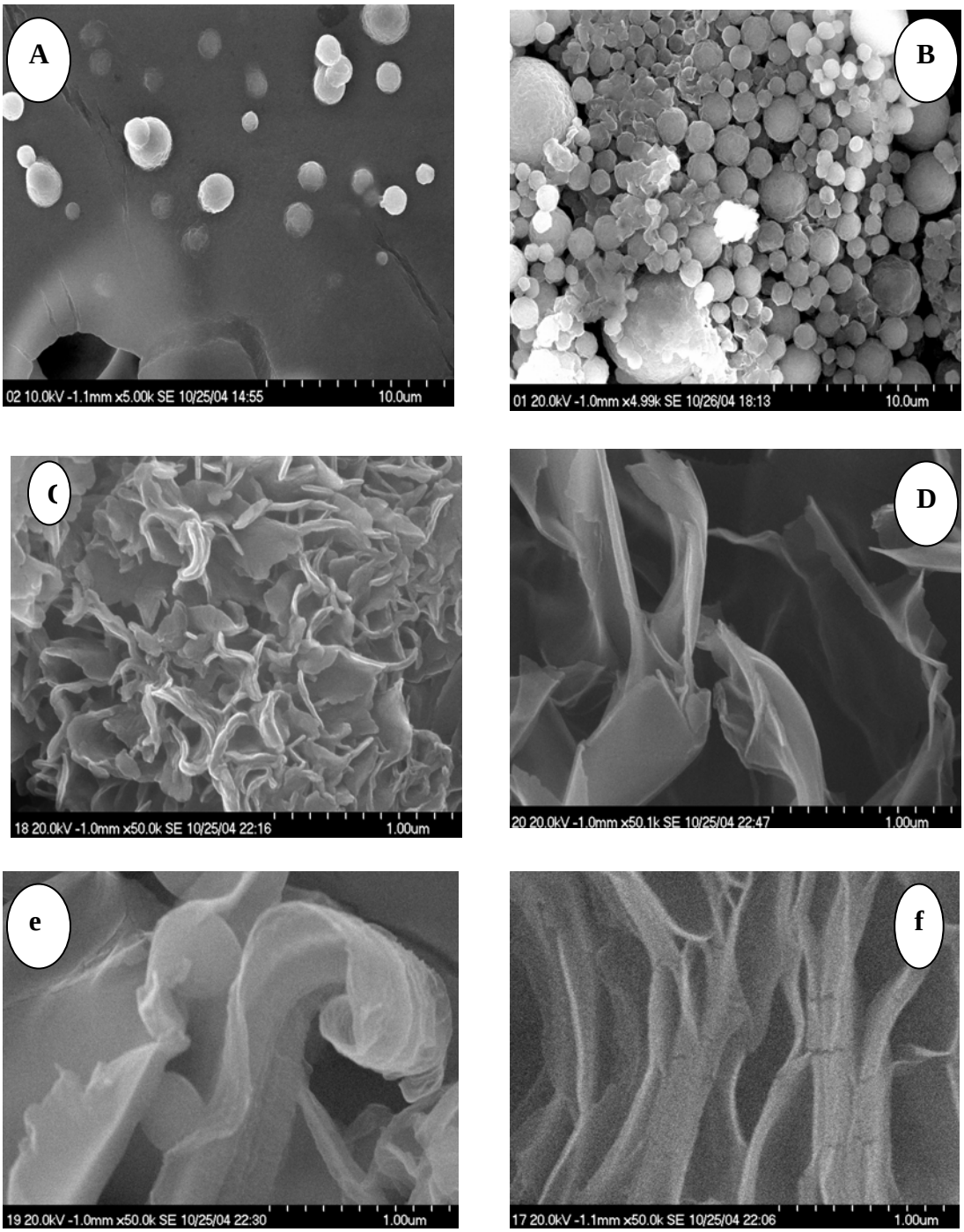

Figure 6.6: *High resolution scanning electron micrograph of 2 wt% polyvinylidene fluoride(PVDF323) crystallized either by (a) L+L demixing prior crystallization,(small crystallite was embedded inside microvoid),or by (b) direct crystallization,(10µm scale bar in bother case). While lamellar structure for different PVDF weight average molecular weight are shown for (c) 15 kg/mol, (d)*

(d) 51 kg/mol, (e) 181 kg/mol, and (f) 207 kg/mol crystallized from $scCO_2$ at 1800 bar with cooling rate 0.2 k/min. (resolution power 1.00μm).

As indicated in the above micrographs, in general for all PVDF samples investigated in this study, it was realize that PVDF can undergo crystallization from $scCO_2$ forming a lamellar structure which is typical for chain folded crystals. The lamellar structure bundles are found to be thickened as the molecular weight of polyvinylidene fluoride increases. As a descriptive example, PVDF15 the lamellas are observed to be less ordered with a very narrow thickness. (Fig. 6.7)

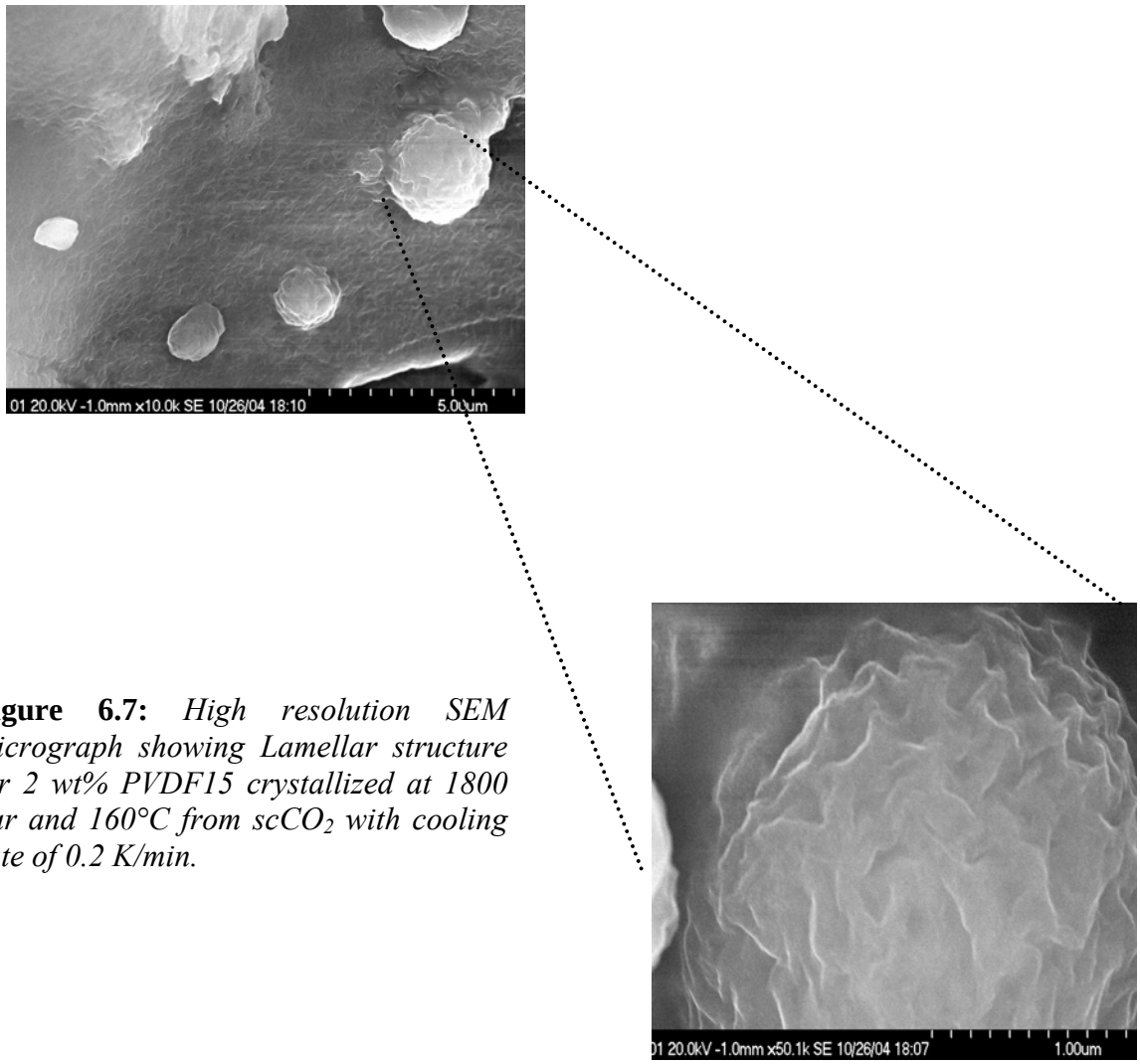

Figure 6.7: *High resolution SEM micrograph showing Lamellar structure for 2 wt% PVDF15 crystallized at 1800 bar and 160°C from $scCO_2$ with cooling rate of 0.2 K/min.*

6.4 Conclusion:

The effect of molecular weight of polyvinylidene fluoride on its precipitation/crystallization border in a solution of carbon dioxide was studied. Where, crystallization occur either (i) directly at high pressure by crossing solid/fluid line, or (ii) indirectly after phase separation at L+L demixing. In the later case liquid droplets are formed consisting of polymer melt swollen by some carbon dioxide, i.e. crystals were formed at higher polymer concentration.

Furthermore, we observed that both higher and lower molecular weights PVDF have the capability of changing the position for both negatively inclined liquid-liquid & liquid-solid boundaries. As an example, for 2 wt% PVDF 323, PVDF 181, and PVDF26 solutions isothermally precipitate from $scCO_2$ at 155°C and 1800 bar; the liquid-Liquid segregation boundaries were measured at 1760, 1510, and 1470 bar, respectively. Consequently, the liquid/solid lines for those 3 sorts of PVDFs were changed. The onset of the crystallization temperature, T_c, for a 2 wt% PVDF 323, 181, 26 isobarically cooled from hot CO_2 at 160°C and 1800 bar, were 146.0, 131.4, and 124.8°C respectively. Polymer polydispersity might be the reason for this behaviour as we have short and long polymeric chains differencing in their solubility in $scCO_2$.

Scanning electron micrograph reveals that PVDF323 can undergo liquid-liquid demixing prior crystallization as obtained by cooling down its homogenous solution with CO_2 at low pressure (i.e. in the vicinity of intersection point between L+L and L+S, point 4 in Fig.6.2). Where, polymer crystals were visualized near structural cavity characterizing PVDF precipitated by L+L demixing, (i.e. sponge likes structure). For other molecular weights PVDF sample crystallized by crossing L+S border, SEM micrograph reveals a well developed lamellar structure.

6.5 References:

[1] Gendron R., and Daigneault L. E., (ed. Lee ST) Foam Extrusion: Principles and practice, Technomic Publishing Co., Inc., 2000.

[2] Lee M., Park C. B., and Tzoganakis C.; Polym. Eng. Sci. 1999, **39**, 99.

[3] Handa Y. P., Zhang Z., and Wong B.; Macromolecules 1997, **30**, 499.

[4] Zhang Z., and Handa Y. P.; Macromolecules 1997, **30**, 8505.

[5] Mizoguchi K., Hirose T., Naito Y., and Kamiya Y.; Polymer 1987, **28**, 1298

[6] Wissinger R. G., and Paulaitis M. E.; J. Polym. Sci., Part B: Polym. Phys. 1991, **29**, 631.

[7] Handa Y. P., Lampron S., and O'Neill M. L.; J. Polym. Sci., Part B: Polym. Phys 1994, **32**, 2549.

[8] Handa Y. P., Kruus P., and O'Neill M.; J. Polym. Sci., Part B: Polym. Phys 1996, **34**, 2635.

[9] Zhang Z., and Handa Y. P.; J. Polym. Sci., Part B: Polym. Phys. 1998, **36**, 977.

[10] Gendron R.; Applied rheology for the extrusion of thermoplastic foams; Proceedings of Foams'99, October1999.

[11] Schultze J. D., Engelmann I. A. D., Boehning M., and Springer J.; Polym. Adv. Technol. 1991, **2**, 123.

[12] Takada M., Tanigaki M., and Ohshima M.; Polym. Eng. Sci. 2001, **41**, 938.

[13] Chiou J. S., Barlow J. W., and Paul D. R.; J. Appl. Polym. Sci. 1985, **30,** 2633.

[14] Chiou J. S., Barlow J. W., and Paul D. R.; J. Appl. Polym. Sci.1985, **30,** 3911.

[15] Beckman E., and Porter R. S.; J. Polym. Sci., Part B: Polym. Phys. 1987, **25**, 1511.

[16] Lambert S. M., and Paulaitis M. E.; J. Supercritical Fluids 1991, **4**, 15.

[17] Kalospiros N., Astarita S. G., and Paulaitis M. E.; Chem. Eng. Sci. 1993, **48**, 23.

[18] Wilson C.W.; J. Polym. Sci. A 1963, **1**, 1305.

[19] Gorlitz M., Minke R., Trautvetter W., Weisengerber G.; Angew. Makromol. Chem. 1973, **29/30**, 137.

[20] Lovinger A.J.; Poly (vinylidene fluoride) in Developments in crystalline Polymers-1, D.C. Bassett, 1 st ed., Applied Science Publishers, London, 1982.

[21] Carlson D.P., Schmiege W.; Fluoropolymers, organic, in Ullmann`s encyclopaedia of Industrial Chemistry, 5th Ed., Gerhartz W., Ed., VCH, Weinheim ,1985.

[22] Richardson A., Hope P.S., Ward I.M.; J. Polym. Sci. Polym. Phys. ed. 1983, **21**, 2525.

[23] Reza Najjar, Ph.D thesis, RWTH-Aachen, in progress.

[24] Juergen Ellmman, PhD thesis, Ulm, Germany, 2001.

[25] Chapter 3, in this thesis.

[26] Costas Kiparrissidas et al. LPREI/CPREI/ AUT.

SUMMARY

This thesis at hand concerned with novel determination of the solubility (liquid/liquid demixing), and crystallization (liquid/solid demixing) of fluorinated polymers in supercritical carbon dioxide by cloud point technique. Due to great importance of semicrystalline PVDF, in particular solubility of this polymer in CO_2 has been investigated in detail either through isothermal depressurization (precipitation) or isobaric expansion (crystallization) procedure technique.

The crystallization (liquid/solid) and precipitation (liquid/liquid) demixing lines of polyvinylidene fluoride in carbon dioxide were studied in temperature and pressure ranges between 110-190°C and 1400-2100 bar, respectively. While the first procedure yielded a solid polymer having micro-porous sponge like morphology containing of interconnected macrovoids, the latter method resulted in fine powders with lamellar structure of typical chain folded crystal, the crystalline powder is characterized by particle diameters in the range of 5-20 µm.

As a major drawback during dispersion polymerization of PVDF in $scCO_2$, a bimodal molecular weight distribution might take place as a result of polymer precipitation in the early polymerization time. By means of cloud point technique we were able to propose different strategic precipitation processes that may occur for polyvinylidene fluoride during its polymerization in supercritical carbon dioxide. First, precipitation may occur by crystallization upon crossing the liquid/solid border. This means crystals are formed directly from homogenous solution. Secondly, crystals are formed after liquid-liquid demixing. In the latter process, liquid droplets are formed consisting of polymer melt swollen by CO_2, i.e. the crystals are formed at high polymer concentration.

To examine the effect of VDF on the miscibility of PVDF/CO_2 binary system was performed. Where, the observed liquid-liquid boundary for the adding gaseous vinylidene fluoride (VDF) on the location of L+L and L+S demixing was investigated. We found at low concentration of VDF (< 42wt %) a decrease in the solubility values

(L+L border) for PVDF/scCO_2 mixture, while at high concentration the situation is reversed. At higher concentration of vinylidene fluoride the crystallization line is not altered from the situation for pure PVDF. Further increase of VDF percentage of (>42 wt %) the monomer was believed to act as antisolvent for the binary mixture of PVDF/CO_2, as liquid-liquid demixing lines were shifted to high values.

The effect of added VDF on the position of liquid/solid demixing pressure and temperature has been studied as well. Where we found a correlation between the decreasing the location of L+S boundary and increasing of added amount of VDF (up to 42 wt %). In all cases the crystallization line were found to despite a negative slope in P-T diagram. This effect was quite similar to what observed regarding effect of adding monomer on the L+L demixing line. On other hand, as the amount of VDF was increased from 42 to 76 wt%, the position of L+S demixing line was shifted to higher temperature value. As the crystallization process becomes faster in the presence of high amount vinylidene fluoride.

For a future work regarding the study of crystallization kinetics for PVDF in scCO_2 , a lot of attention should be addressed to control variety of parameter (ex. cooling rate, presence of nucleating agent) that could influencing either the position at which polymer crystal start to segregate from scCO_2 solution

On another approach regarding the enhancement of molecular weight of PVDF during dispersion polymerization in scCO_2; a novel designed macromolecular stabilizer has been professionally synthesized for the purpose of being used as stabilizer during dispersion polymerization process. For the highest stabilization efficiency during polymerization, macromolecular stabilizer must be completely miscible in CO_2 at operating polymerization condition. However, Impact of molecular structure on the solubility of statistical and block copolymers made up from same constituents i.e. 1H, 1H, 2H, 2H-perfluorodecylacrylate (F8H2A) and methyl methacrylate (MMA) were measured. Whereas, block copolymers are better soluble in CO_2 than statistical copolymers. They simultaneously exhibited a lower solution temperature. Above 50°C the block copolymers solubility hardly depends on the block length ratio. Block copolymers also exhibit a better solubility than statistical copolymer even it has higher molecular weights and containing relatively large amount CO_2-phobic groups. The

results clearly demonstrate that skilful selection of the polymers architecture is of larger importance for creation of CO_2 soluble macromolecules that the simple selection of the "right" composition.

Interestingly, we observed in our study that the impact of fluorination is almost the same for siloxane polymers, whether fluorinated chain exists in the main polymeric chain or in the side chain. Presences of fluoroalkyl-group either in the main chain (α-ω-perfluoroalkyl polysiloxanes) tends to improve solubility at low temperature regime (i.e. lower cloud point) rather than being grafted at side chain, while the at high temperature both sort of fluorosiloxane polymer exhibit the same cloud points characteristics. So, α-ω- Perfluoroalkyl polysiloxanes is better to be used as detergent at low temperature rather than perfluoroalkyl grafted polysiloxanes

Another random and block (palm tree) macromolecule stabilizers have been successfully prepared either by controlled free radical polymerization from P[((PDMS-MMA)$_{1000}$)$_x$]-Br and methylmethacrylate (MMA) or atom transfer radical polymerization technique, respectively. Block copolymers of P[(PDMS-MMA)$_{1k}$]$_x$-b-P[MMA]$_y$ (palm tree) does show both a LCST characteristics in P-T diagram in $scCO_2$ upon increasing temperature. Since PMMA was reported to be $scCO_2$–phobic moiety, increasing weight percent of MMA either in block or random copolymer results in increasing the liquid-liquid demixing pressure to high values i.e. retarding solubility.

Random copolymer of P[((PDMS-MA)$_{1000}$)$_x$-co-MMA$_y$] exhibits a lower cloud point pressure in carbon dioxide and better solubility rather than block copolymer of approximately same composition.

In order to answer an open question whether addition of cosolvent to carbon dioxide can alter its polarity or not? An experimental attempt has been done regarding the effect of adding various classes of low and high molecular weight compounds on the location of liquid/liquid and liquid/solid positions for PVDF/$scCO_2$ system in a temperature range from 110°C to 190°C at pressures between 1400 to 2100 bar. We noticed that low molecular weight additives can considerably influence the solubility of PVDF in CO_2. Moreover, by selection of the type of additive it was possible to lower the L+L demixing pressure and keep the L+L demixing temperature fairly constant or lowering

both, the L+L demixing temperature and the L+L demixing pressures. In the presence of DMF treatment reduces the crystallinity of the polymer only for ~10-15 %.

N,N-dimethylacetamide has a powerful effect on lowering both L+L and L+S segregation line of PVDF in CO_2 as for example 8 wt% can shift the cloud point line by about 800 bar and the onset of the crystallization by ca. 35°C.

The effect of molecular weight of polyvinylidene fluoride on its precipitation/crystallization border in a solution of carbon dioxide was investigated. Where, we observed both higher and lower molecular weights PVDF have the capability of changing the position for both negatively inclined liquid-liquid & liquid-solid boundaries. By comparing SEM micrograph for different crystallized PVDF samples, we noticed that PVDF323 (M_w= 323 kg/mol) can undergo liquid-liquid demixing prior crystallization as obtained by cooling down its homogenous solution with CO_2 at low pressure. Where, roudlich-like droplet structure was visualized. For other molecular weights PVDF sample crystallized by crossing L+S border, SEM micrograph reveals a well developed lamellar structure.

ZUSAMMENFASSUNG

Mit Hilfe einer neu aufgebauten Sichtzelle wurde die Löslichkeit von Polyvinylidenfluorid, PVDF, in überkritischem Kohlendioxid, sc-CO_2, untersucht. PVDF ist ein teilkristallines Polymer. mit einem Gleichgewichtsschmelzpunkt von mehr als 170°C. Aufgrund der wechselnden -CF_2- und -CH_2- Einheiten besitzt PVDF ein starkes Dipolmoment und kann durch eine gleichmäßige Ausrichtung der Ketten in einer all-transplanaren Kristallkonformation ein Elektretmaterial ausbilden, gleichzeitig ist die Polarisierbarkeit der CF_2-Gruppen gering. Dies bedingt, dass sich PVDF selbst in stark polaren aprotischen Lösemitteln wie DMF oder DMAc nur schlecht bzw. nur bei hohen Temperaturen löst. Als Ausgangspunkt dieser Arbeit war bekannt, dass sich PVDF nur bei hohen Drücken (P > 1500 bar und hohen Temperaturen T >100°C) in sc-CO_2 löst. Da sc-CO_2 in jüngerer Zeit besonderes Interesse als ein Lösemittel für Polymerisationsreaktionen insbesondere auch für Fluorpolymere findet, wurde in dieser Arbeit eine genaue Bestimmung der Löslichkeit von PVDF in sc-CO_2 unter Berücksichtigung des Molekulargewichts, der Zugabe niedermolekularer Colsolventien und des Anteils an Monomeren sowie der Zugabe von lösungsvermittelnden Polymeren vorgenommen. Im letzten Fall geht es darum, inwieweit blockartig und statistisch aufgebaute Fluorcopolymere eine makroskopische Segregation des PVDF durch Stabilisierung einer Dispersion verhindern können. Durch die genaue Kenntnis der Löslichkeitsgrenzen soll eine verbesserte Reaktionsführung für die Polymerisation von PVDF in sc-CO_2 erreicht werden.

Es wurde zunächst eine PVT-Apparatur mit Sichtfenstern aufgebaut, in der unter Variation des Volumens und der Temperatur und mit Hilfe eines Multikanal-Photodiodenspektrometers Trübungspunktmessungen durchgeführt werden konnten. Die Trübungsmessungen ermöglichen die genaue Bestimmung des Einsetzens der Phasensegregation, wobei die Wellenlängenabhängigkeit der Trübung auch für eine erste Bestimmung der Teilchenzahl und Teilchengröße genutzt werden kann.

Für binäre PVDF-Lösungen in sc-CO_2 wurde die Molekulargewichtsabhängigkeit der Löslichkeit unter verschiedenen Bedingungen bestimmt. Trübungspunktbestimmungen

durch Abkühlen einer homogenen Lösung des PVDF in sc-CO_2 unter isobaren Bedingungen ermöglichten die Bestimmung der Kristallisationslinie, in einem Temperaturbereich von 100° bis 190°C, d.h. der nukleierten Flüssig-Fest-Entmischung. Auf eine Bestimmung der Schmelzpunktkurven wurde verzichtet, da unter den gewählten Versuchsbedingungen keine gleichmäßige Verteilung der dispergierten Kristallite sichergestellt werden konnte. Trübungspunktbestimmungen durch Entspannung der Lösung (Vergrößerung des Volumens) unter isothermen Bedingungen ermöglichten die Bestimmung der Flüssig-Flüssig-Entmischung in einem Druckbereich zwischen 1400 und 2100 bar. Mikroskopische Untersuchungen der Morphologie der ausgefallenen Teilchen zeigen wie erwartet einen deutlichen Unterschied in der Struktur. Im ersten Fall werden locker gestapelte Lamellenkristalle erhalten, wie es für eine Kristallisation aus Lösung zu erwarten ist. Im zweiten Fall werden je nach Polymerkonzentration tröpfchenförmige, teilkristalline Polymerteilchen oder poröse schwammartige Strukturen erhalten, welche zunächst als hochkonzentrierte Polymerphase aus der Lösung abgeschieden wurden, bevor die Kristallisation beim Abkühlen der Flüssig-Flüssig-Dispersion eintrat.

In einem zweiten Schritt wurde der Einfluss von Zugaben des Monomers Vinylidenfluorid, 1,1-Difluorethylen, auf die Löslichkeit von PVDF in sc-CO_2 bestimmt. Für niedere Anteile an Vinylidenfluorid wurde zunächst eine Erhöhung der Löslichkeit von PVDF in sc-CO_2 festgestellt, Allerdings kann dieser Effekt durch die nicht ausreichende Messgenauigkeit für die Bestimmung kleiner Monomeranteile verfälscht sein. Mit zunehmender Konzentration wurde dann eine Verringerung der Löslichkeit des PVDF in sc-CO_2 bestimmt. Dieser Effekt ist in Übereinstimmung mit der Beobachtung, dass Vinyldenfluorid ein schlechtes Lösemittel für PVDF ist. Andere niedermolekulare Cosolventien insbesondere Dimethylacetamid, Dimethylsulfoxid oder γ-Butyrolacton und N-Methylpyrrolidon ergaben hingegen eine signifikante Verbesserung der Löslichkeit, d.h. Absenkung des Drucks der Trübungspunktlinie. Problematisch ist hier, dass diese Verbindungen alle die radikalische Polymerisation des Vinylidenfluorids inhibieren.

In einem dritten Schritt wurde der Einfluss polymerer Additive auf die Löslichkeit des PVDF in sc-CO_2 untersucht. Als Additive wurden blockartig aufgebaute und statistische Copolymere des 1H,1H,2H,2H-Perfluorodecylacrylats (F8H2A) oder eines PDMS-Methylacrylatmacromonomeren einerseits und des Methylmethacyrlats andererseits ausgewählt. Im Fall der Blockcopolymere des Perfluorodecylacrylats wurde die Länge

des Blocks mit den Perfluoralkylsubstituenten von zwei bis über zweihundert Einheiten variiert. Zum Vergleich wurden statistische Copolymere mit einer ähnlichen Comonomerzusammensetzung herangezogen. Im Fall der Polysiloxanmakromere wurden Blockcopolymere mit einem sehr kurzen Makromonomerblock, so genannte Palmwedelpolymere und statische Copolymer eingesetzt. Hintergrund für die Wahl der ausgesuchten Polymere ist die literaturbekannte Mischbarkeit von PMMA mit VDF und die gute Löslichkeit von Fluorpolymeren und PDMS in sc-CO_2. Damit wurde erwartet dass diese polymeren Additive einerseits die Phasensegregation durch Kristallisation unterdrücken können, andererseits zu einer Stabilisierung kleiner PVDF Tröpfchen und kristalliner Teilchen beitragen können. Die Ergebnisse zeigen, dass die Blockcopolymere im Fall der Fluorpolymere die Löslichkeit des PVDF in sc-CO_2 stärker verbessern als die statistischen Copolymere. Insbesondere zeigte sich im Fall der Fluorpolymere, dass bereits sehr kurze Perfluoralkylacrylatblöcke aus wenigen Monomereinheiten vergleichbare Effekte, wie die längeren Blöcke ergeben. Im Gegensatz hierzu wurde im Fall der Polysiloxanmakromer-Verbindungen gefunden, dass die statistischen Copolymere die Löslichkeit/Dispergierbarkeit des PVDF stärker als die Palmwedel-Polymere verbessern. Weitergehende Untersuchungen zur Bestimmung des Molekulargewichtseinflusses der polymeren Additive und der Hintergründe der beobachteten Verhinderung der Segregation (Trübung) konnten im Rahmen dieser Arbeit nicht mehr durchgeführt werden.

ACKNOWLEDGMENT

First and foremost, I am deeply grateful to my god (*ALLAH*) for his unlimited support & help.

I would like to thank gratefully my advisor **Prof. Dr. rer. nat. Martin Möller**, for the trust he gave me, the big freedom with the selection and treatment of the research contents and the outstanding work conditions. Furthermore, I would like to thank him for the possibility he gave me to present my results in numerous conferences and for the enviable possibility to work in a strongly international team. Also I'd to thank him for his valuable direction as a mentor, excellent teacher and researcher.

I express my grateful to my co-advisor **PD. Dr. Uwe Beginn**, for his co-supervision and guidance. Also I thank him for his critical revision of this thesis, and the time we spent together travelling to various countries to represent my work. Without his assistance this work could not see sunlight. Many thanks Uwe for helping me socially in my early time in Aachen.

I owe my grateful thanks also to **Dr. Ulrich Ziener,** for his support in the early time in constructing a very high pressure system, and dealing with a variety of companies and having a tenth of offers.

I would like to thank **Prof. Dr. Paul Walter**, Section Electron Microscopy, University of Ulm, for the high resolution scanning electron microscopy photographs of polyvinylidene fluoride represented in chapter 3 and 6.

I am grateful to **Dr. Roland Martin**, Solvay, Brussels, Belgium for his generous donation of Solef 1010. Meanwhile, I'd like to thank Elf-Atochem, France for gifting me Kynar 741.

Degussa AG, speciality polymer, Essen, Germany is gratefully acknowledged for flouorsiloxane polymers mentioned in chapter 4.

I want to express my deep thanks to **Prof. Dr. Costas Kiparissides**, Chemical Process Engineering Research Institute (CPERI), Greece for simulation data regarding miscibility of PVDF presented in chapter 3 and 6.

I would like to thank **Prof. Dr. Fanz-Josef Wortmann** for taking over as second referee for this thesis.

I am deeply grateful to **Prof. Dr. W. Leitner** not only for being as a third examiner in my Ph.D committee but also for the great time we had during summer school (Venice, 2003) and VI international conference on green chemistry (Bruchsal, 2004).

My sincere thanks go to **Prof. Dr. rer. nat. Ashraf A. Mansour**, President of the board of trustee, GUC for his support and encouragement whenever needed.

I would like to thank **Prof. Dr. A. Khatab**, Vice Ambassador and cultural consular, Egyptian embassy, Berlin, Germany for her support and physical enforcement.

I'd like to express my warm thanks to Dr. Juergen Ellmann, for his assistance in getting me familiar with high pressure system, and doing my first experiments with kilo bars. Also I thank him for fluorinated block and statistical copolymers mentioned in chapter 4. Also I thank my Iranian colleague Mr. Reza Najjar for the time we spent together and for the synthesis of low molecular weight PVDF26 mentioned in chapter 6. Dr.Ana Morales for palm tree polymers is gratefully acknowledged.

I would like to thank whole co-workers at the mechanical workshop at ITMC/RWTH-Aachen, and at the University of Ulm. Where, in Ulm people help me a lot in constructing high pressure system while at Aachen they help me in repairing high pressure reactor. Without their assistance I couldn't be able to perform this work.

I would like to thank all co-workers at the Deutsche WollforschungsInstitut (DWI) for their wonderful working atmosphere

The European Commission for the financial support (contract no. G1RD-CT-2002-00676) is gratefully acknowledged.

Last but not at least, I express my cordially thanks to my family, my sister Dr. MD. Rania Fahmy and my wife Mrs. Sarah Fahmy for their love and infinite help and support especially in the last time.

List of Publications

1- Published:

◊ "Phase equilibrium behaviour of polyvinylidene fluoride/carbon dioxide mixtures: An experimental and theoretical study" ***Fahmy Sherif***, Beginn Uwe, Moeller Martin, Pladis Prokopis and Kiparrissidas Costas. DECHEMA Monographien (2004), 138 (8 th International workshop on polymer reaction engineering), 375-379.

2- To be submitted:

◊ "Precipitation/crystallization boundaries of PVDF in $scCO_2$" ***Fahmy Sherif***, Beginn U., Ziener U. and Moeller M., 2005

◊ "Phase behaviour of novel molecularly engineered block and statistical copolymer in carbon dioxide" ***Fahmy Sherif***, Beginn U., Ellmann J., Moeller M., 2005.

◊ "Impact of low and high molecular weight additives on the solubility of PVDF in $scCO_2$" ***Fahmy Sherif***, Beginn Uwe, Moeller M., 2005.

◊ "Effect of Molecular weight on the morphology of crystallized polyvinylidene fluoride in $scCO_2$" ***Fahmy Sherif***, Beginn Uwe, Moeller M., 2005.

3- Poster:

◊ "Phase equilibrium behaviour of polyvinylidene fluoride/carbon dioxide mixtures: An experimental and theoretical study" ***Fahmy Sherif***, Beginn Uwe, Moeller Martin, Pladis Prokopis and Kiparrissidas Costas. 8 th International workshop on polymer reaction engineering, Hamburg, Germany, Oct. 4th 2004.

◊ "Polymerization of PVDF in supercritical carbon dioxide" Beginn Uwe, ***Fahmy Sherif***, and Reza Najjar, Polydays Tagung, Potsdam, Germany, 15-16 Oct. 2004.

Lebenslauf

Persönaliche daten:

	Sherif Medhat Fahmy Geb. 19.01.1975 in Kairo/Ägypten Ägypter Verheiratet

Ausbildung:

07.1980-07.1986	Besuch der „ Primary School“ in kairo
10.1986-07.1992	Besuch der „Secondary School“ in kairo, abschluss „Abitur“.
07.1992-07.1996	Studium der Chemie an der Universität Kairo, Ägypten, Abschluss “Bachelor“ (Mit Auszeichnung)
09.1998-12.1998	Forschung Praktikum am „chemisty department, University of Colorado, boulder, USA. group of Prof. Dr. em. John Stevens. thema“ *Synthsis of biodegradable polymer*“
01.1999-10.2000	Studium polymere Chemie am Lehrstuhl für Chemie/ Fakultät für naturwissenschaft and der Universität Kairo, Ägypten, Abschluss „Master of Science“(Mit Auszeichnung) under supervision Prof. Dr. ElShafee Thema „*Compatibility and crystallization behaviour of Poly (3-hydroxybutyrate)/Cellulose acetate butyrate blends*”
08.2001-11.2004	Promotion bei Prof. Dr. Martin Möller in der Abteilung organische chemie III/Makromolekular Chemie der Universität Ulm ab september 2002 am lehrstuhl für Textilchemie und Makromolecular Chemie der RWTH-Aachen thema „ *Solubility of fluorinated polymer in supercritical carbon dioxide*“

Berufstätigkeit:

09.1997-10.2000	Wissenschaftlicher Mitarbeiter in der Lehrstuhl für Chemie /Fakultät naturwissenschaft, Universität Kairo, Ägypten als „Instructor“ .

10.2000-prsent	Wissenschaftlicher Mitarbeiter in der Lehrstuhl für Chemie /Fakultät naturwissenschaft, Universität Kairo, Ägypten als „Assistent Lecturer in polymere chemie“ .
09.1998-09.1999	Wissenschaftlicher Mitarbeiter in der Lehrstuhl für Chemie /Fakultät naturwissenschaft, Amerikanische Universität in Kairo, (AUC) Ägypten als „Instructor“ .
08.2001-09.2002	Wissenschaftlicher mitarbeiter in der Abteilung Organische chemie III/ Makromolekular chemie in der Uni. Ulm.
09.2002-11.2004	Wissenschaftlicher mitarbeiter im Lehrstul für Textilchemie und Makro. Chemie der RWTH Aachen bei Prof. Dr. Martin Moeller.

Erklärung

Ich versichere, dass ich die von mir vorgelegte Dissertation selbstständig angefertigt, die benutzten Quellen und Hilfsmittel vollständig angegeben und die Stellen der Arbeit einschließlich Tabellen und Abbildungen -, die anderen Werken im Wortlaut oder dem Sinn nach entnommen sind, in jedem Einzelfall als Entlehnung kenntlich gemacht habe; dass diese Dissertation noch keiner anderen Fakultät oder Universität zur Prüfung vorgelegen hat.

_____

Sherif Fahmy

Aachen, den 23 Dec., 2005